



ISTITUTO
ITALIANO DI
TECNOLOGIA



UNIVERSITÀ DEGLI STUDI
DI GENOVA

Corso di Dottorato in Neuroscienze
Curriculum Neuroscienze e Neurotecnologie
Ciclo XXXIV

**NRSF/REST impairs brain spatial K⁺ buffering and
glutamate uptake via downregulation of inwardly
rectifying K⁺ channel Kir4.1 and GLT-1 transporter in
cultured cortical astrocytes**

Candidate: Eleonora Centonze

Supervisor: Fabio Benfenati, M.D.

Co-supervisors: Pierluigi Valente, Ph.D.

Fabrizia Cesca, Ph.D.

Contents

1. Abbreviations index	2
2. Abstract	4
3. Introduction	5
3.1. <i>REST in the brain</i>	5
3.2. <i>REST structure, isoforms and regulation</i>	7
3.3. <i>REST and CNS cells</i>	15
3.4. <i>REST and brain disorders</i>	19
3.5. <i>Astrocytes</i>	23
3.6. <i>Potassium and glutamate homeostasis in the CNS</i>	27
4. Aim of the study	34
5. Materials and Methods	35
5.1. <i>Animals and cell culture preparation</i>	35
5.2. <i>Biotinylation, immunoblotting and immunofluorescence</i>	37
5.3. <i>Glutamate uptake assay</i>	38
5.4. <i>Patch-clamp recordings</i>	39
5.5. <i>Statistical analysis</i>	41
6. Results	42
6.1. <i>Astrocytes with REST deficiency preserve a normal cellular morphology</i>	42
6.2. <i>REST deletion in primary astrocytes selectively downregulates an inward rectifier current</i>	44
6.3. <i>REST deletion negatively modulates an inward-rectifier K⁺ current</i>	47

6.4.	<i>Kir4.1 downregulation by REST deletion impairs glutamate uptake by GLT1</i>	53
6.5.	<i>Neurons co-cultured with REST KO astrocytes display altered firing phenotypes</i>	56
7.	Discussion	60
8.	Conclusions	66
9.	Bibliography	67
10.	Acknowledgements	93

1. Abbreviations index

AD = Alzheimer's disease

ALS = amyotrophic lateral sclerosis

AP = action potential

AQP = aquaporin

β TrCP = β -transducin repeat containing E3 ubiquitin protein ligase

BMP = bone morphogenetic protein

BSA = bovine serum albumin

$\text{Ca}^{2+}_{\text{in}}$ = intracellular calcium

CI = circularity index

CNS = central nervous system

CREB = cAMP response element-binding protein

DIV = days in vitro

DL-TBOA = DL-threo- β -benzyloxyaspartic acid

DYRK1A = dual specificity tyrosine-phosphorylation-regulated kinase 1A

EAAT = excitatory amino acid transporters

Erk 1/2 = extracellular signal-regulated kinase 1 and 2

E_K = equilibrium potential for K^+

ESC = embryonic stem cell

FBS = fetal bovine serum

GABA = γ -aminobutyric acid

GBM = glioblastoma multiforme

GLAST = glutamate/aspartate transporter

GLT-1 = glutamate transporter-1

GS = glutamine synthetase

HAUSP = Herpesvirus-associated ubiquitin-specific protease

HCN1 = hyperpolarization-activated and cyclic nucleotide-gated channel

HD = Huntington's diseases

HDAC = histone deacetylase

HIPPI = huntingtin interacting protein 1 protein interactor
IP₃ = inositol-3-phosphate
JAK-STAT = janus kinase signal transducer and activator of transcription
K⁺_{ext} = extracellular potassium
K_v = voltage-gated potassium channel
K_{ir} = K⁺ inward rectifier
KO = knockout
MPP⁺ = 1-methyl-4-phenylpyridinium ion
N_v = voltage-gated sodium channel
NLS = nuclear localization signals
NRSE = neuron-restricting silencing element
NRSF = Neuron-restrictive silencer factor
NSC = neural stem cell
nSR100 = neural-specific Ser/Arg repeat-related protein of 100 kDa
PAG = phosphate-activated glutaminase
PBS = phosphate buffered saline
PD = Parkinson's disease
RE1 = repressor element 1
REST = repressor element 1-silencing transcription factor
RGC = radial glial cell
RILP = REST-interacting LIM domain protein
R_{input} = input resistance
RT = room temperature
SEM = standard error of the mean
SOD1 = superoxide dismutase 1
SZ = schizophrenia
TBP = TATA-binding protein
TCA = tricarboxylic acid
V_h = holding potential
V_{rest} = resting membrane potential
ZF = zinc finger

2. Abstract

Neuron-restrictive silencer factor/repressor element 1 (RE1)-silencing transcription factor (NRSF/REST) regulates many genes and signaling pathways involved in neuronal differentiation, synaptic homeostasis and maintenance of normal glial cell functions. REST activity is progressively downregulated in neurons during development, while it is normally expressed in glial cells. Astrocytes are the most abundant glial cells and play an important role in maintaining the functional integrity of neuronal networks by forming tripartite synapses. In this study, we have explored the in vitro role of REST in astrocyte functions using REST conditional knockout mice (REST-KO). We studied the electrophysiological properties of primary cultures of REST-KO cortical astrocytes by the patch-clamp method. We provided biophysical and pharmacological evidence of a reduced plasma membrane density of the inward rectifying K⁺ channel subtypes 4.1 (Kir4.1). Loss of Kir4.1 causes reduction of the expression and activity of glutamate transporter-1 (GLT-1), accompanied by a decrease in the astroglial glutamate uptake. Because a reduced activity of astrocyte Kir4.1 has been observed in a number of neurological diseases including temporal lobe epilepsy, we have studied the firing properties of neurons co-cultured with REST-KO astrocytes. Loss of Kir4.1 impairs the astrocyte ability to buffer extracellular K⁺ concentration that, increased by neuronal activity, indirectly enhances the action potential firing of neurons co-cultured with REST-KO astrocytes. This study adds a new piece to the discovery of REST-regulated mechanisms in astrocytes and contributes to our understanding of the involvement of Kir4.1 and GLT-1 in a variety of neurological disorders.

3. Introduction

3.1. REST in the brain

The regulation and balance of gene expression is critical for the development and function of the central nervous system (CNS). The CNS works by a complex network of signalling molecules/regulators to maintain a fine control of homeostasis and orchestrate multiple gene expression programs. This function leads to a systematic acquisition and maintenance of neuronal and glial morphological and functional identity. The identification and characterization of these molecules and regulators, the biochemical pathways that they control, as well as their target genes is essential to understanding the regulation of neuronal and glial cell development, function, and pathology. Among these, many recent clues have shown that the neuron-restrictive silencer factor/repressor element 1 (RE1)-silencing transcription factor (NRSF/REST, here called REST) plays a central role under normal conditions, as well as in several brain disorders.

REST is a master transcriptional and post-transcriptional regulator that modulates diverse sets of protein-coding and non-coding genes¹. REST was independently identified by the laboratories of Mandel and Anderson in 1995 that discovered it as a protein expressed in all cells except mature neurons and hence described by both research teams as a repressor of neuronal genes^{2,3}. Subsequent studies of bioinformatics and chromatin immunoprecipitation revealed that over 40% of REST target genes are expressed in the CNS and encode for ion channels, synaptic proteins, neural cell adhesion factors and guidance/migration molecules⁴⁻⁶. Structurally, REST belongs to the Kruppel-type family of zinc finger (ZF) transcription factors, having nine ZF repeats, eight of which located in the N-terminal domain (**Fig. 1**). The multi-zinc protein binds to a conserved 21-23 bp motif that is known as RE-1, also called neuron-restricting silencing element (NRSE) that has been detected in a large number of neuronal genes⁵.

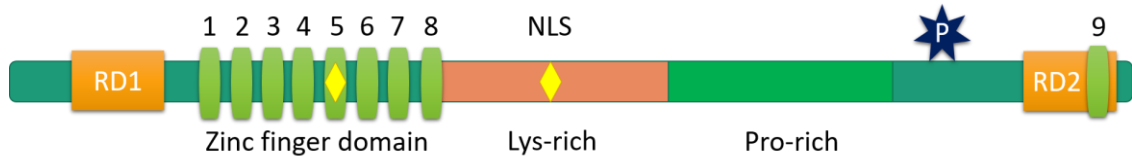


Figure 1. Scheme of the structure of **REST repressor protein**. The REST protein contains a DNA-binding domain of eight ZFs (green cylinders), two repressor domains (RD1 and RD2), lysine- and proline-rich domains, two nuclear localization signals (NLS), a phosphodegron, and a further C-terminal ZF domain (modified from Tang *et al.*, 2021⁷).

Neuronal and glial cells of different brain areas and species express REST⁸. In general, REST is expressed in the whole brain during development, although in adult neurons its expression is strongly decreased^{2,3}. Recent studies described high levels of *REST* mRNA in most non-neuronal tissues, undifferentiated neuronal progenitors, glial cells, endothelial cells and stem cells of areas involved in neurogenesis, such as the dentate gyrus^{2,9-11}. It has been observed that *REST* mRNA is differentially expressed in different types of mature neurons of the adult rat brain where it is involved in the maintenance of neuronal identity by modulation of the expression level of its target genes¹². In the adult rat brain, *REST* mRNA was found in neuron-like cells, including cells of the olfactory system, cerebral cortex, hippocampus, thalamus/hypothalamus, *substantia nigra pars compacta*, pontine nuclei and cerebellum¹². The highest levels were detected in the neurons of the hippocampus, pons/medulla, and midbrain¹². Moreover, it has been observed that rat neurons express REST splice variants¹². All these findings collectively lead to the idea that gene regulation by REST could have different levels of activity depending on the presence of co-factors and its affinity for the target genes¹³. In addition, REST might act only above a threshold concentration to control the expression level of target genes in the various neuronal populations¹².

Although numerous studies have demonstrated that *REST* mRNA levels decrease during brain development, it seems that its expression increases with physiological aging¹⁴. For example, in prefrontal cortex extracts, REST expression was significantly higher in aged individuals compared with young adults¹⁴. These studies suggest that REST could be important as a neuroprotective modulator, through the suppression of genes potentially involved in cell senescence.

3.2. REST structure, isoforms and regulation

The human *REST* gene comprises 24 kb of genomic DNA, composed of (i) three non-coding alternative 5' exons associated with different promoters, (ii) three coding exons (IV-VI) and (iii) an internal exon with alternative splicing, exon N, containing a premature stop codon, between exon V and VI (**Fig. 2**¹⁵). Exon N can give rise to six alternative transcripts^{12,16}. Structural analyses of the human, mouse and rat genomes demonstrated that the structure of *REST* exons and introns is highly conserved across these species.¹⁶

The three 5' exons, designated as "a", "b" and "c", are depicted in Figure 2. *REST* transcripts begin at any of such exons. The transcripts starting at exon "a" are the most abundant (about 80%), whereas the transcripts under control of exons "b" and "c" are less common (19% and 1%, respectively)¹⁵. The presence of three 5' exons suggests that *REST* contains at least three promoters. Promoter "a" is the most active in non-neuronal cells, whereas "b" is more active in neuronal cells, and "c" has weak activity in non-neuronal cells and neural progenitors and none in neuronal cells.¹⁷ Hence, "c" acts as a strong silencer of the other two *REST* promoters¹⁵. The cell-type-specific regulation of *REST* promoters by adjacent or distal enhancers/repressors depends on the action of trans-acting factors binding to these regions¹⁸. In the promoter of *REST*, GC boxes are located before exon "a", which are *cis*-acting transcriptional regulatory elements containing the sequence 5'-GGGCGG-3'. The GC boxes allow the increase of transcription of the *REST* gene by potentiating the promoter activity (**Fig. 2**). The TATA-like sequence and the CAAT box, two non-coding sequences of nucleotides that influence gene transcription, are located upstream of the GC boxes in the promoter. Both elements have a low interspecies conservation and their modulatory effect on human *REST* has not yet been proved¹⁶. Additionally, 2 kb away from exon "a", binding sites for the transcription factors Nanog and Oct4, required to maintain the pluripotency and self-renewal of cells, were identified^{15,18} (**Fig. 2**).

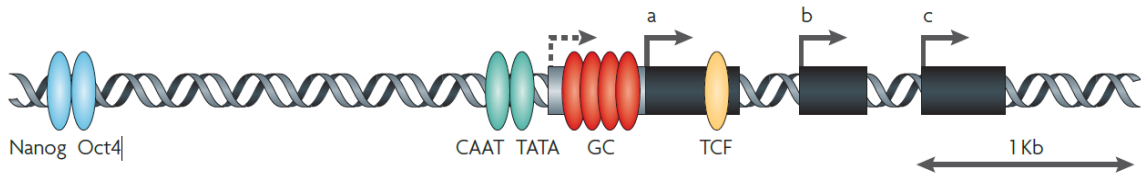


Figure 2. Schematic representation of *REST* promoter region. *REST* transcripts begin at one of three alternatively used 5' exons (indicated by black boxes labeled "a", "b", and "c"). Upstream of exon A TATA and CAAT boxes are located and 2 kb away, binding sites for Nanog and Oct4 (represented as ovals) are found¹⁵.

REST undergoes alternative splicing to produce variants with different capacities to mediate gene repression^{12,19}. In addition to full-length *REST* (isoform 1), the *REST* mRNA splicing variants identified and characterized thus far, include *REST1*, *REST4* (named also *sNRSF*), *REST-N62*, *REST-N4*, and *REST-5FΔ*^{12,19}. The *REST1* transcript contains only exon 1 and encodes for isoform 2²⁰. Three distinct transcripts encode for isoform 3, also called *REST4* or *sNRSF*: (i) the *REST-N62* transcript, generated by insertion of exon N, (ii) the *REST-N4* transcript that has an alternative splicing-mediated addition of 4 bp within exon N, and (iii) the *sNRSF* transcript, identified in human small cell lung cancer, that has a missing C-terminal repressor domain^{16,21} (**Fig.3**). The *REST-5FΔ* resulting from skipping exon V and exon N, encodes for isoform 4.

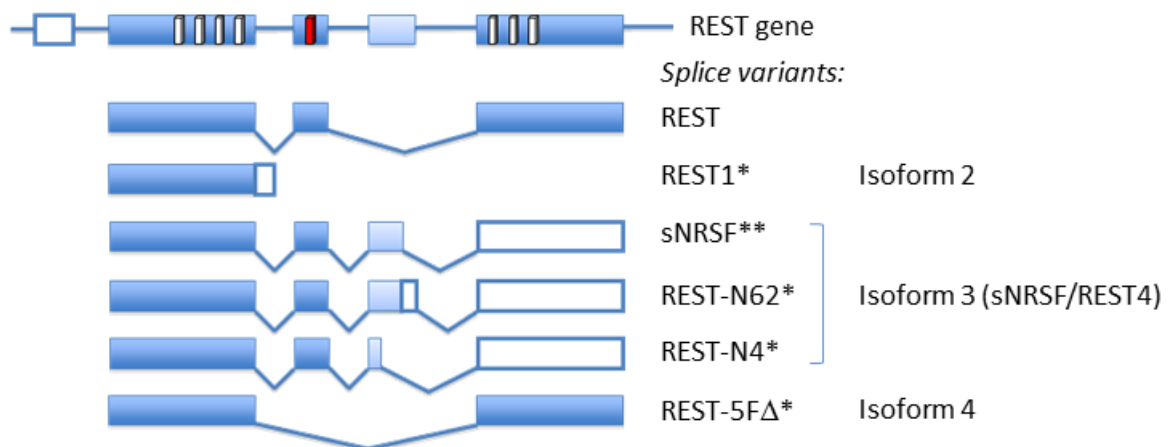


Figure 3. *REST* mRNA and alternative splice variants. The human *REST* gene comprises three alternative non-coding 5' exons (represented by the first white box on the left), three coding exons (dark blue) and the alternative N exon (light blue). The smaller boxes represent the ZFs containing the DNA binding domain (white) and the NLS (red). The six *REST* splicing isoforms are represented (modified by Faronato and Coulson, 2011²¹).

Among the splicing variants, only REST4 and REST5 have been detected in neurons¹², with REST4 being the most investigated one. The biological function of REST4 is not yet fully understood, albeit it is highly conserved in humans, mice and rat¹⁶. REST4 comprises the N-terminal repressor domain and only five ZFs, having an additional exon between exons 3 and 4 that leads to a premature stop codon²². Therefore REST4 lacks the critical domains required for REST-mediated transcriptional silencing of target genes and, in particular, the seventh ZF domain, which is thought to be responsible for binding to DNA²². As a consequence, it should not be able to bind the RE-1 site on DNA. When REST4 was identified in 1998, it was shown to be capable of repressing gene expression even without direct DNA binding¹². In subsequent years, the hypothesis that REST4 operates as a de-repressor has emerged²³. In this context, it was proposed that REST and REST4 interact to form an inactive heterodimer complex capable to prevent the REST binding to the RE-1 sequence, causing de-repression^{23,24}. It was found that *REST* transcript could give REST4 by the action of a splicing regulator, i.e. the neural-specific Ser/Arg repeat-related protein of 100 kDa (nSR100), which directly induces alternative splicing of REST transcripts to produce REST4¹². Consequently, REST has a greatly reduced repressive activity, resulting in the expression of REST targets in neural cells. Blockade of nSR100 expression in the developing mouse brain impairs neurogenesis²⁵. In addition, REST directly silences the expression of nSR100, thereby preventing the expression of REST4 and other neural-specific alternative splicing variants in non-neural cells²⁵. REST isoforms themselves play a key role in the physiological control of REST¹⁹. Nakano and colleagues reported that post-transcriptional inactivation of REST by alternative splicing is essential for the de-repression of many neuronal genes and, in particular, is required for hearing in humans and mice¹⁹.

REST undergoes diffuse, context-dependent alternative splicing, leading to approximately 45 mRNA variants that result in structurally and functionally different isoforms of the REST protein²⁶. REST mutations that affect alternative splicing could impair the proper action of REST, leading to a variety of pathological conditions including different cancer types^{16,20,26}. Chen and Miller in 2013 examined the *REST* pre-mRNA splicing repertoire in 27 patients with kidney, liver and lung cancer and discovered that

all patients presented differential expression of REST splicing variants in both cancer cells and neighboring normal cells²⁶. Moreover, loss of REST and increased splicing of REST4 have been detected in an aggressive subset of breast cancers and have also been correlated with the development of prostate cancers with a neuroendocrine phenotype^{27,28}. In addition, REST-N62 and sNRSF have been found in human neuroblastoma and lung cancers, respectively^{16,22}. These studies in humans have provided insight into several isoforms with context-specific alternative splicing, relating them to different cancer types and providing further insights into the complexity of REST gene regulation.

In contrast to the regulation of REST target genes, little is known concerning the regulation of REST expression. It is possible that *REST* gene expression is defined not at the transcriptional level, but rather by post-transcriptional and/or post-translational modifications in a cell-specific manner. In this context, structural analyses of genomes have shown that the structure of exons and introns is conserved and that there are three 5' exons where promoter "c" acts as a strong silencer of the other two promoters^{15,18} (**Fig. 2**).

The transcriptional regulation of REST involves several positive/negative elements²⁹, including the cAMP response element-binding protein (CREB), the specificity-protein 1 and 3, the dual-specificity tyrosine-phosphorylation-regulated kinase 1A (DYRK1A), the huntingtin-interacting protein 1 protein interactor (HIPPI), the Wnt signaling cascade and microRNAs. The cellular transcription factor CREB half-site, located in the first REST promoter fragment, operates as a positive REST regulator following CREB application²⁹. Also the interaction of specificity protein 1 and 3 are important to fine-tune REST transcription during neuronal differentiation³⁰. DYRK1A affects the local spatial-temporal changes of REST levels, according to its dose and kinase activity³¹. HIPPI binds the promoter of *REST*, increasing its expression in both neuronal and non-neuronal cells³². Moreover, REST is a direct target of the canonical Wnt signaling cascade³³. Wnt and its receptors are expressed in a controlled spatial-temporal fashion during CNS development and are important for the normal growth of neural tissue³³. In fact, the Wnt pathway controls neural stem cell differentiation by direct REST regulation³³.

Finally, *REST* mRNA stability is regulated by several microRNAs such as miR-218 and miR-9/miR-9*³⁴. The first one negatively regulates *REST* expression³⁵, whereas the bifunctional miR-9/miR-9* targets two components of the *REST* complex: miR-9 targets *REST* and miR-9* targets CoREST³⁴. The latter mechanism implies that *REST* can regulate its expression by a double negative feedback involving *REST*-dependent expression of a specific microRNA³⁴.

REST shows different apparent molecular weights due to the presence of post-translational modifications that control *REST* activity²⁴. Among these, the most common *REST* post-translational modification is glycosylation, consisting in a covalent addition of one or more carbohydrates residues (“glycans”), during or after the synthesis of the protein. Although little is known about full-length *REST* glycosylation, experimental data obtained on REST4 indicated that *REST* might be O-glycosylated on the C-terminal region, a post-translation modification that is not required for *REST* DNA-binding activity²⁴.

Phosphorylation/dephosphorylation processes also play a key role in the stability/degradation of the *REST* protein^{36–38}. *REST* contains two nearby but distinct degron motifs that serve as binding sites, one containing E1009 and S1013³⁷ and the other containing S1024, S1027, and S1030³⁶. Phosphorylation of these serine residues by casein kinase 1 (CK1) facilitates the binding to a chaperone protein (β -transducin repeat-containing E3 ubiquitin protein ligase; β TrCP) that transports *REST* to the proteasome for degradation³⁹. These data support the important role of phosphorylation in the regulation of the stability and half-life of the *REST* protein across a conserved phosphodegron³⁶. A number of kinases involved in tuning *REST* levels through phosphorylation have been identified over time^{39,40}. CK1, mentioned earlier, has been found as a major upstream factor regulating *REST* expression through phosphorylation of two neighboring phosphodegrons³⁹. Various phosphodegrons are present within the *REST* protein sequence and different kinases can phosphorylate the same residue. For example, polo-like kinase 1 directly phosphorylates the *REST* phosphodegron acting a potent regulator of *REST* stability⁴⁰. Nesti and colleagues identified S861/S864 as a target of phosphorylation by extracellular signal-regulated

kinase 1 and 2 (Erk 1/2)⁴¹. Furthermore, the phosphodegron can be targeted by protein phosphatases⁴⁰. The C-terminal domain small phosphatase 1 controls the stability of the REST complex through dephosphorylation of the same site (S861/S864) at the C-terminus of REST, protecting REST from degradation^{41,42}.

The REST sequence has a specific consensus site for a Herpesvirus-associated ubiquitin-specific protease (HAUSP), which acts as a de-ubiquitinase, counterbalancing the activity of β TrCP⁴³. Thus, even HAUSP plays a key role in the regulation of REST expression during neural differentiation. The downregulation of HAUSP, together with the upregulation of β TrCP in neuronal progenitors, leads to a negative modulation of REST protein levels, enabling neuronal differentiation⁴³. Several pieces of evidence have been recently collected showing that the dysregulation of REST phosphorylation leads to several brain pathologies^{40,44}. For example, the phosphorylation-mediated degradation of REST is critical in the progression of triple-negative breast cancer, and breakdown of this mechanism impairs cancer transformation, progression and formation of metastasis⁴⁰. REST phosphorylation has also been related to the acquisition of neuroendocrine phenotype in prostate cancer. This evidence has highlighted the impact of phosphorylation on REST stability under physiological and pathological conditions.

REST binds the conserved 21-23 bp RE-1 motif also known as NRSE, distributed in the target genes' regulatory regions^{2,10}. RE-1 has been found in more than 1,000 genes involved in fundamental neuronal specific traits, including voltage-gated ion channels and neurotransmitter receptors, synaptic vesicle proteins and neurotransmitter synthesis⁶. Moreover, *in silico* analysis identified nearly 2000 putative REST targets in the mammalian genome, in both coding and non-coding genes^{6,45}.

REST performs active gene repression by its central DNA-binding domain consisting of C₂H₂ ZFs, small DNA recognition units that are usually organized in tandem, and by two repressor domains that reside at the N- and C-terminals⁴⁶⁻⁴⁸. Thanks to its domain organization, REST acts as a scaffold recruiting multiple co-repressors, such as mSin3 and CoREST at the N- and C-terminal, respectively^{13,49,50}. These two important co-repressors recruit additional factors/enzymes involved in chromatin remodeling and histone modification. They are controlled at multiple levels ensuring a reliable repression of

their target genes^{13,50}. mSin3 interacts with several histone deacetylases (HDACs) and with the methylated CpG-binding protein, MeCP2^{13,50}. CoREST action involves histone methyltransferases, HDACs and chromatin remodeling complexes, such as Brg1, G9a and others¹⁵ (**Fig. 4**). The chromatin remodeling complexes change the chromatin state by adding factors for gene repression, as H3K9me2, and/or removing markers for gene activation, as H3K4, thus producing a more condensed and less accessible state of chromatin⁵¹. Among these factors the Brg1 enzyme, recruited by the C-terminal repressor domain, stabilizes the interaction between REST and RE-1 sites using its ATP-dependent remodeling activity⁵². Once associated with chromatin, REST mediates repression through histone deacetylase, histone demethylase and histone methylase activities^{53,54}. Furthermore, REST also plays a direct role in transcriptional gene repression interacting with both TATA-binding protein (TBP) and small C-terminal domain phosphatases, two proteins involved in the transcription machinery^{55,56}. In particular, the interaction between REST and TBP inhibits the formation of the transcription pre-initiation complex⁵⁵. The small C-terminal domain phosphatase is a transcriptional regulator that silences neuronal genes and is localized by REST to the C-terminal domain of RNA polymerase II, where induces polymerase deactivation by dephosphorylation^{55,56}.

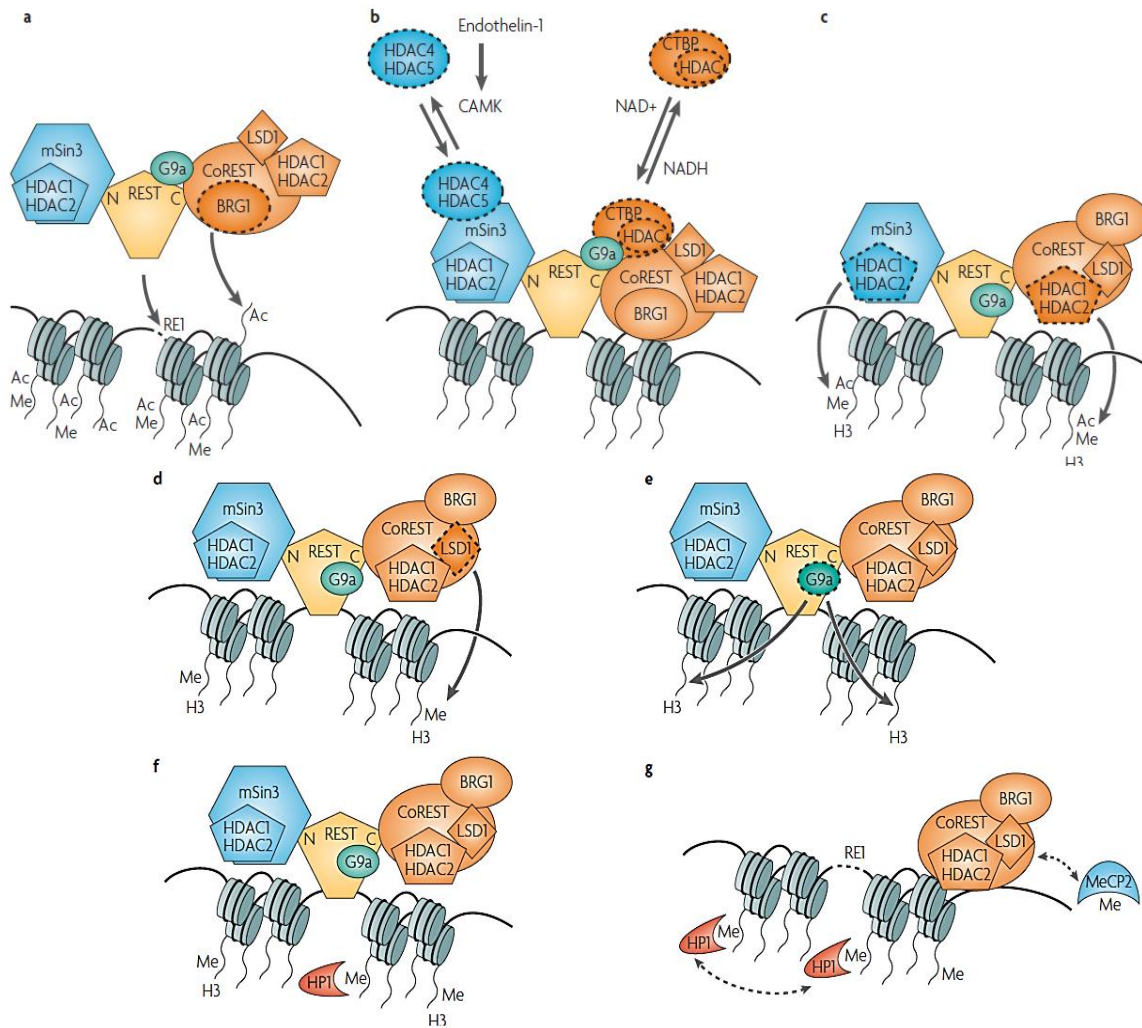


Figure 4. Schematic representation of long-term gene silencing mediated by REST. After REST binding to the RE-1 motif, the corepressors mSin3 and CoREST bind the N- and C-terminals of the protein, respectively. Both corepressors recruit HDACs, whereas CoREST at the same time recruits other enzymes such as G9a, LSD1, and BGR1. After several steps, long-term silencing of target genes may be determined by the interactions of recruited HP1 proteins to adjacent nucleosomes, which generate the compact chromatin state¹⁵.

According to its expression in different tissues, REST mediates both transient and long-term silencing, either by remaining associated with RE-1 sites itself or by leaving CoREST attached after its dissociation^{13,49}, thus representing an efficient mechanism of gene modulation across multiple RE-1 sites. The REST-CoREST complex triggers different mechanisms of epigenetic silencing depending on whether it is required to inactivate neuronal genes in terminally differentiated non-neuronal cells or to inhibit neuronal genes in embryonic stem and progenitor cells⁵⁷. In cells where long-term silencing of

neuronal genes is required, the REST-CoREST complex needs to enroll chromatin modifiers, such as HP1 proteins, which are recruited to adjacent nucleosomes, as shown in several studies (**Fig. 4d**)^{54,57,58}. In contrast, in stem cells, neuronal genes undergo epigenetic modifications that result in an inactive, but reversible, chromatin state that is available for subsequent activation^{13,57}.

3.3. REST and CNS cells

A basic feature in vertebrates concerning the CNS development is that the diverse cell types inside it are generated sequentially: first neurons, followed by oligodendrocytes and then astrocytes^{59,60}. At the beginning of neural development, during the expansion phase, neural stem cells (NSCs) undergo limited amplification, mainly symmetric divisions, producing a first pool of cortical progenitors that generates apical radial glial cells (RGCs). During the neurogenic phase, most apical RGCs divide asymmetrically to generate nascent projection neurons, either directly or indirectly through intermediate progenitor cells or basal RGCs⁶¹⁻⁶⁴. At the end of neurogenesis, RGCs become gliogenic and cortical progenitors revert to symmetric divisions generating oligodendrocytes and astrocytes⁶⁵.

In general, individual cell categories are defined by the expression of a unique repertoire of coding and non-coding transcripts⁶⁶⁻⁶⁸. A complex set of extracellular spatial and temporal factors determines the fate of stem and progenitor cells inside the nervous system. These factors induce the sequential activation and/or inactivation of selective classes of genes and combinations of transcription factors, leading to functionally different cells and determining neuronal and glial fate specification⁶⁶⁻⁶⁸. The acquisition and maintenance of neuronal and glial identity are epigenetically driven through the regulation of neural genes by transcriptional repressors and corepressors⁵.

REST is involved in several key biological processes, such as the determination of neuron-specific gene expression after differentiation, and the control of the pathways that underlie neuronal gene expression during early embryogenesis. Indeed, the loss of REST is critical for the acquisition of the neuronal phenotype, promoting both context-

dependent gene repression/activation, gene activation and long-term gene silencing^{2,3}. In the case of gliogenesis, however, REST represses the expression of numerous neural-specific genes in neural progenitor cells (NPCs)^{1,69-71}. The importance of the REST function was demonstrated by studies using REST-KO models. The mouse REST-full KO embryos have a normal development until embryonic day 9.5, but after this stage, they undergo cellular disorganization and widespread apoptotic cell death producing an insufficient CNS growth and malformations of development, leading to death at embryonic day 11.5⁷².

Together with its corepressors, REST inhibits the expression of numerous neural-specific genes in embryonic stem cells (ESCs), in NPCs and in terminally differentiated non-neural tissues⁷³. REST is expressed in neural progenitors, where it performs epigenetic remodeling to repress a wide array of neural-specific genes, including genes involved in the formation and maintenance of synaptic contacts, axon guidance, synaptic plasticity and structural remodeling, synaptic vesicle proteins, ion channels, receptors and transporters^{4,13,15}. In this context, the loss of REST during the final stages of neuronal differentiation is critical for the acquisition of the neuronal phenotype, because REST reduction subtends the selective upregulation of neural-specific genes^{6,13,74}. Neuron progenitors differentiate into mature neurons by a mechanism that allows the dissociation of the REST repressor complex from the RE-1 site of neuronal genes¹³. At the end, when mature neurons are formed, REST protein reaches undetectable levels of expression^{13,43}.

Several studies have started to identify the specific components of REST regulatory machinery during development⁷⁵. We have described above that the low expression of REST allows the transcription of a large panel of genes, which are necessary for the acquisition of the unique phenotype of neuronal cells^{13,76}. By this, REST plays a role in controlling neurogenesis in the adult hippocampus, in the maintenance of a pool of adult neural stem cell and in the control of stage-specific differentiation by the coordinated regulation of neuronal, ribosome biogenesis and proliferation genes^{11,77}. However, recent studies suggest that REST function inside the brain is also associated with the regional glial lineage specification and differentiation. In glial cells, REST supports the

expression/repression of many genes involved in the lineage differentiation, maturation, preservation of the specific phenotype, as well as for their transformations under several brain diseases^{1,57}. In this context, numerous studies have well characterized the developmental stage-specific profiles for REST and CoREST target genes in glial cells^{1,75,78}.

During neural development, the transition from neurogenesis to gliogenesis implies a return to symmetric division of progenitors and a sequential differentiation in oligodendrocytes and astrocytes⁷⁹. REST is a critical factor driving significant changes in the signaling environment of progenitor NSCs^{57,73}. REST is important to maintain and regulate general glial functions, as a function of the context and the developmental stage^{13,75,80}. REST supports oligodendrocyte specification and maturation by targeting genes involved in their developmental pathways, such as sonic hedgehog, platelet-derived growth factor and fibroblast growth factor¹. The morphogen sonic hedgehog is secreted by NSCs and promotes oligodendrogenesis by inducing the expression of Olig1 and Olig2, two essential determinants of oligodendrocytic fate. PDGF promotes the growth of oligodendrocytic glial progenitor cells and allows their early differentiation. Fibroblast growth factor signaling has also been shown to promote oligodendrogenesis at high concentrations in progenitor cultures^{1,79}.

REST has also been shown to stimulate progenitor specification to astroglial fate by targeting key genes, encoding for Notch, bone morphogenetic protein (BMP), Janus kinase (JAK) and signal transducer and activator of transcription (STAT)^{1,80-82}. Many studies have reported the importance of Notch signaling in astrocyte formation, since it is a pro-proliferation factor critical for embryonic specification of NPCs^{79,81,83,84}. BMP signaling is strictly involved in astroglialogenesis^{80,85} and particularly the subtype 2 (BMP2) that up-regulates and supports REST transcription during astrocytic differentiation of NPCs, by the downstream protein Smad. This transcription factor binds to Smad-binding elements in the regulatory region RE-1 of the *REST* gene⁸⁰. BMP and Notch, which promote astrogenesis, require pre-activation of the JAK-STAT pathway^{79,82,86}. It has been postulated that the JAK-STAT pathway is fully active in early neural progenitors working as regulator of mechanisms that promote astrocyte development and, at the same time,

deter neuronal differentiation in the embryonic cortex⁸⁶. In this sense, REST is involved in mechanisms that maintain a finest ratio between neurons and glial cells during differentiation. REST is also critical to ensure a constant self-renewal of HSCs and NPCs, because when it is reduced to low levels for neuronal differentiation, its expression in cells generated from NPCs designated to the astroglialogenesis remains unaffected⁸⁷.

As mentioned above, when astrocytes are differentiated, REST is normally associated with typical neuronal genes containing the RE-1 binding site⁷⁵. Several studies observed that when REST repressive function was suppressed in astrocytes, the neuronal genes were de-repressed, confirming that REST prevents neuronal phenotype development in astrocytic cells^{78,87}. Indeed, Abrajano and colleagues described that REST is involved in the recruitment of epigenetic and regulatory co-factors that control glial gene expression⁷⁵. REST together with the cofactor CoREST, targets a large number of genes encoding epigenetic factors, such as DNA methylation factors, DNA methyltransferases and methyl-CpG binding domain proteins, histone modifying enzymes, deacetylases/demethylases and switch/sucrose non-fermentable chromatin-remodeling complex¹. These gene panels demonstrate that REST, together with corepressors, plays key roles in encoding glial cell identity and function^{1,75}.

Furthermore, REST is critical in glial responses against neuroinflammatory conditions and pathological degeneration, when the nervous tissue environment must change rapidly^{88,89}. In rat NPC cultures, signaling from inflamed tissue leads to expression of REST⁷⁸. In turn, it responds to these abnormal stimuli by reducing their neurogenic capacity and promoting gliogenesis, resulting determinant in the NPC-specific response to innate immunity under pathophysiological conditions⁷⁸.

Immunocytochemistry studies on human cortex show that individual astrocytes have strong variability in REST expression⁹. In fact, REST astrocytic expression varies enormously, from low levels similar to those observed in neurons, to very high levels as those observed in microglia⁹. The extreme heterogeneity of astrocytes in terms of shape, size, protein and receptor expression is well-known, but at the moment has not been totally explained^{90,91}. The described variable levels of REST could play a central role in this high heterogeneity.

3.4. REST and brain disorders

The role of REST in brain disorders has been discussed in several recent articles^{8,92}. REST is a critical gene regulator, by direct and indirect mechanisms, in several pathological processes of CNS. As of now, numerous pieces of evidence indicate that REST is also an important transcriptional regulator in mature neurons characterized by a high plasticity and rearrangement. In this context, REST plays a key role in the regulation of genes important for synaptic plasticity and homeostasis⁹³. Moreover, REST is also involved in normal aging mediating neuroprotective pathways by the negative modulation of genes involved in neuronal death⁶⁴. Thus, REST activation levels inside CNS control the dualism of neuroprotection-neurodegeneration in the aging brain.

Dysregulation of REST is implicated in several neurodegenerative disorders, including Alzheimer's (AD), Parkinson's (PD) and Huntington's diseases (HD) (for a recent review see⁸). The final action of REST on its target genes depends on several distinct elements, including the nature of target itself, the cell environment and the function of REST effectors. Hence, the perturbation of REST function may be due to the impairment of several pathways, which may result in a wide spectrum of disorders⁷⁴.

Different central diseases are linked to REST dysfunction in diverse brain cells. For example, a negative modulation of REST is associated to Schizophrenia (SZ)⁹⁴. The downregulation of REST in a neuronal cell line leads a deregulation of SMARCA2 gene, which encodes BRM subunit in the switch/sucrose non-fermentable chromatin-remodeling complex, which in turn produces an alteration of dendritic spine morphology, an intermediate phenotype of SZ⁹⁴.

While, during normal brain aging, REST increments have a neuroprotective role⁷⁴, in AD REST is markedly downregulated in selected vulnerable neuronal populations¹⁴. In particular, REST loses its normal nuclear localization and co-localizes with amyloid- β in light chain 3-positive autophagosomes along with misfolded pathological proteins¹⁴. This phenomenon leads to a depression of genes that promote cell death and the development of hallmarks of AD pathology, and at the same time, positively modulates

the expression of stress response genes that delay the disease progression¹⁴. In HD patients, opposite to what happens in AD patients, an abnormal REST accumulation in the nucleus of selectively vulnerable striatal neurons is observed, triggering the pathological events that underlie the HD⁹⁵. Mutant huntingtin, a protein essential for normal development before birth, impaired the interaction between REST nuclear localization complex and huntingtin-associated protein-1, thus altering the appropriate nuclear localization of REST^{95,96}.

The role of REST in PD has been recently investigated. When the human dopaminergic neural cell line, named SH-SY5Y, was treated with 1-methyl-4-phenylpyridinium ion (MPP+), a potent inhibitor of dopamine neurons known to produce a PD-like disease, an increase in REST rising that produced a general protective effect was observed⁹⁷. The same REST-dependent effect was described also *in vivo*, when nigrostriatal dopaminergic neurons were exposed to MPP+ and REST levels were increased^{98,99}.

REST expression is also upregulated during stroke¹⁰⁰. Normally, serine/threonine CK1 acts as an upstream signal regulating the stability of REST by phosphorylating REST serine residues and allowing the recognition and the binding of REST by E3 β -TrCP ligase³⁹. It has been shown that in differentiated neurons, global ischemia reduces CK1 and E3 β -TrCP ligase levels, resulting in an increase of REST expression and, subsequently, a down-regulation of REST pro-survival target genes¹⁰⁰. Moreover, molecular and genetic approaches have shown that *REST* mRNA and protein levels are consistently upregulated in selectively sensitive mature hippocampal neurons after ischemic injury. These increases correlate with the reduction of histone acetylation and gene silencing of the AMPA receptor GluR2 subunit¹⁰¹. Calderone and colleagues reproduced an *in vitro* model of ischemia consisting in oxygen-glucose deprivation of rat hippocampal slices, to study the role of REST during ischemia¹⁰¹. They observed that when REST was selectively downregulated by antisense oligodeoxynucleotides, the levels of GluA2 were also downregulated, and this negative modulation significantly lowered neuronal death¹⁰¹. These findings strongly suggest that REST plays a key role in the intracellular signaling pathways mediating cell death after insults¹⁰¹.

The expression of REST is upregulated in neuropathic pain¹⁰², a state where pain thresholds to common stimuli are decreased and analgesic effects are attenuated¹⁰³. The repressive effect of REST may be involved in downregulation of ion channels and analgesia genes that cause neuropathic pain. Indeed, it was found that two subtypes of voltage-gated sodium (Nav) and potassium channels (Kv), Nav2.1 and Kv4.3¹⁰⁴ respectively, are downregulated in dorsal root ganglia after injury, likely lowering the pain turn-on threshold¹⁰⁵.

As observed in neurodegenerative diseases, a dysregulation of REST levels was also observed in diverse brain tumors. Under these conditions, REST was down- or up-regulated in a tumor-specific manner⁸. Blom and colleagues, in a study encompassing 161 nervous system tumors, found no activating or inactivating mutations regulating the REST gene, suggesting that its dysregulation in the different tumor forms depends on external factors.¹⁰⁶ The downregulation of REST expression has been detected in several neuroblastoma cell lines, such as in NS20Y, NIE11, and in NIH3T3 cells¹⁰⁷. In contrast, in medulloblastoma cells and associated tumors, REST showed high levels of expression¹⁰⁸. In human glioblastoma multiforme (GBM), REST is highly expressed in tumorigenic-competent self-renewing GBM cells, and its knockdown strongly reduces their *in vitro* self-renewal and *in vivo* tumorigenic capacity, indicating that REST contributes to GBM maintenance¹⁰⁹.

The dysregulation of REST and the repression of its target genes are also implicated in the pathogenesis of several forms of epilepsy¹¹⁰. Under physiological conditions, REST expression is low in the adult hippocampus, but its levels increase after seizures^{110–112}. The question concerning the physio-pathological significance of this increase is not yet completely understood^{110,113}. A REST-dependent regulatory region has been identified in the gene encoding for the hyperpolarization-activated and cyclic nucleotide-gated channel (HCN1) that is persistently down-regulated after a proepileptogenic insult^{110,114}. The blockade of REST-mediated *HCN1* gene repression in a mouse model of temporal lobe epilepsy significantly suppressed the development of seizures, suggesting its important role in epilepsy¹¹¹. Successive investigations found that gene repression resulting from increased REST was not limited to HCN1 genes, but also extended to

genes encoding other channels and signaling proteins^{99,111}. The use of specific decoy oligonucleotides to impair REST binding to the RE-1 DNA sequence of its target genes elicited a reduction in the initial seizure pattern^{99,111}.

A further link between REST dysfunction and epilepsy is caused by mutation of the REST-interacting LIM domain protein (RILP), which normally binds and keeps REST in the cytoplasm, thus inhibiting and gene silencing activity¹¹⁵. A mutation in RILP causes mislocalization of REST in the progressive myoclonic epilepsy-ataxia syndrome¹¹⁶. In a study concerning this syndrome, several families were found to have a mutation (R104Q) in the RILP translocator¹¹⁶. When this mutation was cloned *in vitro*, it caused a block of the normal REST translocation from the nucleus to cytosol¹¹⁶. These results suggest that tissues bearing mutant RILP have constitutively active REST, which inappropriately downregulates its target genes¹¹⁶. The progressive myoclonic epilepsy - ataxia syndrome may occur when brain regions expressing mutant RILP display an altered expression of REST target genes, resulting in dysregulation of neurotransmission factors and hyperexcitability^{105,116}.

The increasing knowledge in REST physiology and pathology is promising for future developments in new therapies for brain diseases^{92,99}. An interesting approach in this sense, has been developed for HD⁹⁹. As previously mentioned, one of the mechanisms contributing to the pathogenesis of HD is the accumulation of REST in neuronal nuclei resulting in an increased repression of targets⁹⁵. Two pharmacological approaches able to reduce REST complex formation that pathologically accumulates in the nucleus of HD cells were developed and subsequently tested in various cell lines and *in vivo*. The first drug called quinolone-like 91 decreased the nuclear accumulation of mSin3b, the corepressor of the N-terminal REST operating complex⁹⁵. The second compound, X5050, decreased REST levels in cells by stimulating its breakdown¹¹⁷. After application of these drugs, several REST target genes increased⁹⁵.

In several pain models, drugs against REST have been developed and tested. Notably, two peptidomimetics that compete with the N-terminus of REST, called mS-11 and C737, have been formulated to inhibit mSin3 binding and mitigate gene repression^{118,119}. In a mouse model of sciatic nerve injury, mS-11 administration restored the threshold for

pain stimulation of C-fibers to basal levels¹¹⁸. C737 injection treated weight loss induced by cold stress and acted as a therapeutic protector¹¹⁹.

The most concrete therapeutic attempts regarding REST have been developed in different cancer therapies⁹². In the therapy of medulloblastoma, the interaction between REST and its co-repressor mSin3 is targeted by some drugs that prevent their binding. However, these drugs are still under investigation^{92,120}. Other REST-targeted anticancer drugs have an epigenetic function, affecting the viability of medulloblastoma cells¹²¹. Moreover, other drugs act binding enzymes such as LSD1¹²² and deubiquitinase USP37, which are considered as anti-medulloblastoma factors¹²³. Moreover, when REST transcription was blocked in glioblastoma, a block of tumor progression was observed⁹². Another therapeutic approach against breast cancer is based on demethylation of REST¹²⁴.

Various types of epilepsy are treated with valproic acid¹²⁵. The precise mechanism of action of this drug is unclear. Its pharmacological effects seem to involve the control of GABA levels, the negative modulation of Nav channels and the inhibition of histone deacetylase¹²⁵. In this context, valproic acid is a high-affinity inhibitor of histone deacetylase but it is not specific for forms 1 and 2 of the enzyme, which are critical for transcriptional repression by REST. Valproic acid is also known to act on sixteen other forms of the enzyme, so its mechanism of action remains under investigation to develop therapeutics specific for the first class deacetylases¹²⁵. Such drugs could be useful in treatments for neurodegenerative disorders and learning and memory defects^{99,126}.

Potentially all the above-mentioned therapies, either being used to treat brain disorders or being investigational, have the common goal of modulating REST activity in neuronal and non-neuronal cells.

3.5. Astrocytes

Glial cells surround and envelop neuronal cell bodies as well as blood vessels, axons and synapses throughout the nervous system¹²⁷⁻¹³⁰. Nervous system glial cells are classified based on morphology, function and location inside nervous system as microglia,

Schwann cells, oligodendrocytes and astrocytes¹³¹. Microglia keep the brain under surveillance for damage or infection¹³². Schwann cells and oligodendrocytes wrap myelin around axons in peripheral nervous system and in CNS, respectively¹³³.

Astrocytes are the most abundant glial cells in the CNS and play a fundamental role in the maintenance of homeostasis and neuronal physiology^{134–136}. Astrocytes, in addition to define the microarchitecture of the brain and have trophic support functions, play important roles in the maintaining the functional integrity of the whole brain. It is known that a single astrocyte connects about 10^5 neurons, forming the so-called “tripartite synapses”, consisting of presynaptic terminal, postsynaptic side and the peri-synaptic feet of astrocytes^{137,138}. By this architecture, astrocytes are actively involved in the regulation of synaptic function and information processing¹³⁹. They directly support neurons in terms of energy and metabolic precursors used to synthesize neurotransmitters. By this mechanism, they provide a discrete and precise encoding of synaptic signals and neurotransmission inside the neuronal network.

Although they are not neurons, astrocytes display exocytotic release of gliotransmitters¹³⁷ that occurs primarily at tripartite synapses^{140,141}. They secrete factors that regulate essential processes such as the number of synapses, postsynaptic activity through up-regulation of postsynaptic receptor expression and the enhancement of the release probability at the presynaptic level^{142–146}.

Astrocytes are central elements in the control of extracellular water homeostasis inside the nervous system^{147,148}. To do this, they express a particular type of channel protein called aquaporin (AQP) on the membrane surface^{149,150}. AQPs are a family of small membrane channels that facilitate bidirectional water transport in response to osmotic gradients⁹⁷. Aquaporin type 4 (AQP4) is a member of this family and is the main water channel in the brain and spinal cord^{150,152}. Highly expressed in astrocytes, AQP4 are localized to specialized membrane domains on astrocytic endfeet, and are close to both blood vessels and astrocyte compartments that encompass glutamatergic synapses^{150,152}. The central role of AQP4 in astrocytic function was demonstrated in 1997 when AQP4-KO mice were generated¹⁵³. AQP4 play a central role in the modulation of extracellular space diffusion¹⁵⁴, in synaptic plasticity and memory formation¹⁵⁵, as

well as in K⁺ buffering¹⁵⁶ cooperating with other membrane proteins such as K⁺ channels¹⁵⁰.

Astrocytes also contribute to the homeostatic control of blood supply to the brain by their functional interactions with the vascular system, forming a closely associated structure with blood vessels¹⁵⁷. The functional coupling between astrocytes and endothelial cells is essential to set-up the blood-brain barrier¹⁵⁷. The blood-brain barrier is a biochemical barrier that regulates the passage of compounds between the circulating blood and the brain¹⁵⁸, composed of endothelial cells, astrocytes and pericytes. Thanks to the close interaction with the vascular system, astrocytes control local blood flow using their processes and by releasing several autacoids including prostaglandins, nitric oxide and arachidonic acid^{159,160}. In this way, they are actively involved in the fine control of energetic requirements, controlling regional increases in blood flow, that in turn regulates the concentration of oxygen and glucose in the brain regions^{159,160}.

Several astrocytic functions that underlie brain homeostasis are due to intracellular calcium concentration (Ca²⁺_{in}) fluctuations inside the astroglial syncytium¹⁶¹. Several factors modulate the increase Ca²⁺_{in} in astrocytes, most of which are released during neuronal activity. Among these, glutamate, γ -aminobutyric acid (GABA) and ATP are the most important^{162–164}. In particular ATP, released during synaptic activity, acts through the activation of G-protein-coupled receptors on astrocytic membrane surface. This in turn activates the inositol-3-phosphate (IP₃) pathway, leading to IP₃ receptor activation and Ca²⁺ release from the endoplasmic reticulum (**Fig. 5**)^{161,165}.

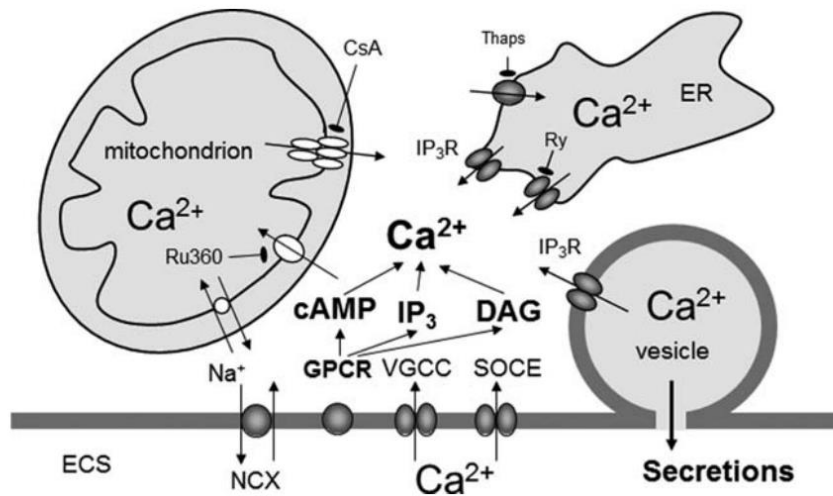


Figure 5. Ca^{2+} sources for vesicle-based secretion in astrocytes¹⁶⁶.

The increase of Ca^{2+}_{in} propagates along astrocyte processes through gap-junctions between adjacent glial cells, allowing Ca^{2+} waves to propagate over long distances inside the syncytium¹⁶⁷. The consequence of the increase of Ca^{2+}_{in} in astrocytes is the release of gliotransmitters, such as ATP, glutamate, D-serine and GABA^{141,167}. In addition, the release of several vasoactive factors at vascular endings are also regulated by Ca^{2+} waves. Among these, arachidonic acid, prostaglandins, 20-hydroxyeicosatetraenoic acid, epoxyeicosatrienoic acids, phospholipase C and adenosine have been recently well characterized¹⁵⁹. Several studies have reported that the malfunction of the Ca^{2+} signaling mechanism in astrocytes could be an important molecular determinant in several neurological disorders, including epilepsy, AD and HD^{140,168,169}.

Thanks to the discovery of Ca^{2+} channel expression on astroglial membrane, as well as of other ion channels such as K^{+} channels, astrocytes are now seen as fundamental functional actors inside CNS^{128,170}. In this context, astrocytes are fundamental cells in the homeostatic control of neuronal network also through the so called spatial K^{+} buffering¹⁷¹. This process is functionally coupled to another important astrocytic mechanism of control, glutamate buffering¹⁷². The K^{+} and glutamate buffering work together to avoid hyperexcitation of the neuronal network and the fine tuning of the whole CNS functionality¹⁷².

3.6. Potassium and glutamate homeostasis in the CNS

During sustained neuronal activity, the extracellular K^+ concentration is temporarily raised causing depolarization of neighboring neurons, which if uncorrected would produce network hyperexcitability¹⁷³. K^+ buffering is performed rapidly by astroglial cells primarily by the Kir channels¹⁷¹.

Kir channels are classified into seven different subfamilies (Kir1.0-Kir7.0) that include more than twenty members, depending on their electrophysiological and molecular properties^{174,175}. At the astrocytic level, K^+ buffering is mainly mediated by the Kir channels containing the 4.1 subunit (Kir4.1), encoded by the *KCNJ10* gene¹⁷⁶. Astrocytes from Kir4.1-KO mice have a dramatic reduction of Kir currents, cellular depolarization and reduced K^+ buffering capacity¹⁷⁷. Other than the homomeric Kir4.1 channel, heteromeric Kir channels have been described, formed by Kir4.1/Kir5.1 and Kir4.1/2.1 subunits, albeit much less expressed¹⁷⁸. The expression of Kir4.1 in both brain and spinal cord astrocytes increases during development^{171,179,180}. Under physiological conditions, and normal neuronal activity, astrocytes remove the excess of K^+ from the extracellular space through Kir4.1 channels, redistributing it through the astrocytic syncytium to distant sites where extracellular K^+ concentration (K^+_{ext}) is low¹⁸¹. Because Kir4.1 channels show both weakly rectifying properties and lack of intrinsic voltage-dependence, they enable both K^+ influx and efflux by electrochemical gradient¹⁷⁵. In addition, they are actively involved in the maintenance of the negative membrane potential of astroglial cell¹⁷⁵. The control of negative resting membrane potential is crucial for the regulation of Na^+ -dependent glutamate uptake¹⁸². Because Kir4.1 channels are strictly voltage- and K^+_{ext} -dependent, K^+ uptake occurs in the hyperpolarized astrocyte when K^+_{ext} is high. Conversely, K^+ release occurs when the astrocyte is depolarized and K^+_{ext} is low¹⁷⁵. The K^+ released during neuronal activity will be absorbed by astrocytes with strong negative membrane potential and redistributed through gap junctions to astrocytes with weakly negative membrane potential¹⁸³. These astrocytes in turn will have a strong tendency to release K^+ where its concentration is low, such as around blood vessels¹⁷⁵.

Several studies have evidenced that some brain diseases have a common denominator in the deficiency of astrocyte Kir4.1-mediated currents^{184–189}. In this context, reduced expression of Kir4.1 has been found in mouse models of neurodegenerative diseases characterized by impaired K⁺ homeostasis, such as HD and amyotrophic lateral sclerosis (ALS)^{185,187,188}. HD mouse models have been associated with a decreased functional expression of Kir4.1 channels, resulting in high extracellular striatal K⁺ *in vivo*, thereby enhancing neuron excitability. Rescuing the loss of astrocytic Kir4.1 channels resulted in an improvement of various symptoms associated with HD in mouse models. These findings indicate the astrocytic Kir4.1 as a potential cellular target for therapeutic strategies in HD¹⁶⁴.

A number of studies have established that Kir4.1 channels play a role in the onset and progression of ALS^{185,187,190}. In glial cells of the spinal cord of the superoxide dismutase 1 (SOD1)^{G93A} mouse model, a mutation that causes ALS, a progressive loss of Kir4.1 was revealed¹⁸⁵. Since exposure of motor neuron to high extracellular K⁺ concentrations resulted in cell death, it is likely that the loss of Kir4.1 impairs perineural K⁺ homeostasis and contributes to motor neuron degeneration through an excitotoxic mechanism in the SOD1^{G93A} mutant mice¹⁸⁵. A subsequent study has also revealed impaired expression of Kir4.1 in the brainstem and cortex of the SOD1^{G93A} ALS rat¹⁸⁷. Patch-clamp recordings on cultured cortical SOD1^{G93A} ALS astrocytes displayed a significantly reduced Kir4.1 current density, at different extracellular K⁺ concentrations¹⁸⁷.

Downregulation of Kir4.1 channel expression has been reported in reactive astrocytes a few days after global cerebral ischemia¹⁸⁶. Using the patch-clamp technique, the membrane properties of hippocampal astrocytes were studied at various intervals after ischemia (from 2 h to 5 weeks). Astrocytes progressively depolarized starting 3 days after ischemia, which coincided with Kir4.1 down-regulation in reactive astrocytes¹⁸⁶.

Mutations in *KCNJ10*, the gene encoding the Kir4.1 subunits, have been associated with seizure susceptibility in both mice and humans^{184,189}. In the mouse gene, a single nucleotide polymorphism (Thr262Ser) appears to be involved in seizure susceptibility control¹⁸⁹. In the human gene, a single nucleotide polymorphism leads to an Arg271Cys substitution in *KCNJ10* that is a risk factor for epilepsy¹⁸⁴. Recently, rare mutations in the

Kir4.1 channel subunits have been reported to strongly impair channel conductance, leading to severe clinical syndromes, including epilepsy^{191,192}.

As evidenced by the genetic ablation of Kir4.1 in astrocytes, impairment of extracellular K⁺ buffering is functionally coupled to the alteration of astroglial glutamate uptake^{182,193}. The expression of Kir4.1 sets the resting membrane potential near equilibrium potential for K⁺ (E_K), typically around -85 mV, that ensures the maximal glutamate transport rates through glial specific transporters, which work more efficiently at negative potentials¹⁷¹. By this mechanism, astrocytes preserve neuronal integrity by removing the excess glutamate resulting from synaptic transmission. Thanks to this buffering, astrocytes prevent a general excitotoxicity associated with the excessive activation of glutamate receptors and the activation of oxidative-dependent stress pathways^{194–196}. The excess of glutamate is collected by specific astrocyte transporters known as excitatory amino acid transporters (EAAT)^{197,198}. Once inside astrocytes, glutamate is converted to α -ketoglutarate by glutamate dehydrogenase or by a transaminase reaction, and then conveyed into the astrocytic tricarboxylic acid (TCA) cycle¹⁷³. Alternatively, it is converted to glutamine by the enzyme glutamine synthetase (GS)¹⁹⁹. Glutamine is extruded by the Na⁺-driven glutamine transporter SNAT3 into the extrasynaptic space and taken up by neurons that convert it back to glutamate via phosphate-activated glutaminase (PAG), restoring the presynaptic glutamate stores^{200–202}. This glutamate-recycling pathway represents a vital pathway inside CNS²⁰³ and it is known as the glutamate-glutamine cycle (see **Fig. 6**).

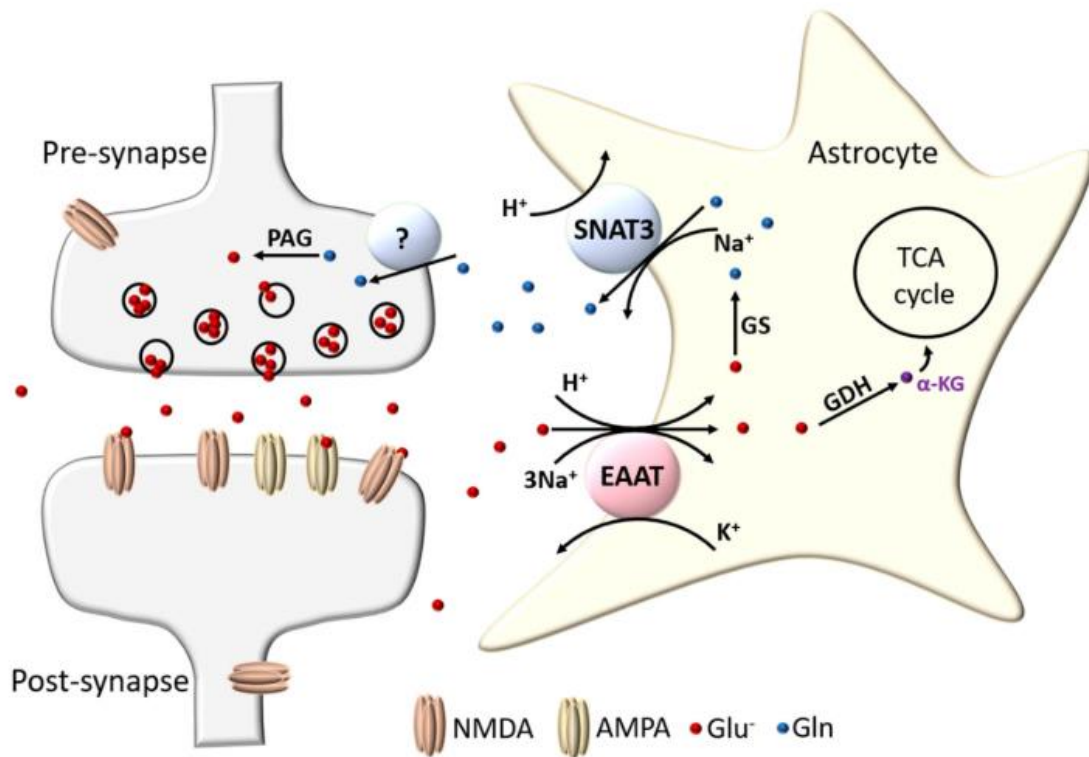


Figure 6. The glutamate–glutamine cycle. Astrocytic glutamate transporters, EAATs, recover the excess glutamate released during synaptic activity. Astrocytes convert glutamate to α -ketoglutarate by glutamate dehydrogenase or a transaminase reaction to join the TCA cycle. Alternatively, glutamate is converted to glutamine by the GS enzyme. SNAT3 then transports glutamine into the extracellular space where it is captured by neurons. Here, PAGs convert glutamine back to glutamate and deliver it back into synaptic vesicles²⁰³.

Currently, five human isoforms of EAAT transporters are known, named EAAT1, EAAT2, EAAT3, EAAT4 and EAAT5^{197,198}. The glutamate transporters EAAT1 and EAAT2 and their rodent homologs glutamate-aspartate transporter (GLAST) and glutamate transporter-1 (GLT-1) respectively, are those most expressed in the astrocytic plasma membrane. Both GLAST and GLT1 have a similar structure and retain the 65% of homology at the amino acid level¹⁹⁷. Functionally, both transporters have the same affinity for glutamate and are capable to reduce the extracellular glutamate concentration to the same level^{204,205}. However, they differ in the expression profile inside the brain and are differentially regulated during development^{206,207}. GLAST is found throughout the CNS, but in different concentrations in different regions. After birth, radial glial cells and immature astrocytes in the forebrain and cerebellum express GLAST. In adulthood, it is mostly found in Bergmann's glial cells in the cerebellum^{208,209}, Müller's glia in the

retina²¹⁰, and circumventricular organs²¹¹, while it has a limited expression in the forebrain.

In rodents, GLT-1 is expressed at postnatal week 3 and reaches the adult levels by week 5²¹². In the adult brain, GLT-1 represents the major EAAT expressed by mature astrocytes²⁰⁸. GLT-1 is mostly abundant in forebrain regions, with the highest levels in astrocytes of the caudate nucleus, cortex and hippocampus²⁰⁸.

Within the synaptic cleft, glutamate concentration can transiently increase from < 20 nM to 1 mM following action potentials²¹³. Meanwhile, cytosolic glutamate concentration varies from 1 to 10 mM in different cell types²¹⁴. Under physiological conditions, astrocytes maintain the extracellular glutamate level below the toxic threshold in order to avoid neuronal hyperexcitability or receptor desensitization¹⁷². To do this, astrocytes can change the expression and/or the activity of the transporter at the plasma membrane, thereby fine-tuning the clearance of glutamate. In cultured astrocytes, the expression of both transporters is stimulated by dibutyryl-cAMP or by growth factors, in association with the morphological and biochemical maturation of astrocytes²¹⁵.

Alterations of the expression of astrocytic glutamate transporters underlie multiple neurological diseases, such as traumatic brain injury, epilepsy²¹⁶ and ALS²¹⁷. In particular, several data showed that in the brain tissue of patients suffering of ALS, epilepsy, PD, AD and HD, the levels of GLT-1 and GLAST proteins are lower²¹⁸⁻²²³.

Abnormal levels of EAAT genes are associated with SZ²²⁴. Mice lacking EAAT1 showed behavioral alterations like enhanced locomotor activity in new environment, but not in the home cage²²⁵. EAAT- KO elicited spontaneous lethal seizures in homozygous mice, high susceptibility to brain injury, and short lifespan²¹⁶. Heterozygous EAAT2-KO mice showed abnormalities when compared with wild-type, such as increased locomotion in a novel environment and improved freezing responses in the conditioned fear test²²⁶.

Early research documented decreased EAAT1 and EAAT2 expression levels in AD brains²²⁷. Later analyses showed that astrocytic expression of EAAT2 was lower in AD subjects with dementia than in patients with mild cognitive impairment²²⁸, suggesting a protective role for EAAT2 expression in astrocytes. Indeed, gene loss accelerates

cognitive deficits given by AD²²⁹. In classic AD transgenic models with global overexpression of mutant proteins, a decrease in EAAT1 and EAAT2 levels has been observed, together with impaired glutamate re-uptake activity and altered glutamatergic neurotransmission^{230,231}. Some studies in astrocyte cultures argue that EAATs expression or localization is influenced by Amyloid- β , which is the causative factor in AD and this would provide an explanation for the decreased glutamate re-uptake seen in AD²³¹.

Studies performed *in vitro*, in transgenic models, and patients with HD have found abnormalities in EAAT2 transcript levels. In particular, lower levels of the EAAT2 transcript were detected in tissues from patients with HD compared to control groups²³². Strikingly, mutant huntingtin can directly reduce transporter expression, since when mutant huntingtin was induced in astrocytes, this was sufficient to decrease EAAT2 transcription and cause the HD phenotype in mice²³³.

In ALS patients, glutamate levels in plasma and cerebrospinal fluid were significantly elevated in comparison with healthy patients^{234,235}. Increases in glutamate levels were attributed to altered glutamate uptake. Later studies actually found a marked downregulation of EAAT2 levels in the spinal cord of ALS patients²³⁶. Importantly, an EAAT2 gene mutation has been identified that compromises glutamate transport likely due to a defect in glycosylation that reduces its surface exposure²³⁷.

There are several investigations concerning epileptic seizures and their influence on EAATs expression levels^{238–240}. Amount and function of glial EAATs decrease in the chronic phase of epilepsy in both rodents and patients, and this likely contributes to brain damage and epileptogenesis. EAAT2-KO, in particular, leads to seizures and death in mice^{239,241}. In contrast, EAAT2 overexpression in astrocytes reduces chronic seizure frequency and mortality in an epilepsy model^{239,241}.

GLT-1 and GLAST are antiporters that carry a glutamate molecule inside to cell together with three Na²⁺ and one H⁺ ions while one K⁺ ion transported to extracellular space. Since Kir4.1 channels are responsible for maintaining a negative resting potential in astrocytes, they ensure maximal glutamate transport rates through GLT-1 and GLAST^{242,243}. Indeed, blocking Kir4.1 channels with Ba²⁺ inhibits glutamate clearance,

supporting the significant role of membrane hyperpolarization in glutamate clearance^{171,244}. In addition, KO mice for Kir4.1 experience a drastic reduction of glutamate uptake and, accordingly, show high susceptibility to seizures¹⁸².

4. Aim of the study

The transcriptional regulator REST negatively controls several neuronal genes including those encoding for neurotransmitter receptors/synthesizing enzymes, synaptic vesicle proteins, adhesion factors and ion channels¹⁰. It is ubiquitously expressed in non-neuronal cells, such as glial cells, where it suppresses the expression of genes important for neuronal differentiation⁸⁰. Kir4.1 in astrocytes is largely responsible for K⁺ buffering and for maintaining the astrocytic resting membrane potential. The setting up of a negative membrane potential would ensure maximal clearance rates of glutamate via GLT-1 that has a higher density in the astrocytic membrane as well²⁴⁵.

The primary aim was to investigate the role of REST in the function of astrocytes *in vitro*. We focused our attention on the functional consequences of REST deletion in primary cultures of mouse cortical astrocytes by studying the changes in the two main homeostatic functions of astrocytes, namely K⁺ clearance and glutamate uptake. Given its close association with Kir4.1 and its importance in glutamate clearance, we also sought to explore the relationships between REST and GLT-1. We also investigated the consequences of deleting REST in astrocytes on neurons co-cultured with them, testing the hypothesis that impairment of Kir4.1 and GLT-1 would cause hyperexcitability and seizures.

5. Materials and Methods

5.1. Animals and cell culture preparation

All experiments were carried out in accordance with the guidelines established by the European Community Council (Directive 2010/63/EU of 22 September 2010) and were approved by the Italian Ministry of Health (Authorization #73-2014-PR on Dec 5, 2014). Wild-type C57BL/6J were obtained from Charles River (Wilmington, MA) and heterozygous GTinvREST mice⁷¹ were kindly provided by Gail Mandel (Portland, United States). They exploited a mouse line carrying a GT in the Rest intron (RestGT) between non-coding exon 1a-c and the first coding exon, exon 2. The GT cassette contains a splice acceptor site upstream of a promoter-less β -galactosidase and neomycin gene fusion (b-geo) and a polyadenylation sequence²⁴⁶. RestGT mice were crossed to mice expressing the Flpe recombinase transgene²⁴⁷ and this resulted in the inversion of the GT cassette (GTinv) to restore normal splicing of Rest exons 1a-c to exon 2, obtaining RestGTi mice, heterozygous for the inverted allele. RestGTi homozygous mice were provided to us by the above-mentioned laboratory.

Sequences containing either active or inactive Cre-recombinase were cloned respectively into pLenti-PGK-Cre-EGFP or pLenti-PGK- Δ Cre-EGFP plasmids^{248,249}. The production of VSV-pseudo typed third-generation lentiviruses was performed as previously described²⁵⁰. The transfection of astrocytes, obtained from RestGTi mouse cortex, with lentiviral particles expressing Cre results in re-inversion of the GTinv cassette, terminating transcription upstream of remaining Rest sequence.

The mouse was bred at the San Martino (GE, Italy) SPF animal facility, maintained on a C57BL/6J background and propagated in homozygosity. Two females were housed with one male in standard Plexiglas cages (33 x 13 cm), with sawdust bedding and metal top. After two days of mating, male mice were withdrawn and dams were housed individually in Plexiglas cages and daily checked. Mice were maintained on a 12:12 h light/dark cycle (lights on at 7 a.m.). The temperature was maintained at 22 \pm 1 °C and relative humidity

at 60±10%. Animals were provided drinking water and complete pellet diet (Mucedola, Settimo Milanese, Italy) ad libitum. Mice were weaned into cages of same sex pairs. Primary cultures of cortical astrocytes were prepared from both genotypes as described before^{251,252}. All efforts were made to minimize suffering and reduce the number of animals used. Briefly, new-born pups (P0 to P2) were sacrificed and, after removal of the meninges, cortical tissue was enzymatically dissociated. Astrocytes were plated on poly-D-lysine-coated (0.01 mg/ml) cell culture flasks and incubated for about 2 weeks at 37 °C, 5% CO₂, 90% humidity in medium consisting of DMEM (Gibco/Thermo-Fischer Scientific) supplemented to reach the final concentration of 1% glutamine, 1% penicillin/streptomycin and 10% Foetal Bovine Serum (FBS; Gibco/Thermo-Fischer Scientific). Typically, cultured astrocytes are grown in a medium supplemented with FBS because, even though it does not represent a physiological condition, it contains growth factors and fulfils several metabolic requirements of cultured cells that allow rapid proliferation^{253,254}. At confluence, astrocytes were enzymatically detached (trypsin–EDTA) and plated on petri dishes (33-mm diameter) at a density of 40,000 or 100,000 cells/ml, depending on the experiment. Cultures were incubated and maintained in the humidified incubator at 37 °C, 5% CO₂. Cells were subjected to infection with lentivirus containing Δ-Cre and Cre enzymes, 3 days after plating on petri dishes. Astrocytes were infected with lentiviruses at n=10 multiplicity of infection. After 24 h from infection, half of the medium was replaced with fresh medium. All experiments were performed after 7 days *in vitro* (div) of lentivirus incubation. Transduction efficiency was always above 75% of astrocytes and was verified thanks to the nuclear expression of the GFP reporter. For experiment concerning astrocytic/neuronal co-cultures, astrocytes were seeded on poly-D-lysine-coated (0.01 mg/ml) on petri dishes (33-mm diameter) at a density of 200,000 cells/ml. After 3 days of incubation, astrocytes were subjected to infection with lentivirus containing Δ-Cre and Cre enzymes and the medium was replaced after 24 h. Six days later, the complete DMEM medium was replaced with the Neurobasal medium (Gibco/Thermo-Fischer Scientific) supplemented to reach the final concentration of 10% FBS, 1% glutamine, 1% penicillin/streptomycin and 2% B27 (Gibco/Thermo-Fischer Scientific). The day after, enzymatically dissociated hippocampal neurons obtained from

18-day mouse embryos were plated on the top of astrocytes at a density of 200,000 cells/ml in complete Neurobasal medium, as described above. Two hours later, all the medium was replaced with a Neurobasal supplemented with 1% glutamine, 1% penicillin/streptomycin and 2% B27.

5.2. Biotinylation, immunoblotting and immunofluorescence

After 7 days from infection, cultured cortical astrocytes were washed three times with cold PBS. Astrocytes were incubated with 1 mg/mL biotin (EZLink Sulfo-NHS-LC-Biotin, Thermo Fisher Scientific, #21335) in phosphate buffered saline (PBS) pH 8.0 for 30 min at 4 °C. After removing biotin, astrocytes were washed twice with Tris 50 mM pH 8, waiting 5 min between each wash. Then astrocytes were washed twice with PBS pH 8. Astrocytes were lysed with lysis buffer (150 mM NaCl, 50 mM Tris-HCl, pH 7.4, 1 mM EDTA, 1% Triton X-100) supplemented with protease inhibitors. After 10 min of incubation on ice, cell lysates were collected and clarified by centrifugation (10 min at 10,000 x g at 4 °C). Supernatants were incubated with NeutrAvidin agarose resin (Thermo Fisher Scientific, #29202) for 3 h. Proteins were eluted from the agarose resin, resolved by SDS/PAGE and analyzed by immunoblotting.

The following antibodies were used: mouse monoclonal anti-Kir4.1 (1C11, Santa Cruz, sc-293252), rabbit polyclonal anti-EAAT2 (Cell Signaling Technology, #3838). Signal intensities were quantified using the ChemiDoc MP Imaging System (GE Healthcare BioSciences, Buckinghamshire, UK).

After 7 days from infection, cultured cortical astrocytes were fixed in PBS with 4% paraformaldehyde (PFA) for 15 min at room temperature (RT) and then washed with PBS. Cells were then permeabilized with 0.1% Triton X-100 in PBS for 5 min and blocked with 2% bovine serum albumin (BSA) in PBS for 30 min at RT. Then cells were incubated with primary antibodies in PBS 2% BSA overnight at 4 °C. Astrocytes were immunostained with antibodies against mouse monoclonal anti glial fibrillary acidic

protein (GFAP, Sigma Aldrich, Milan, Italy #G3893). After several PBS washes, astrocytes were incubated for 1 h with the fluorescent secondary antibodies in blocking buffer solution. Astrocytes were then washed three times in PBS and then stained with Hoechst for nuclei detection. After several washes in PBS, coverslips were mounted with Mowiol mounting medium. All images used for quantification of the immunofluorescence intensity were acquired with a Leica SP8 confocal microscopy (Leica Microsystems, Wetzlar, Germany).

Images were obtained using a 63x oil objective at a resolution of 1024 × 1024 pixels and Z-stacks were acquired every 300 nm. For each set of experiments, all images were acquired using identical exposure settings. Offline analysis was performed using the ImageJ software.

Astrocyte morphology was quantified in ImageJ, using the “Polygon Selections” feature tool Analyze-Measure function, to quantify the following shape descriptors: field area (μm^2), field perimeter (μm) and circularity index (CI). The circularity function calculates object circularity using the formula: $\text{circularity} = 4\pi (\text{area}/\text{perimeter}^2)$; circularity range from 0 (infinitely elongated polygon) to 1.0 (perfect circle).

5.3. Glutamate uptake assay

For glutamate uptake experiments, astrocytes were plated at concentration of 2×10^5 cell/ml in 6-well plates and experiments were performed as previously described²⁵². Briefly, astrocyte cultures were washed three times with pre-warmed (37 °C) HEPES-buffered Hanks' balanced salt solution. 1 $\mu\text{Ci}/\text{ml}$ of [³H] l-glutamate (NET490001MC, Perkin Elmer, Milan, Italy) was added to unlabelled l-glutamate (#G8415, Sigma) to reach a final concentration of 50 μM to isolate Na^+ -dependent transport in standard bath saline contained (in mM): 140 NaCl, 4 KCl, 2 MgCl₂, 2 CaCl₂, 10 HEPES, 5 glucose. To isolate Na^+ -independent transport, NaCl was replaced by choline chloride (#C7017, Sigma). To isolate Kir4.1-mediated glutamate uptake oversaturation (600 μM) of Ba²⁺ (#342920, Sigma) was added to the Na^+ solution. To block glutamate transporters 100 μM of GLT-1 blocker DL-threo- β -benzyloxyaspartic acid (DL-TBOA, #2532, Tocris) was

added to the Na⁺ solution. Cultures were incubated with the isotope on a heating plate at 37 °C for 10 min. After three washes with PBS, cells were harvested into 400 ml of 1 M NaOH solution in MilliQ water. The samples for radioactivity detection were moved to vials containing 2 ml of aqueous scintillation mixture and counted using a liquid scintillation counter (1450 LSC & Luminescence Counter, MicroBete TriLux, Perkin Elmer).

5.4. Patch-clamp recordings

Infected astrocytes of both genotypes were used for patch-clamp electrophysiological recordings using the whole-cell configuration as previously described²⁵⁵. The experiments were performed 7 div after infection, using an EPC-10 amplifier controlled by PatchMaster software (HEKA Elektronik, Lambrecht/Pfalz, Germany) and an inverted DMI6000 microscope (Leica Microsystems GmbH, Wetzlar, Germany). Patch electrodes fabricated from thick borosilicate glasses were pulled to a final resistance of 4–5 MΩ when filled with the standard internal solution. Recordings with leak current >200 pA or series resistance >10 MΩ were discarded. All recording were acquired at 50 kHz. Experiments were carried out at RT (20–24°C).

Salts and other chemicals were of the highest purity grade (Sigma, St. Louis, MO). For experiment involving astrocyte, the standard bath saline contained (mM): 140 NaCl, 4 KCl, 2 MgCl₂, 2 CaCl₂, 10 HEPES, 5 glucose, pH 7.4, with NaOH and osmolarity adjusted to ~315 mOsm/l with mannitol. The intracellular (pipette) solution was composed of (mM): 144 KCl, 2 MgCl₂, 5 EGTA, 10 HEPES, pH 7.2 with KOH and osmolarity ~300 mOsm/l. Experiments carried out under various extracellular K⁺_{ext} were done using external solutions with K⁺ salts replaced equimolarly. Aliquots of BaCl₂ were prepared in MilliQ and 0.2 mM of Ba²⁺ were added to the extracellular solution to block K⁺ channels, in the presence of the internal solution described above. In experiments conducted with L-glutamate, were used external solutions with L-Glutamate previously aliquoted into extracellular solution. 1 mM L-Glutamate was added to the extracellular solution to stimulate GLT-1 channels. To isolate the currents generated by GLT-1, 10 μM of the

amino-5,6,7,8-tetrahydro-4-(4-methoxyphenyl)-7-(naphthalen-1-yl)-5-oxo-4H-chromene-3-carbonitrile (UCPH), the selective GLAST channel-specific blocker, was added to the solution. To block glutamate transporters, 100 μ M TBOA (#2532, Tocris) was added to the Na⁺ solution.

The different saline containing the pharmacologic agents were applied with a gravity-driven, local perfusion system at a flow rate of \sim 200 μ l/min positioned within \sim 100 μ m of the recorded astrocytes. The experiments with IL1 β were performed incubating astrocytes with IL1 β (10 ng/ml) or corresponding amount of vehicle (water) and patch-clamp experiments were conducted 24 h after incubation.

For experiments involving astrocyte/neuron co-cultures, cells were maintained in standard Tyrode solution containing (in mM): 140 NaCl, 4 KCl, 2 CaCl₂, 1 MgCl₂, 10 HEPES, 10 glucose, pH 7.3 with NaOH and osmolality \sim 315 mOsm/l. For the analysis of neuronal excitability, D-(-)-2-amino-5-phosphonopentanoic acid (D-AP5; 50 μ M), 6-yano -7 notroquinoxaline-2,3-dione (CNQX; 10 μ M), and bicuculline methiodide (30 μ M), were added to block NMDA, non-NMDA, and GABA_A receptors, respectively. The standard internal solution was (in mM): 126 K Gluconate, 4 NaCl, 1 MgSO₄, 0.02 CaCl₂, 0.1 BAPTA, 15 glucose, 5 HEPES, 3 ATP, 0.1 GTP (pH 7.2 with KOH). For recording miniature excitatory postsynaptic currents (mEPSCs), bicuculline methiodide (30 μ M), CGP58845 (5 μ M), D-AP5 (50 μ M) and tetrodotoxin (TTX; 300 nM) were added to the extracellular solution to block GABA_A, GABA_B, NMDA receptors and generation and propagation of spontaneous action potentials (APs).

Current-clamp recordings of neuronal firing activity and the following analysis were performed as previously described²⁵⁶. Neuronal cells were held at potential of -70 mV and APs were induced by injection of 10 pA current steps of 1 s in pyramidal neurons morphologically identified by their teardrop-shaped somata and characteristic apical dendrite after 12-16 div^{257,258}. The mean firing frequency was calculated as the number of APs evoked by minimal current injection, whereas the instantaneous frequency was estimated as the reciprocal value of the time difference between the first two evoked APs. The rheobase was calculated as the minimum depolarizing current needed to elicit

at least one AP. Current-clump recordings were acquired at a 50 kHz and filtered at 1/5 of the acquisition rate with a low-pass Bessel filter.

Miniature excitatory postsynaptic currents (mEPSCs) were recorded from low-density hippocampal neurons in standard external solution containing the following: TTX (1 μm ; Tocris Bioscience), D-AP5 (50 μm), CGP 58845 (10 μm), and bicuculline (30 μm). The amplitude and frequency of mEPSCs were calculated using a peak detector function with appropriate threshold amplitude and threshold area using the Minianalysis program (Synptosoftware).

5.5. Statistical analysis

Data are expressed as means \pm standard error of the mean (SEM) for number of cells (n) or mouse preparations as detailed in the figure legends. Normal distribution of data was assessed using the D'Agostino-Pearson's normality test. The F-test was used to compare variance between 2 sample groups. To compare 2 normally distributed sample groups, the unpaired or paired 2-tailed Student's t -test was used. To compare 2 sample groups that were not normally distributed, the nonparametric Mann-Whitney's U -test was used. To compare more than 2 normally distributed sample groups, we used one- or two-way ANOVA, followed by the Bonferroni's test. When data were not normally distributed, one- and two-way ANOVA were substituted with the Kruskal-Wallis's and Friedman's two-way ANOVA tests, respectively, followed by the Dunn's post-hoc multiple comparison test. Alpha levels for all tests were 0.05% (95% confidence intervals). Statistical analysis was carried out using OriginPro-8 (OriginLab Corp., Northampton, MA, USA) and Prism (GraphPad Software, Inc.) software.

6. Results

6.1. Astrocytes with REST deficiency preserve a normal cellular morphology

We investigated the role of REST in astrocyte differentiation and function using genetically modified REST^{fl/fl} mice⁷¹. We have acutely knocked-out REST by infecting primary astrocyte cultures derived from mice homozygous for the floxed mutant alleles of the *REST* with lentiviruses expressing recombinant Cre. We cultured primary cortical astrocytes from new-born homozygous REST knock-in mice and, after re-plating them on petri dishes at 15 div, we infected them with lentiviruses expressing mutant Cre recombinase (Δ -CRE) or functional Cre recombinase (Cre) enzymes at 18 div for 24 h. The Δ -CRE is a defective, non-functional enzyme that represents our control condition (Ctrl), while Cre is the functioning enzyme, which acts by silencing REST (KO). Infected astrocytes were cultured until 25-28 div when were analysed morphologically, biochemically, and electrophysiologically. Both Cre and Δ -CRE constructs also contain the gene encoding for Green Fluorescent Protein (GFP), which offers the advantage to optically identify infected cells, showing a nuclear localization. The level of astrocytic infection was very similar under both conditions (\sim 70%, **Fig. 1A-C**). As expected, cells infected by Cre showed very low levels of REST mRNA and protein compared to astroglial cells infected by Δ -Cre, with the efficiency of cell infection (\sim 75%) similar under both conditions (**Fig. 1D**). Astrocytes *in vivo* exhibit a process-bearing shape (for a review²⁵⁹). Since there is evidence that *in vitro* the activation of REST influences the morphological differentiation of primary astrocytes⁸⁰, we measured various morphological parameters from immunocytochemical images obtained by confocal microscopy. Cells were co-stained with anti-GFAP antibodies to detect astroglia, anti-GFP to detect infected cells and Hoechst to visualize nuclei. Among the morphological parameters we measured perimeter, area and CI of astrocytes under both conditions (**Fig. 1E**). The results clearly indicate that the astrocyte morphology was not affected by REST deletion, as none of

the investigated parameters was significantly changed between Ctrl and REST-KO astrocytes.

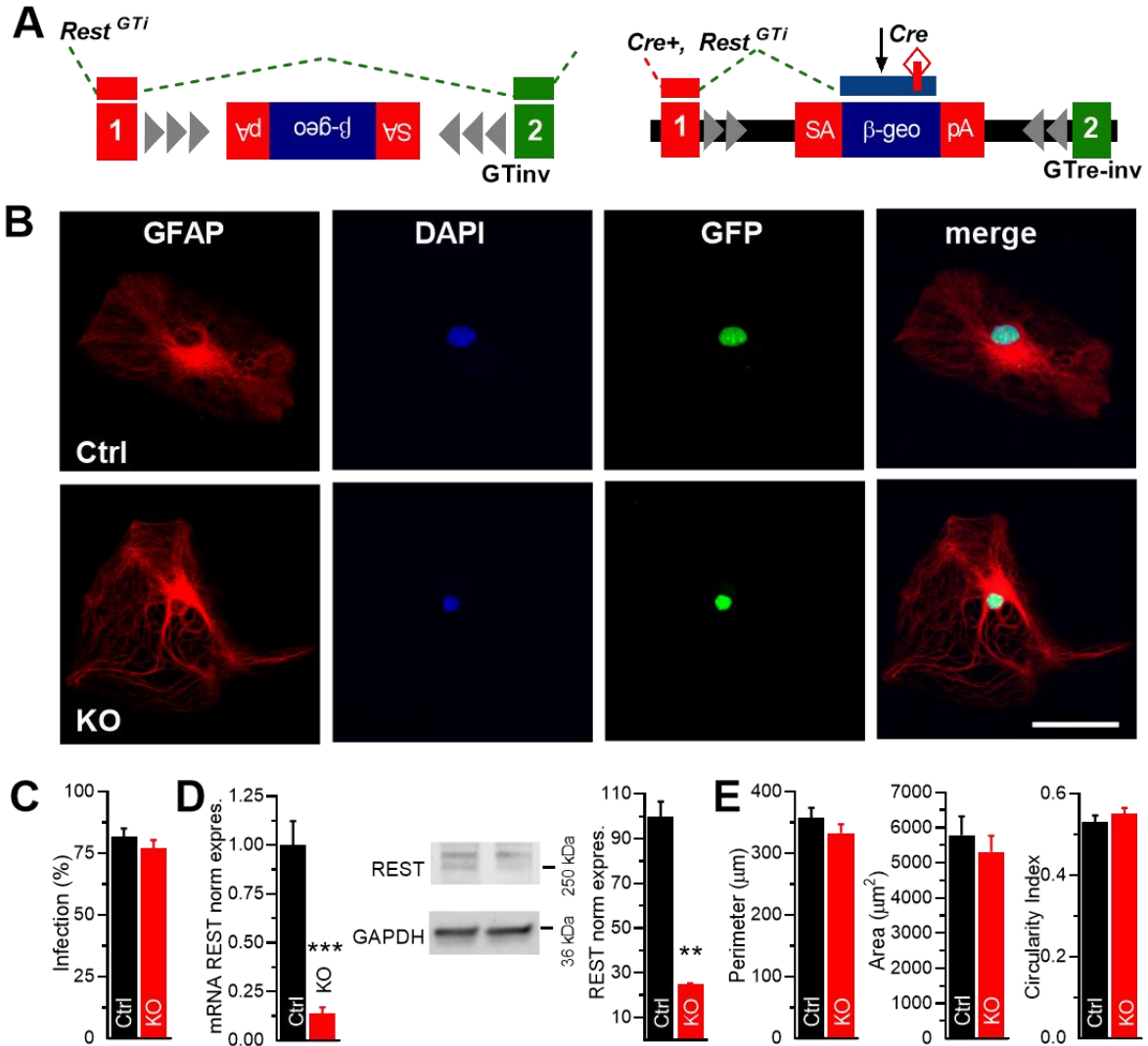


Figure 1. REST deletion did not produce changes in cell morphology of primary cultured astrocytes.

A. KO strategy. Mice with the inverted GT cassette *Rest* GTInv, resulting in normal splicing, were generated by mating *Rest*^{GTi} mice to mice containing the Flpe transgene (left). The infection of postnatal astrocytes with Cre-recombinase-encoding lentivirus, resulted in re-inversion of the GTInv cassette, splicing of exons 1a–c to the β -geo gene instead of exon 2, and terminating transcription upstream of remaining *REST* sequences (right). **B.** Representative confocal images of GFAP immunostaining (red) in Ctrl and REST-KO mouse primary culture of astrocytic cells (25 div). DAPI staining was used to label cell nuclei (blue) and GFP (green) as reporter for infected cells. Merge panels represent the superimposition of all images. Scale bars, 20 μ m. **C.** Percentage of astrocytes infected with Cre and Δ Cre lentiviruses, in control (Ctrl, black) and REST-KO (KO, red) cortical astrocytes (17–20 div). The percentage of infected cells in both conditions was the same ($p > 0.05$, Student's *t*-test/Mann Whitney's *U*-test). **D.** Bar-graph of mRNA (left) and protein (right) expression levels of REST evaluated by real-time PCR and western blotting analysis in Ctrl and REST-KO

astrocytes. **E.** Analysis of Ctrl and REST-KO astrocytic morphology. From left to right, bar-graphs represent the perimeter, area and the CI calculated for Ctrl (n=178) and KO (n=176) astrocytes from 3 independent preparations. All data are expressed as means±SEM **p<0.01, ***p<0.001, Student's *t*-test/Mann Whitney's *U*-test.

6.2. REST deletion in primary astrocytes selectively downregulates an inward rectifier current

To analyse the effects of REST deletion on the electrical membrane properties of primary astrocytes, macroscopic currents were recorded by patch-clamp using whole-cell configuration on isolated Ctrl and REST-KO cultured cells. Compared to Ctrl astrocytes, REST-KO cells displayed significantly more depolarized resting membrane potentials (V_{rest}) (**Fig. 2A**). To address the possibility that the depolarized V_{rest} could be due to a change in background membrane conductance, we applied a slow voltage ramp that allows monitoring the background conductance in a large range of membrane voltages. Astrocytes, voltage clamped at the holding potential (V_h) of -70 mV, were hyperpolarized for 200 ms at -100 mV before the application of a slow depolarizing ramp to +80 mV (**Fig. 2B**, inset). The results show that while Ctrl cells had an outwardly rectifying ramp current profile with physiological inward currents at negative voltages, REST-KO astrocytes had no significant current at low potentials (**Fig. 2B**, red and black trace, respectively). The mean current densities (J =pA/pF) at -100 mV and +80 mV in REST-KO astrocytes indicate that the conductance was not significantly altered at positive voltage, it was two-fold smaller at -100 mV with respect to Ctrl astrocytes (**Fig. 2C**). The lack of inward current in REST-KO astrocytes was accompanied by an increase in the rectification profile of macroscopic conductance.

We next sought to determine the voltage-dependent kinetics of astrocyte currents in the presence and absence of REST. A family of 200 ms-voltage steps (increments of 10 mV) from a V_h of -70 mV were used to activate voltage- and time-dependent membrane currents from -100 mV to +80 mV (inset in **Fig. 2D**). Ctrl astrocytes exhibited sustained non-inactivating negative currents at potentials below -70 mV and non-inactivating, quasi-instantaneous positive currents at potentials above -70 mV (**Fig. 2D, E**; black

line/symbols). By contrast, only non-inactivating positive currents with an outwardly rectifying profile were evoked at potentials above -40 mV in REST-KO astrocytes (**Fig. 2D, E**; red line/symbols). The absence of this inward current in REST-KO astrocytes was accompanied by a significant increase of the input resistance (R_{input} , **Fig. 2F**). In addition to the sustained inward current, in a subset of astrocytes belonging to both experimental groups, depolarizing steps above -50 mV induced rapidly activating fast inactivating currents (**Fig. 2G**). This transient voltage-dependent conductance peaked at -30 mV and was abolished when extracellular Na^+ (140 mM Na^+_{ext}) was replaced with choline (0 mM Na^+_{ext}) or when the classical Na^+ channel blocker Tetrodotoxin (TTX, 1 μM) was added to the physiological recording solution (**Fig. 2H**). Importantly, the percentage of astrocytes that exhibited this *bona fide* transient Na^+ current was the same for both genotypes (**Fig. 2I**). Collectively, the results clearly demonstrate that primary astrocytes in which REST is deleted exhibit a selective downregulation of the hyperpolarization-activated, non-inactivating inward current and a depolarized resting membrane potential.

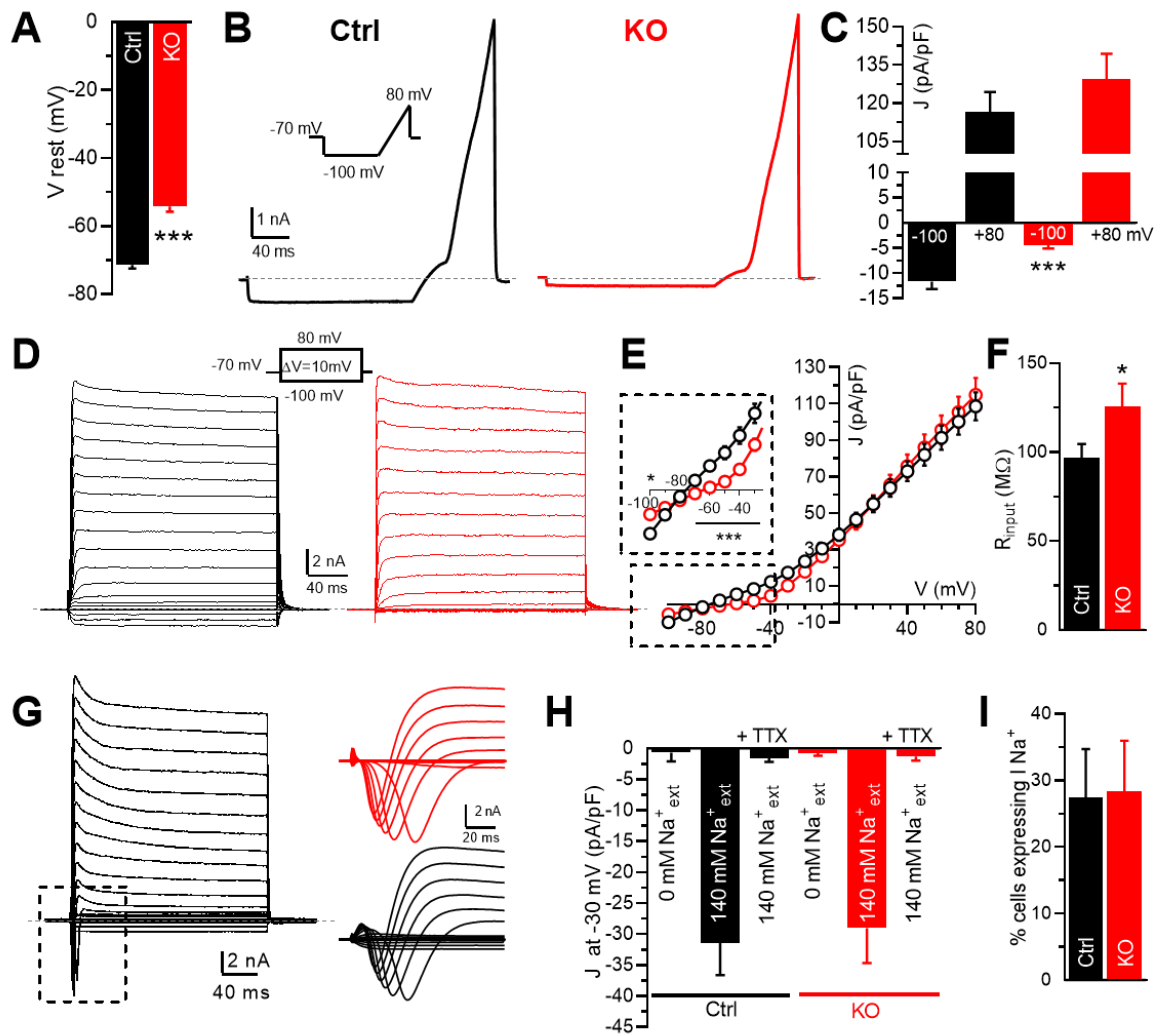


Figure 2. Effects of KO of REST on astrocyte whole-cell macroscopic currents **A.** REST-KO astrocytes show a more positive resting membrane potential compared to Ctrl cells. **B.** Representative macroscopic currents recorded in Ctrl (black) and REST-KO (red) astrocytes evoked with a voltage ramp protocol shown in the inset. **C.** Ramp current densities (J) of both genotypes measured at -100 and +80 mV using the protocol depicted in (B) show that REST-KO cells have a significant reduction of inward current compared to Ctrl. **D.** Representative family of voltage- and time-dependent membrane currents evoked by the protocol showed in the inset. The non-inactivating inward currents were recorded only in control astrocytes. **E.** Current density vs. voltage relationship of currents elicited show the same level of outward current under both conditions, but a significant reduction of inward component in KO cells (inset). **F.** R_{input} bar-graph calculated for both genotypes. **G.** Representative recordings of voltage-step currents for Ctrl cells illustrating the expression of a transiently activated inward current. The inset shows the magnification of this component for both genotypes. **H.** Statistical analysis of transient inward current density studied at peak potential (-30 mV) for Ctrl and REST-KO astrocytes in external solution containing 140 mM, 0 mM of Na^+ and in presence of TTX (1 μ M). **I.** Percentage of expression of this conductance in both genotypes across different culture preparations ($n=5$). About 30% of both Ctrl and REST-KO recorded astrocytes show

this Na⁺-dependent transiently activated inward current. All data are expressed as means±SEM *p<0.05; ***p<0.01, Student's *t*-test/Mann Whitney's *U*-test. n=109 and n=97 for Ctrl and REST-KO astrocytes, respectively.

6.3. REST deletion negatively modulates an inward-rectifier K⁺ current

The previous results clearly indicate that primary astrocytes expressing REST displayed both positive and negative sustained currents that changed polarity at around -70 mV, while REST-deficient cells exhibited only positive currents activated at potentials above -40 mV. We hypothesized that REST is necessary for the upregulation of a background K⁺ conductance, which also contributes to define the negative V_{rest} observed in control astrocytes (see **Fig. 2A**). To address this point in detail, electrophysiological experiments were carried out under various extracellular K⁺ concentrations (K^+_{ext}). When K^+_{ext} was increased from 4 to 40 mM in Ctrl, but not in REST-KO astrocytes, the evoked ramp currents changed polarity at more positive potentials, an effect that was paralleled by a reduction in current rectification (**Fig. 3A**). The quantitative analysis of the *J* values recorded under these conditions for Ctrl/ REST-KO genotypes using a family of 200 ms-voltage steps protocol, corroborate these findings (**Fig. 3B**). The analysis of V_{rest} as function of K^+_{ext} in the two genotypes clearly indicates that this K⁺ current directly contributes to set the V_{rest} in primary astrocytes expressing REST (**Fig. 3C**).

Altogether, these results support the tenet that, in control astrocytes, the functional expression of a background K⁺ conductance has a relevant role for setting the very negative V_{rest} . The K^+_{ext} dependence of the current evoked at negative potentials suggests that this conductance is mediated by inward rectifier K⁺ channel (Kir) and in particular by the 4.1 subtype, which several studies have identified to be largely expressed by astrocytes in many brain regions *in vivo*^{148, 178,260,261} and *in vitro*²⁶².

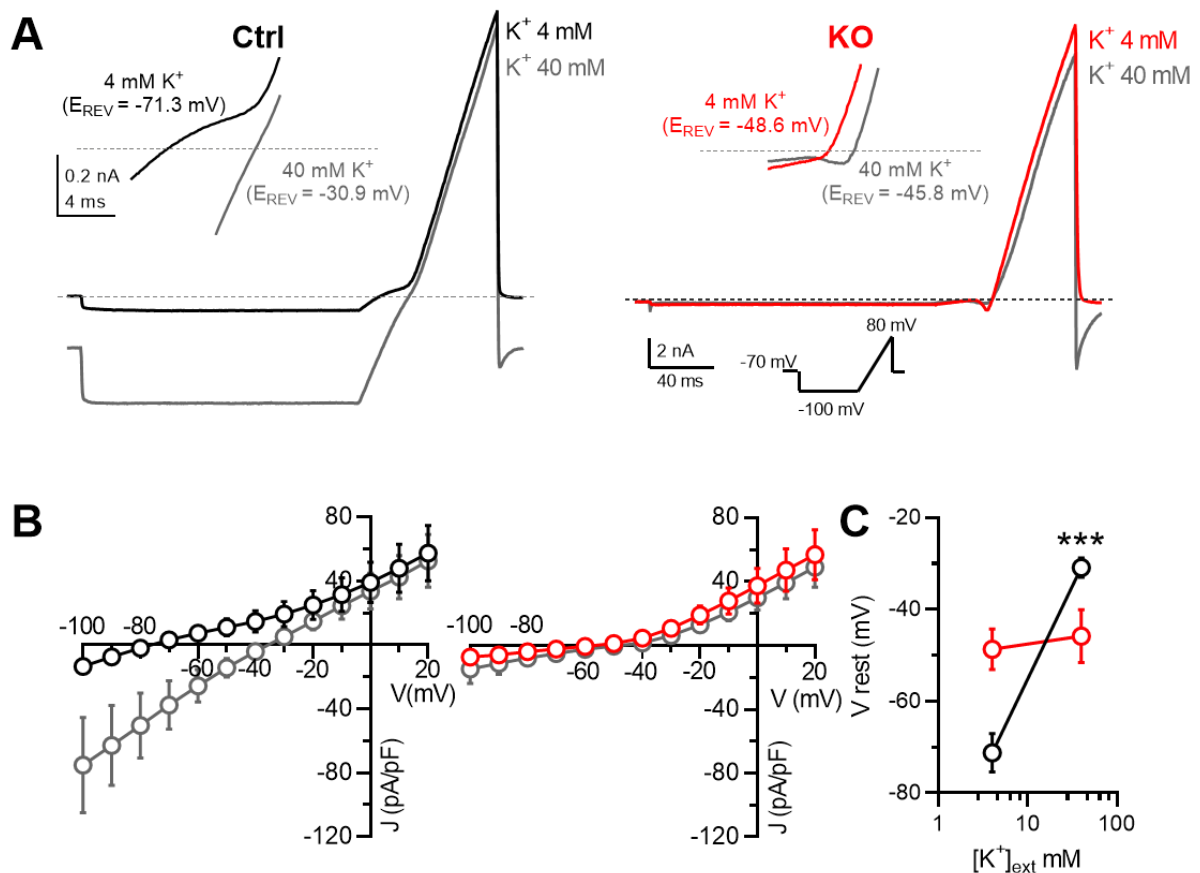


Figure 3. REST deletion decreases the astrocytic inward-rectifier K⁺ conductance. **A.** Representative current traces of Ctrl and REST-KO astrocytes evoked in 4 mM and 40 mM extracellular K⁺ (K⁺_{ext}) by replacing equimolarly Na⁺. The increase in K⁺_{ext} positively shifts the reversal potential (E_{rev}) of Ctrl current, but not of REST-KO current. The shift in E_{rev} to more positive potentials is accompanied by a reduction of rectifying profile, which indicates the activation of an inward-rectifier K⁺ channel that approximates the behaviour predicted by the constant field theory for simple K⁺ electrodiffusion. **B.** J-V plot of steady-state currents evoked in 4 mM and 40 mM of K⁺_{ext} with a voltage step protocol in Ctrl and REST-KO astrocytes. The statistical analysis confirms the data presented in A. **C.** The shifts in E_{rev} measured in 4 mM and 40 mM of K⁺_{ext} were fitted by a least-squares linear regression. All data are expressed as means±SEM (Ctrl, n=9; KO, n = 9) ***p <0.001, paired Student's *t*-test/Wilcoxon's test.

A distinctive feature of astrocytic Kir4.1-mediated current is its full blockade by low micromolar concentrations of extracellular Ba²⁺^{180,255}. To corroborate the hypothesis that under our experimental conditions the background K⁺ current in REST-expressing astrocytes was mediated by Kir4.1 channels, comparative experiments were performed in both Ctrl and REST-KO astrocytes in the presence or absence of Ba²⁺. In Ctrl astrocytes,

the extracellular administration of Ba²⁺ (200 μM) resulted in the complete inhibition of the negative ramp currents but did not affect the positive current evoked at depolarized potentials (**Fig. 4A**, left). The voltage intercept of ramp current before and after Ba²⁺ exposure was at ~-75 mV confirming that, in these astrocytes, the background conductance was mediated by a Ba²⁺-sensitive K⁺ channel. By contrast, in REST-KO astrocytes the Ba²⁺ challenge did not modify the evoked ramp current (**Fig. 4A**, right). Notably, the profiles of the current following Ba²⁺ administration in Ctrl and REST-KO astrocytes perfectly overlapped, adding further support to the concept that REST specifically controls the functional expression of the Ba²⁺-sensitive Kir4.1 current (data not shown). The same results were achieved by means of a voltage-step protocol (**Fig. 4B**) that was also used to calculate the current density at -100 mV and +80 mV in the presence or absence of Ba²⁺ in astrocytes from both genotypes (**Fig. 4C**). The analysis of the net effect of Ba²⁺ calculated in both Ctrl and REST-KO astrocytes at -100 mV and +80 mV (**Fig. 4D**) confirms the strong Ba²⁺-sensitivity of the current activated at negative potentials, a result that reasonably rules out the possibility that other K⁺ channels subtypes contribute to the negative K⁺ current evoked in REST-expressing primary astrocytes.

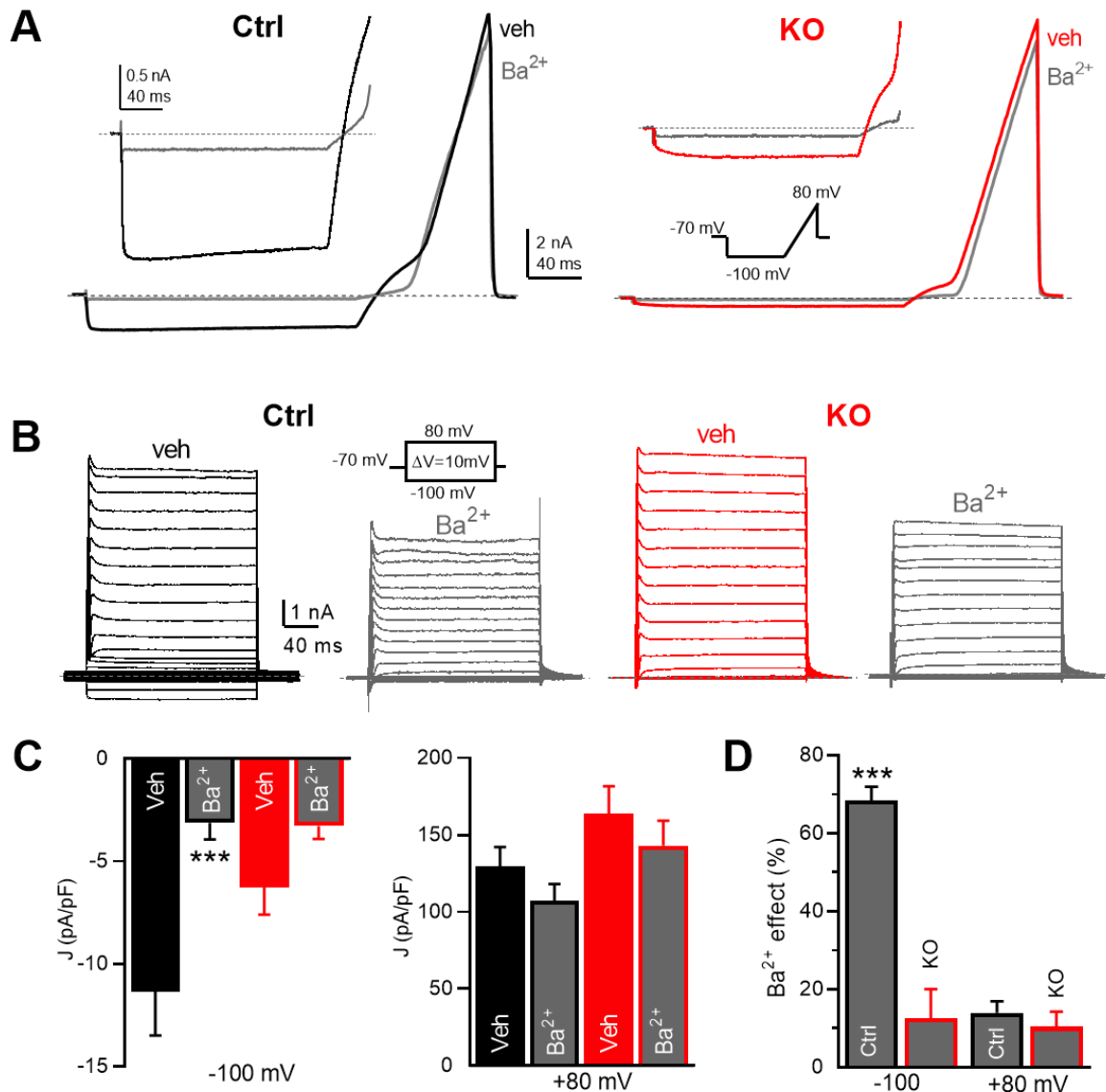


Figure 4. The inward-rectifier K⁺ current down-regulated by REST deletion is mediated by Kir4.1 channels. **A.** Representative ramp current traces elicited in Ctrl and KO astrocytes before (black/red) and after (grey) acute treatment with extracellular solutions contain Ba²⁺ (200 μM). Magnification of the currents at negative potentials is shown in the inset. **B.** Representative current traces evoked by a family of voltage steps before (left) and after acute treatment of the Ctrl/REST-KO cells with Ba²⁺ (right). **C.** Statistical analysis of J recorded at -100 (left) and +80 mV (right) for both genotypes studied with or without Ba²⁺ as in (A) with the protocol depicted in (B). ***p<0.001, 2-way ANOVA followed by Bonferroni's multiple comparison test (Ctrl, n=24; REST-KO, n=22). **D.** Bar-graph of Ba²⁺ effect at -100 and +80 mV for Ctrl and REST-KO cells showing the selective and complete blockade of the inward current expressed in Ctrl cells. All data are expressed as means±SEM (Ctrl, n=24; REST-KO, n=22). ***p<0.001, unpaired Student's *t*-test/Mann Whitney's *U*-test.

To further confirm that REST controls Kir functional expression, we took advantage of the evidence that interleukin 1 β (IL1 β) downregulates the Kir4.1-mediated current in astroglial cells²⁶³. To address this issue, primary astrocytes of both genotypes were incubated for 24 h with either IL1 β (10 ng/ml) or vehicle (veh). Under these conditions, IL1 β potently and specifically decreased the number of astrocytes that displayed inward current elicited by ramp stimulation in Ctrl astrocytes (20% of IL1 β -treated astrocytes vs. 77.5% of vehicle-treated astrocytes) but had no effect in REST-KO cells. (**Fig. 5A, C**). Accordingly, long-term IL1 β exposure caused a depolarization of mean V_{rest} in Ctrl astrocytes, which was not apparent in REST-KO cells (**Fig. 5B**).

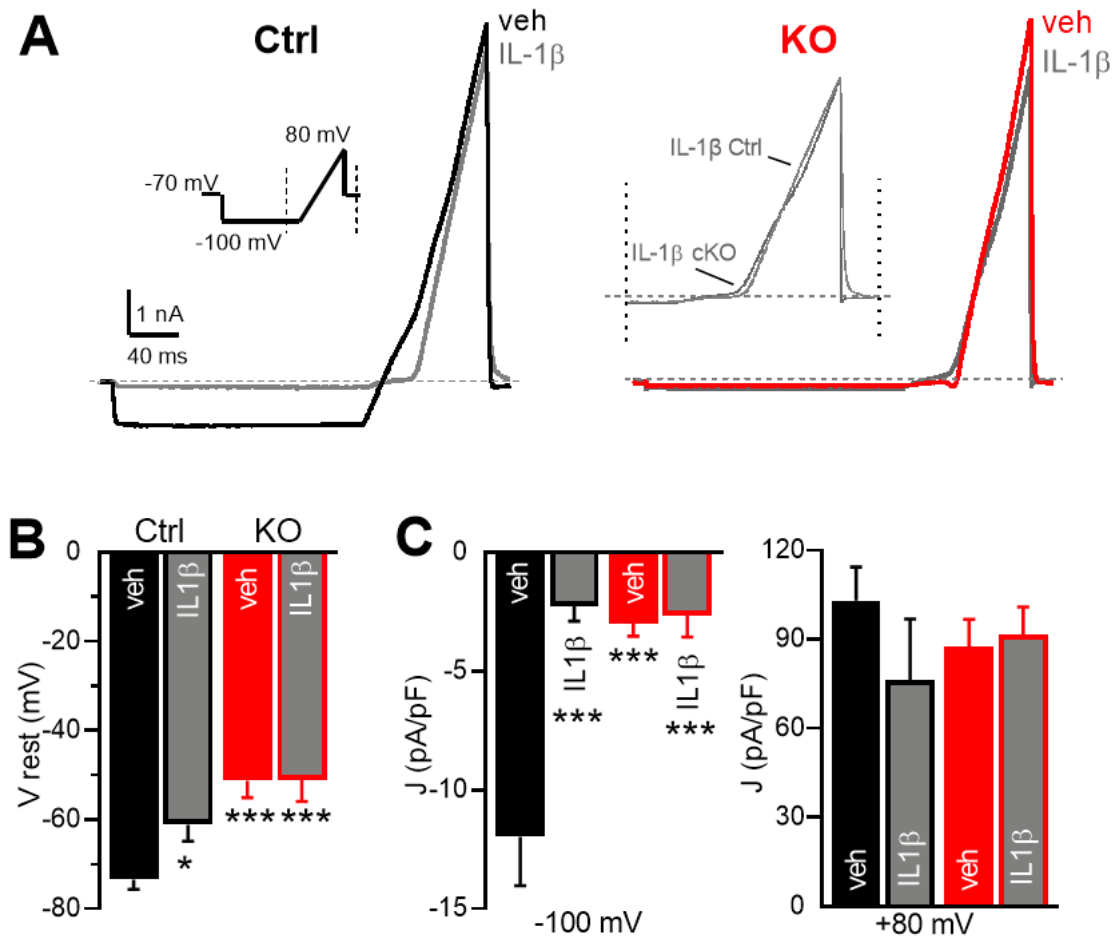


Figure 5. Kir4.1 channels are downregulated by chronic treatment with IL1β in control astrocytes, but not in REST-KO cells. A. Representative ramp current recordings in Ctrl and REST-KO cells treated for 24 h with either vehicle (black) or IL1β (10 ng/ml, grey). **B.** Ctrl astrocytes treated with IL1β show a reduction of membrane potential value compared to REST-KO cells. * $p < 0.05$, *** $p < 0.001$, Student's *t*-test/Mann Whitney's *U*-test **C.** Statistical analysis of *J* recorded at -100 and +80 mV for both genotypes treated in the presence or absence of IL1β. *** $p < 0.001$, 2-way ANOVA followed by Bonferroni's multiple comparison test ($n = 22, 16$ and $n = 15, 15$ for Ctrl/Veh, Ctrl/IL1β and REST-KO/Veh, REST-KO /IL1β astrocytes, respectively). All data are expressed as means \pm SEM.

The functional and pharmacological analyses indicated that primary astrocytes expressing REST exhibit Kir4.1-mediated currents, while REST deletion caused a downregulation of Kir expression. To get insight at the molecular level into the mechanism underlying the observed effects, we addressed the expression level of Kir4.1 in subcellular compartments of both Ctrl and REST-KO primary astrocytes.

Immunoblotting and surface biotinylation experiments showed that, although REST deletion did not change total Kir4.1 protein expression, it significantly decreased its exposure at the plasma membrane (Fig. 6A, B). Taken together, these results support the hypothesis that REST controls the functional expression of Kir4.1 channels and that its absence alters the post-translational processes that govern the plasma membrane targeting and turnover of Kir4.1.

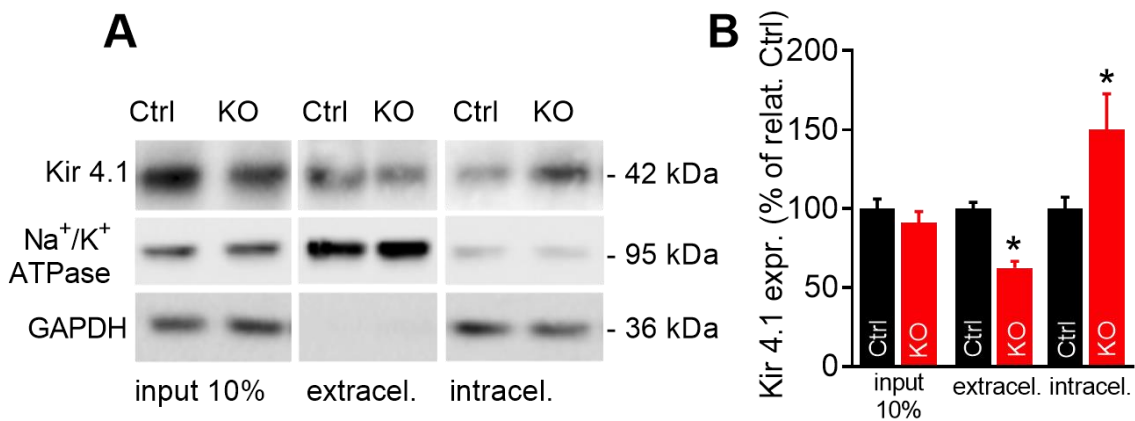


Figure 6. Kir4.1 channels are less expressed at the plasma membrane in REST-KO astrocytes. A. Representative immunoblots of cell surface biotinylation performed in Ctrl and REST-KO primary astrocyte cultures against Kir4.1. Total cell lysates (input), biotinylated (cell surface, extracellular), and non-biotinylated (intracellular, intracellular) fractions were analysed by immunoblotting. Na/K-ATPase and GAPDH were included as markers of the plasma membrane and cytosolic fractions, respectively. **B.** Statistical analysis of the biotinylation experiments. Data were normalized to the mean value of control astrocytes treated with vehicle and expressed as means±SEM. *p<0.05, Student's *t*-test/Mann Whitney's *U*-test (n=4 independent preparations).

6.4. Kir4.1 downregulation by REST deletion impairs glutamate uptake by GLT1

The activity of Kir4.1 channels is associated with glutamate uptake by setting V_{rest} close to the negative reversal potential of K^+ , hence increasing the maximal transport rates via the Na^+ -dependent GLT-1 transporter²⁶⁴. To demonstrate that the functional impairment of Kir4.1 channels in REST-KO primary astrocytes affects glutamate uptake, we assayed of 3H -glutamate (3H -Glu) uptake in Ctrl and REST-KO astrocytes. Cells were infected and maintained for one week in culture (the same time-window used for the

electrophysiological experiments) before assay. The day of the experiment, the cell medium was replaced with physiological solution containing $^3\text{H-Glu}$ in the presence or absence of choline, to isolate the Na^+ -dependent glutamate transport, or of Ba^{2+} to inhibit Kir4.1. To rule out the potential role of GLAST²⁶⁵ under our experimental conditions, the specific GLAST inhibitor UCPH (10 μM) was added to the bath solution. To test for the specificity of glutamate uptake by GLT-1, we replaced extracellular Na^+ with choline or challenged the assay with the competitive GLT-1 blocker DL-TBOA (100 μM). Under both conditions, a strong decrease in glutamate uptake was observed in Ctrl astrocytes. Moreover, the dependence of glutamate uptake on a full functionality of Kir4.1 channels was confirmed by the significantly decreased glutamate uptake in the presence of Ba^{2+} in control cells (**Fig. 7A**). Compared to Ctrl astrocytes, REST-KO cells showed a significantly decreased basal uptake of glutamate that was not further affected by Ba^{2+} . Altogether, these results show that the ability to uptake glutamate is significantly impaired in REST-KO astrocytes and confirm the important contribution of Kir4.1 channel activity to the Na^+ -dependent glutamate uptake²⁶⁶.

To confirm that glutamate uptake after REST deletion is defective, we measured glutamate-evoked currents in astrocytes of both genotypes under conditions of blockade of GLAST (by the antagonist UCPH) and of the ionotropic glutamate receptors (CNQX and AP5). As previously described²⁶⁷, a reversible inward current was evoked in astrocytes clamped at -70 mV and challenged with L-glutamate (1 mM). Of note, compared to Ctrl astrocytes, in REST-KO cells the glutamate-evoked, TBOA-sensitive inward currents were significantly diminished (**Fig. 7B**).

Since the results clearly indicate that REST-KO astrocytes display a reduced basal capacity of glutamate uptake, we next evaluated whether this effect was reflected by a change in GLT-1 expression in REST-KO, in view of the recent report of a positive control exerted by REST on GLT-1 expression²⁶⁸.

The results showed that the repression of REST decreased both GLT-1 mRNA and protein levels in KO astrocytes compared to Ctrl (**Fig. 7C, D**). While the GLT-1 protein level at the plasma membrane, analysed by surface biotinylation, was significantly decreased in REST-KO astrocytes (**Fig. 7E**). These results suggest that the absence of REST, in addition

to downregulating Kir4.1 channel, also causes an impairment in astroglial glutamate uptake by reducing the expression of GLT-1, especially at the plasma membrane.

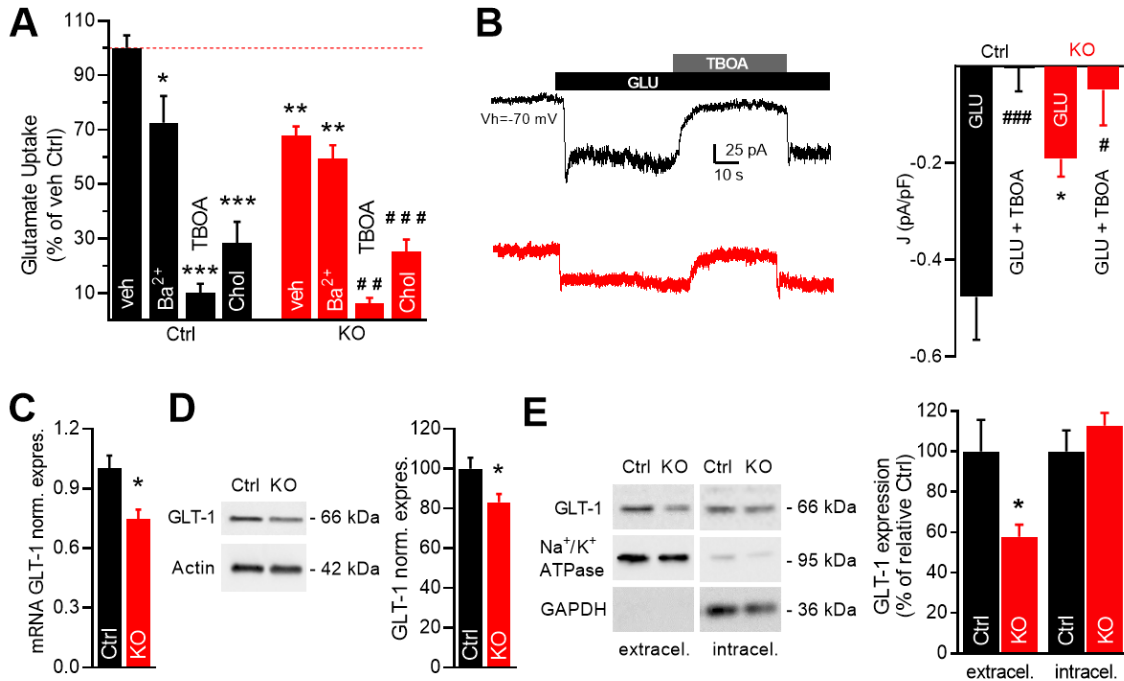


Figure 7. Glutamate uptake was altered in astrocytes with Kir4.1 downregulated by REST deletion.

A. Quantitative analysis of glutamate uptake by both control and REST-KO astrocytes (21-24 div). Data were normalized to the mean value of Ctrl astrocytes. **B.** On the left the representative traces of currents obtained during whole-cell voltage-clamp recording from astrocytes clamped at a holding potential of -70 mV. L-glutamate (1 mM) evoked inward currents that were completely blocked by 100 μM TBOA. On the right, the current density (J) is shown from Ctrl and REST-KO astrocytes recordings, in an external solution containing L-Glutamate and in presence of TBOA. # p<0.05, ## p<0.01, paired Student's *t*-test/Wilcoxon's test; *p<0.05, Student's *t*-test/Mann Whitney's *U*-test (n=20 and n=10 for Ctrl and REST-KO astrocytes, respectively). **C.** Bar-graph of mRNA expression levels of GLT-1 evaluated by real-time PCR in Ctrl and REST-KO astrocytes (n=4 independent preparations) *p<0.05, Student's *t*-test/Mann Whitney's *U*-test. **D.** Representative immunoblots and quantification of protein expression levels of GLT-1 evaluated by western blotting analysis in Ctrl and REST-KO astrocytes (n=4 independent preparations). *p<0.05, paired Student's *t*-test/Wilcoxon's test. **E.** Surface biotinylation of Ctrl and REST-KO primary astrocytes. *Left:* representative immunoblots labelled with antibodies to GLT-1 showing biotinylated (extracellular), and non-biotinylated (intracellular) fractions. Na/K-ATPase and GAPDH were included as markers of the plasma membrane and cytosolic fractions, respectively. *Right:* statistical analysis of the experiment presented in E (n=4 independent preparations). Data were normalized to the mean value of control astrocytes (n=4 independent preparations). *p<0.05, Student's *t*-test/Mann Whitney's *U*-test. All data are expressed as means±SEM.

6.5. Neurons co-cultured with REST KO astrocytes display altered firing phenotypes

We next sought to determine whether the described changes in the expression of relevant astrocyte homeostatic proteins in primary REST-KO astrocytes could affect the neuronal function in term of single cell excitability. To this end, wild-type hippocampal neurons were co-cultured with Ctrl (Astro Ctrl) or REST-KO (Astro KO) astrocytes for 14 days before performing measurements of neuronal excitability. Excitatory pyramidal neurons were visually identified in co-cultures and analysed by patch-clamp under current-clamp configuration^{257,258} (**Fig. 8A**). Neurons co-cultured with Ctrl or REST-KO astrocytes did not show any difference in V_{rest} or R_{input} (**Fig. 8B, C**). Moreover, they responded to the injection of a depolarizing current with similar firing of action potentials (APs) with no overt differences in the minimum amount of current necessary to evoke the first AP (Rheobase, **Fig. 8D**).

The instantaneous firing frequency was studied by delivering constant current pulses (1-s duration) of increasing amplitude (10 pA) and measuring the resulting AP firing rate. The analysis revealed that REST ablation in primary astrocytes strongly increased the high-frequency firing activity evoked by intense depolarizing currents in co-cultured neurons (**Fig. 8F**). The same level of hyperactivity in these neurons was observed by counting the number of APs evoked by injection of 1 s-step of 300 pA of depolarizing current (**Fig. 8G**).

Finally, the analysis of the shape of the first AP evoked by minimal current injection showed that the neurons co-cultured with Ctrl or REST-KO astrocytes exhibited the same amplitude and maximal rising slope of APs. However, neurons co-cultured with REST-KO astrocytes experienced a decreased amplitude of after-hyperpolarization, a phase that strictly depends on the extracellular K^+ concentration (**Fig. 8H, I**).

Collectively, these results show that neurons co-cultured with REST-KO primary astrocytes display increased intrinsic excitability that emerges under conditions of intense electrical activity. Whether these effects are causal consequences of the deficits in homeostatic proteins such as Kir4.1 and GLT-1 observed in the co-cultured REST-KO astrocytes remains to be established and warrants further studies.

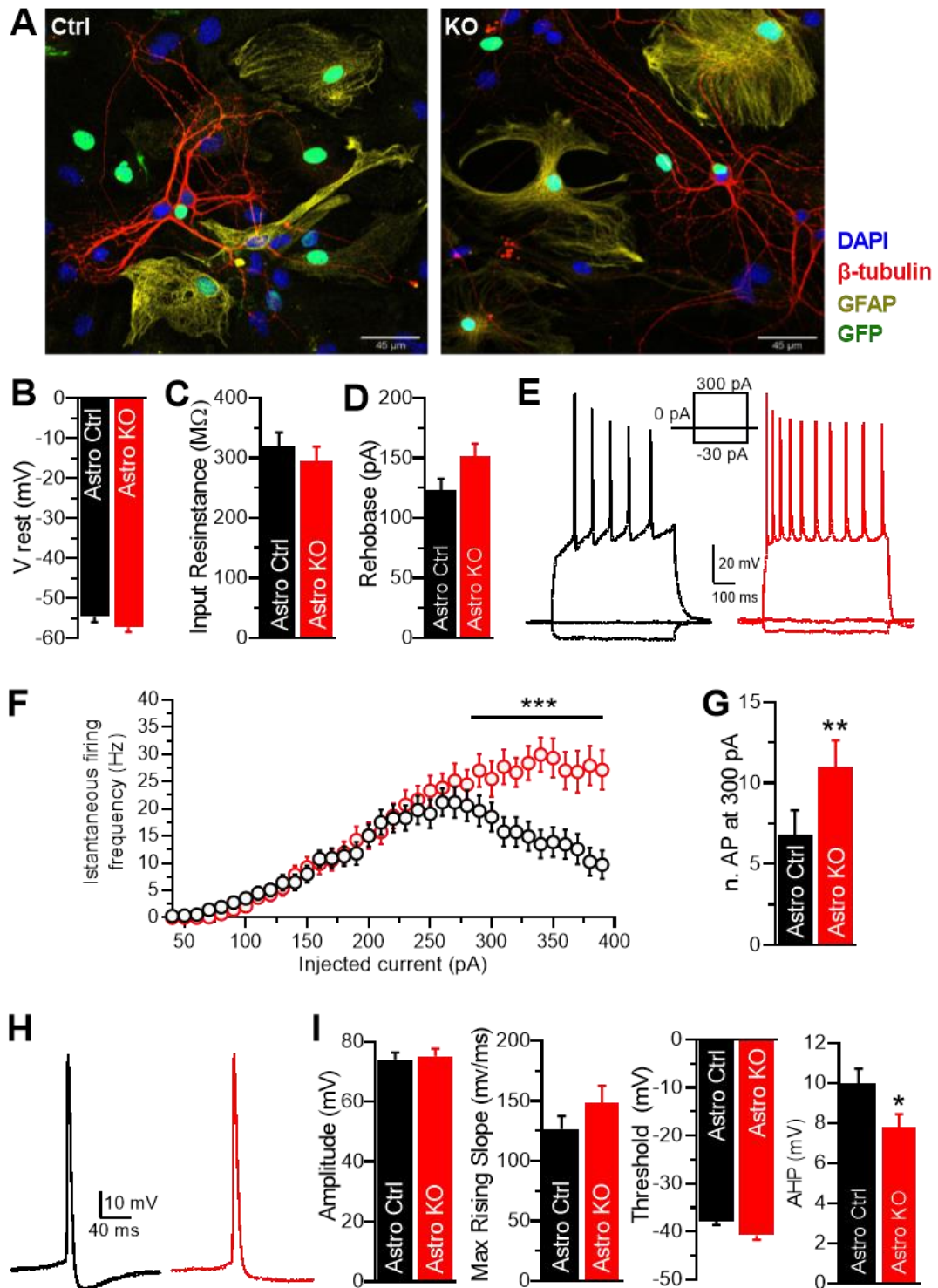


Figure 8. The excitability of neurons co-cultured with REST-KO astrocytes is increased at large current injections. A. Representative merged images of hippocampal neurons (14 div) co-cultured with Ctrl and REST-KO astrocytes. Cells were immunostained with DAPI (blue, nuclei), β -tubulin (red,

neurons), GFAP (yellow, astrocytes), and GFP (green, Ctrl/KO infected cells). Scale bar, 45 μ m. **B.** Neuronal resting membrane potential was not significantly different between the two groups. **C, D.** Bar-graph of neuronal R_{input} (**C**) and rheobase (**D**) recorded in neurons co-cultured with Ctrl/REST-KO astrocytes. **E.** Representative current-clamp recordings of neuronal APs induced by the injection of -30, 0 and +300 pA steps for 1 s in neurons co-cultured with Ctrl (black) and REST-KO (red) astrocytes. **F.** Instantaneous firing frequency as a function of injected current for neurons co-cultured with Ctrl and REST-KO astrocytes. In the presence of REST-KO astrocytes, neurons displayed a higher evoked instantaneous firing frequency with a significant difference observed at large current injections (>300 pA). **G.** Number of APs evoked at 300 pA of injected current in neurons co-cultured with Ctrl and REST-KO astrocytes. **H.** Representative traces of the shape of the first AP evoked by minimal current injection recorded in neurons co-cultured with Ctrl (black) and REST-KO (red) astrocytes. **I.** Values of the AP amplitude, maximum rising slope, threshold and after-hyperpolarization potential (AHP) estimated in neurons co-cultured with Ctrl (black) and REST-KO (red) astrocytes. All data are expressed as means \pm SEM with n=56 and n=55 for neurons co-cultured with Ctrl and REST-KO astrocytes, respectively, from 8 independent cultures. *p<0.05; **p<0.01, Student's *t*-test/Mann Whitney's *U*-test.

We have previously shown that silencing REST impairs GLT-1 expression and functionality. Thus, we tested the hypothesis that a decrease in the clearance of glutamate in the synaptic environment by perisynaptic astrocytes enhances post-synaptic activity. To this end, we studied the mEPSCs in wild-type hippocampal neurons co-cultured with either Ctrl or REST-KO astrocytes (**Fig. 9A**).

A significant increase in the amplitude in neurons co-cultured with REST-KO astrocytes (**Fig. 9B**) was observed, while the mEPSC frequency, charge, decay, and rise times (**Figure C–F**) were not significantly altered.

Since the mEPSC frequency depends on both the density of active synapses impinging onto the patched neuron and the probability of release of single vesicles, while the mEPSC amplitude reflects the quantal size, i.e., the neurotransmitter content of a single synaptic vesicle and the density of postsynaptic receptors²⁶⁹, the specific increase in amplitude indicates a more intense postsynaptic effect of single glutamate quanta that, in the absence of changes in neuronal properties can be attributed to a lower clearance/uptake of the released glutamate by perisynaptic REST-KO astrocytes.

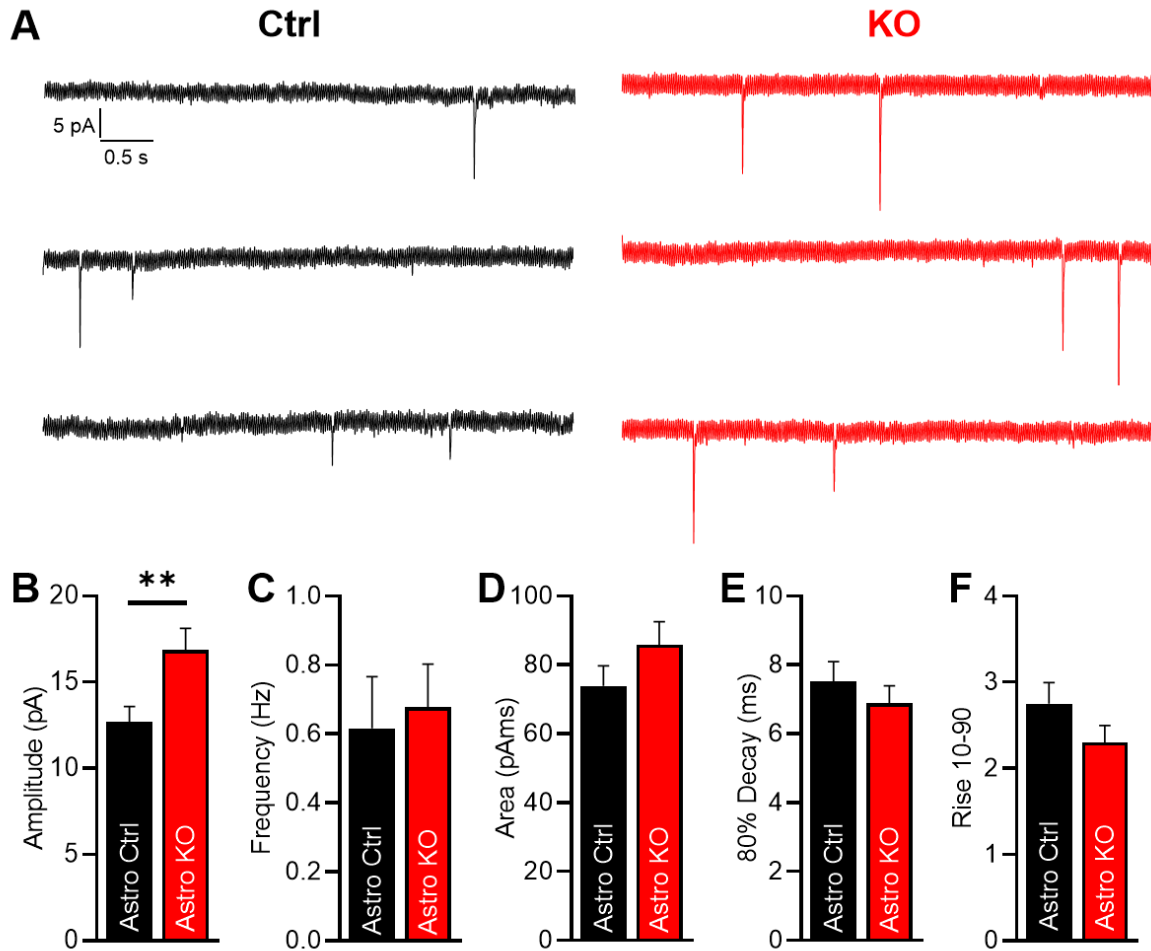


Figure 9. mEPSCs of neurons co-cultured with REST-KO astrocytes reveal a postsynaptic effect. **A.** Representative traces of mEPSCs from wild-type hippocampal neurons co-cultured with either Ctrl (black) or REST-KO (red) astrocytes. **B-F.** Analysis of mEPSCs. From left to right, mEPSC amplitude, frequency, area (charge), 80% decay time, and 10%-90% rise time are shown. Data are expressed as means \pm SEM with n=30 and n=34 for neurons co-cultured with Ctrl and REST-KO astrocytes, respectively, from 4 independent cultures. **p<0.05, Student's *t*-test/Mann Whitney's *U*-test.

7. Discussion

Functional relevance of REST in astrocyte functions

REST was initially known for its ability to repress the expression of neuronal genes in non-neuronal tissues^{2,10}, such as astrocytes. A number of studies have confirmed that it also plays a major role in orchestrating the lineage and maintenance of the astrocyte phenotype^{13,75,80}. Once astrocytes are differentiated, REST persists, repressing the expression of neuron-specific genes containing the RE-1 binding site^{1,80}. Previous studies have shown that deletion of REST in astrocytes resulted in de-repression of neuronal genes, supporting the assumption that REST prevents the development of the neuronal phenotype in astrocytic cells¹. Recently, it has been shown that REST, by binding to RE-1 consensus sites, can also activate and enhance gene transcription in astrocytes^{268,270-272}.

Within the nervous tissue, astrocytes play central roles maintaining bidirectional communication with neurons and buffering ions and molecules that are released during normal and sustained firing and synaptic activity^{137,138}. During neuronal activity, the extracellular K⁺ concentration is temporarily elevated causing depolarization of nearby membranes. Astrocytes play a key role in the control of K⁺_{ext} homeostasis by Kir channels, avoiding the hyperexcitation of the neuronal network associated with increased extracellular K⁺_{ext}¹⁸¹. Although several Kir channel subtypes are present in glial cells, numerous lines of evidence consistently reveal that Kir4.1 is the major pore-forming subunit in these cells and is directly linked to astrocyte function^{180,182,273,274}. In this context, several data obtained in spinal and cortical astrocytes further prove that the genetic deletion of Kir4.1 is sufficient to dramatically reduce the K⁺ permeability mediated by Kir channels^{180,264}.

One of the most important astrocytic functions is the clearance of synaptically released glutamate that terminates the synaptic action of the transmitter. Potassium buffering by astrocyte is directly linked with the uptake of released glutamate. Indeed, glutamate clearance by astrocytes occurs via GLT-1 and GLAST transporters, which function much more efficiently at negative resting potentials, made possible by Kir4.1.

The goal of the thesis work was to determine if and how the absence of REST affects the physiology of astrocytes and how these changes reflect neuronal physiology. To avoid the compensatory effects of constitutive KO of genes, we induced an acute deletion of the REST gene in primary cortical astrocytes from a conditional cKO mouse (Cre/REST^{fl/fl}) using lentiviruses expressing mutant (Ctrl) or functional (KO) Cre recombinase.

REST and astrocyte K⁺ buffering

REST KO does not alter astrocyte morphology or induce astrocyte activation. However, astrocytes in which REST was deleted experience a dramatic reduction of inward current accompanied by a marked depolarization of resting membrane potential, indicating that REST-KO astrocytes lack either an inward cationic current or an outward anion current (i.e., chloride current). This is also evident by the values of V_{rest} at zero current, which are positive in REST-KO astrocytes and by the increased R_{input} , both indicators of impairment of a K⁺ conductance. It is known that astrocytes are characterized by a highly selective membrane permeability to K⁺ and a negative resting potential²⁷⁵. Thus, the positively shifted V_{rest} , the augmented R_{input} and the reduction of inward current can all be explained by a specific loss of a Kir4.1-related current. Our findings are consistent with previous reports based on studies of retinal Muller cells, spinal oligodendrocytes, and complex glia in CA1 *stratum radiatum* in which a lack of Kir4.1 was shown to depolarize the resting membrane potential of glial cells associated with complete loss of inward currents^{177,182,273}.

We employed biophysical and pharmacological tools to demonstrate that the impairment in Kir4.1 function was the main signature of REST deletion in astrocytes. A typical distinctive feature given by Kir4.1 expression is that the inward current increases with increasing K⁺_{ext} concentration (in proportion of the square root of K⁺_{ext})^{276,277}. Indeed, REST KO astrocytes are not able to change the V_{rev} to more positive values in response to the E_K change. This alteration indicates that there are not sufficient K⁺ channels available to support the entry of K⁺ ions into the cell. The involvement of Kir4.1 channels is also confirmed by the absence of effect of Ba²⁺ in REST-KO cells²⁷⁸, a

treatment that, as observed in previous studies, causes a depolarization of astrocyte membrane depolarizes up to 35 mV²⁷⁸. Biophysical and pharmacological tests indicate that in astrocytes the probability of Kir4.1 opening at resting membrane potentials is high. This contributes to their negative resting membrane potential near the E_K ²⁷⁹ and to a large portion of K⁺ permeability, which, in turn, is required for extracellular K⁺ clearance. In REST KO astrocytes, the resulting opening probability of Kir4.1 is impaired, suggesting that the channel may be directly or indirectly regulated by REST.

Changes in Kir4.1 expression have been recently related to a dysregulation of immune-inflammatory function of astrocytes, inducing seizure generation in epilepsy of various etiologies^{263,280,281}. It has been observed that after *status epilepticus*, a peak in expression of IL1 β in the temporal cortex occurs in concomitance with a strong reduction in the expression of Kir4.1 mRNA, suggesting that IL1 β regulates Kir4.1²⁶³. Interestingly, REST-KO astrocytes are also insensitive to prolonged treatment with IL1 β , further indicating that REST silencing results in negative modulation or a reduction of membrane expression of astrocyte Kir4.1 channels. Our hypothesis was supported by surface biotinylation experiments, which confirmed that the membrane expression of Kir4.1 in REST-KO astrocytes is indeed significantly decreased. In the absence of gross changes in the total astrocyte expression of Kir4.1, consistent with the absence of RE-1 sites in the promoter region of the *Kcnj10* gene, these data suggest that REST controls Kir4.1 channel trafficking and membrane localization at the post-transcriptional level, by regulating some other factor responsible for Kir4.1 membrane targeting.

Hence, it is obvious that if a high concentration of K⁺ in the extracellular space, following sustained neuronal activity, is not buffered by astrocytes, it can cause general neuronal network hyperexcitability. In this context, a fine-tuning of the Kir4.1 expression and function is functionally relevant. In fact, it has been demonstrated that K⁺ channel expression and function is involved in the pathogenesis of a variety of neurological diseases including ischemia, HD, ALS, AD, and epilepsy^{184–189}. Several studies have established that Kir4.1 channels are down-regulated in regions interested by injury^{179,282}. Such observations strongly indicate that the functional expression of astrocytic Kir4.1 *in vivo* can be regulated in a variety of physio-pathological conditions²⁸³.

REST and astrocyte glutamate transport

The alteration of ion gradients and membrane depolarization resulting from Kir4.1 deficiency can result in a reduced activity of other ion gradient- and voltage-dependent transporters. Indeed, these alterations have been shown to affect glutamate transporter function and occasionally cause transporter reversion with release of glutamate^{284,285}. Astrocytes express high levels of Na⁺-dependent excitatory amino acid transporters (EAATs) that localize in the proximity of glutamatergic synapses and perform properly at very negative membrane potentials near the E_K: EEAT1 or GLAST and EEAT2 or GLT-1. In particular, the latter transporter is responsible for 90% of the clearance of glutamate released into the synaptic cleft¹⁹⁸.

Thus, we tested the possibility that the decrease in Kir4.1 currents by REST KO results in an impaired glutamate uptake by GLT-1. Indeed, REST knocked out astrocytes show an impaired glutamate uptake that is not further affected by Ba²⁺-mediated blockade of Kir4.1 channels. This phenotype is due to a decreased transcription of the GLT-1 gene in REST KO astrocytes associated with a decreased membrane targeting of the transporter. The decreased expression of GLT-1 mRNA and protein after REST KO is in full agreement with a recent report showing a positive transcriptional effect of REST on the GLT-1 gene²⁶⁸. Indeed, it has been shown that, although the main action of REST is to repress a variety of target genes, the occupancy of promoter RE-1 sites can occasionally induce transcriptional activation^{272,286,287}.

REST KO astrocyte profoundly alter neuronal network activity

Extracellular K⁺ and glutamate clearance are among the fundamental functions of astrocytes, as they prevent hyperexcitability in the neuronal network^{288,289}. It has been shown that a functional failure in the regulation of extracellular K⁺ and glutamate homeostasis negatively impacts on neuronal network excitability^{182,225,282}. In particular, an impairment of the Kir4.1 subtypes leads to hyperexcitability of the perisynaptic environment and results in seizure susceptibility in both mice and humans^{184,189}. Furthermore, a decrease in the expression and function of glial EAATs was found to be

associated with the chronic phase of epilepsy in either rodents or humans. EAAT2-KO, in particular, leads to seizures and death in mice^{239,241}. Because both Kir4.1 and GLT-1 are downregulated in REST-KO astrocytes, we thought that these changes may affect excitatory neurotransmission. Indeed, normal neurons cultured with REST-deleted astrocytes exhibit impaired after-hyperpolarization potentials following APs and dramatically increased firing frequencies evoked by strongly depolarizing current pulses. These results are highly suggestive of an impaired extracellular K⁺ buffering by REST-KO astrocytes and indicate that neurons co-cultured with astrocytes lacking REST become hyperexcitable.

On the other hand, impaired glutamate clearance may also alter neuronal network activity by hyperactivating post-synaptic AMPA receptors. This possibility was also addressed in a synaptic environment influenced by the presence of REST KO astrocytes co-cultured with normal neurons. Under these conditions, mEPSCs of co-cultured neurons are characterized by augmented mEPSC amplitude, indicative of an increased quantum size of released glutamate that may reflect a higher amount of glutamate retention in the perisynaptic space due to impaired glutamate clearance by astrocyte perisynaptic endfeet. The impact of this result is noteworthy, since the deficit in GLT-1 can be partially compensated by other glutamate transporters expressed by astrocytes, such as GLAST. However, the latter transporter, that normally contributes to a small fraction of glutamate uptake, was recently shown not to be affected by REST²⁶⁸.

REST and the inter-relationships between astrocyte Kir4.1 and GLT-1

REST deletion in astrocytes result in an impaired function, but not altered expression, of Kir4.1, consistent with the fact that *Kcnj10* is not a direct REST target gene. The concomitant changes in GLT-1 can explain this strict interdependence between Kir4.1 channel functionality and expression of REST protein. It is known that Kir4.1 conductance affects the strength of electrogenic glutamate uptake in a dual manner: (i) it sets the level of astrocyte membrane potential, thus providing the driving force for transport; and (ii) it limits the spread of transport-associated electrical signals by providing a large shunt conductance^{171,182,261,290,291}. It has also been shown that Kir4.1

KO or Ba²⁺-mediated inhibition are associated with significant reductions in glutamate transport by GLT-1, providing evidence for the tight coupling of the two transporters^{292,293}. In addition, previous data^{212,294,295} have shown that both Kir4.1 channels and GLT-1 co-distribute in spots on astrocyte processes wrapping glutamatergic synapses by forming supramolecular complexes.

Much less is known on the reverse effect, i.e., the possibility that primary changes in GLT-1 expression, membrane targeting and/or activity affect the function of Kir4.1 channels. REST has been recently shown to increase GLT-1 expression at the transcriptional level by directly binding the two RE-1 sites present in the GLT-1 promoter²⁶⁸, a report that is fully consistent with the significant decrease in GLT-1 mRNA and protein we observed in REST KO astrocytes.

This study helps reveal the role of REST in non-neuronal cells and, concurrently, adds new insights into the role of Kir4.1 and GLT-1 in astrocyte physiopathology. The effects of REST in astrocytes, uncovered by REST deletion, are coherent with an overall homeostatic function of REST in the nervous tissue under physiological conditions. It has been shown that the low levels of REST expression in neurons can be increased by hyperactivity, resulting in a downscaling of intrinsic excitability and excitatory synapses and a concomitant upscaling of inhibitory synapses onto excitatory neurons^{113,296,297}. Here, we show that the high constitutive levels of REST in astrocytes tonically support GLT-1 expression and, through GLT-1/Kir4.1 supramolecular relationships, the membrane exposure and function of Kir4.1 channels. This reveals a previously unknown role of astrocyte REST in homeostatic plasticity by boosting K⁺ buffering and glutamate clearance, which are the paramount “housekeeping” functions of astrocytes in the brain environment. Such multi-faceted homeostatic mechanisms could be exploited as a target for therapies aimed at neurological diseases caused by network hyperexcitability, such as epilepsy and other CNS disorders.

8. Conclusions

The results presented in this thesis demonstrate that REST positively modulates inward K^+ currents mediated by Kir4.1, notwithstanding the fact that the Kir4.1 gene promoter lacks RE-1 binding sites. The associated impairment in the expression and function of GLT-1 glutamate transporter in the absence of REST, confirms the positive transcriptional effect of REST on the GLT-1 promoter. Moreover, it offers a molecular explanation for the observed impairment in Kir4.1 function, given the fact that these two membrane actuators work in concert on the astrocyte membrane. The functional changes observed in REST knocked out astrocytes are reflected by functional changes in wild type neurons co-cultured with them that denote a decrease in K^+ buffering and a decreased clearance of released glutamate. Overall, this study reveals an overall homeostatic role of REST in astrocytes and adds new insights into the role and regulation of Kir4.1 and GLT-1 in astrocyte function.

9. Bibliography

1. Abrajano, J. J. *et al.* Differential deployment of REST and CoREST promotes glial subtype specification and oligodendrocyte lineage maturation. *PLoS One* **4**, (2009).
2. Chong, J. A. *et al.* REST: A mammalian silencer protein that restricts sodium channel gene expression to neurons. *Cell* **80**, 949–957 (1995).
3. Schoenherr, C. J., & Anderson, D. J. The neuron-restrictive silencer factor (NRSF): a coordinate repressor of multiple neuron-specific genes. *Science (New York, N.Y.)*, **267**, 1360–1363 (1995).
4. Brivanlou, A. H. Should the master regulator Rest in peace? *Nat. Genet.* **20**, 109–110 (1998).
5. Hsieh, J. & Gage, F. H. Chromatin remodeling in neural development and plasticity. *Curr. Opin. Cell Biol.* **17**, 664–671 (2005).
6. Bruce, A. W. *et al.* Genome-wide analysis of repressor element 1 silencing transcription factor/neuron-restrictive silencing factor (REST/NRSF) target genes. *Proc. Natl. Acad. Sci. U. S. A.* **101**, 10458–10463 (2004).
7. Tang, Y., Jia, Z., Xu, H., Da, L. T. & Wu, Q. Mechanism of REST/NRSF regulation of clustered protocadherin α genes. *Nucleic Acids Res.* **49**, 4506–4521 (2021).
8. Zhao, Y. *et al.* Brain REST/NRSF Is Not Only a Silent Repressor but Also an Active Protector. *Mol. Neurobiol.* **54**, 541–550 (2017).
9. Prada, I. *et al.* REST/NRSF governs the expression of dense-core vesicle gliosecretion in astrocytes. *J. Cell Biol.* **193**, 537–549 (2011).
10. Schoenherr, C. J. & Anderson, D. J. Silencing is golden: negative regulation in the control of neuronal gene transcription. *Curr. Opin. Neurobiol.* **5**, 566–571 (1995).
11. Gao, Z. *et al.* The master negative regulator REST/NRSF controls adult neurogenesis by restraining the neurogenic program in quiescent stem cells. *J. Neurosci.* **31**, 9772–9786 (2011).
12. Palm, K., Belluardo, N., Metsis, M. & Timmusk, T. Neuronal expression of zinc finger transcription factor REST/NRSF/XBR gene. *J. Neurosci.* **18**, 1280–1296

- (1998).
13. Ballas, N., Grunseich, C., Lu, D. D., Speh, J. C. & Mandel, G. REST and its corepressors mediate plasticity of neuronal gene chromatin throughout neurogenesis. *Cell* **121**, 645–657 (2005).
 14. Lu, T. *et al.* REST and stress resistance in ageing and Alzheimer's disease. *Nature* **507**, 448–454 (2014).
 15. Ooi, L. & Wood, I. C. Chromatin crosstalk in development and disease: Lessons from REST. *Nat. Rev. Genet.* **8**, 544–554 (2007).
 16. Coulson, J. M., Edgson, J. L., Woll, P. J. & Quinn, J. P. A splice variant of the neuron-restrictive silencer factor repressor is expressed in small cell lung cancer: A potential role in derepression of neuroendocrine genes and a useful clinical marker. *Cancer Res.* **60**, 1840–1844 (2000).
 17. Koenigsberger, C., Chicca, J. J., Amoureux, M. C., Edelman, G. M. & Jones, F. S. Differential regulation by multiple promoters of the gene encoding the neuron-restrictive silencer factor. *Proc. Natl. Acad. Sci. U. S. A.* **97**, 2291–2296 (2000).
 18. Kojima, T., Murai, K., Naruse, Y., Takahashi, N. & Mori, N. Cell-type non-selective transcription of mouse and human genes encoding neural-restrictive silencer factor. *Mol. Brain Res.* **90**, 174–186 (2001).
 19. Nakano, Y. *et al.* Defects in the Alternative Splicing-Dependent Regulation of REST Cause Deafness. *Cell* **174**, 536-548.e21 (2018).
 20. Chen, G. L. & Miller, G. M. Extensive Alternative Splicing of the Repressor Element Silencing Transcription Factor Linked to Cancer. *PLoS One* **8**, (2013).
 21. Faronato, M. & Coulson, J. REST (RE1-silencing transcription factor). *Atlas Genet. Cytogenet. Oncol. Haematol.* **15**:208-213 (2011).
 22. Palm, K., Metsis, M. & Timmusk, T. Neuron-specific splicing of zinc finger transcription factor REST/NRSF/XBR is frequent in neuroblastomas and conserved in human, mouse and rat. *Mol. Brain Res.* **72**, 30–39 (1999).
 23. Shimojo, M., Paquette, A. J., Anderson, D. J. & Hersh, L. B. Protein Kinase A Regulates Cholinergic Gene Expression in PC12 Cells: REST4 Silences the Silencing Activity of Neuron-Restrictive Silencer Factor/REST. *Mol. Cell. Biol.* **19**, 6788–6795

- (1999).
24. Lee, J. H., Shimojo, M., Chai, Y. G. & Hersh, L. B. Studies on the interaction of REST4 with the cholinergic repressor element-1/neuron restrictive silencer element. *Mol. Brain Res.* **80**, 88–98 (2000).
 25. Raj, B. *et al.* Cross-Regulation between an Alternative Splicing Activator and a Transcription Repressor Controls Neurogenesis. *Mol. Cell* **43**, 843–850 (2011).
 26. Chen, G.-L. & Miller, G. M. Disorders of the Nervous System Alternative REST Splicing Underappreciated. **5**, 2–7 (2018).
 27. Wagoner, M. P., Gunsalus, K. T. W., Schoenike, B., Richardson, A. L. & Roopra, A. The Transcription Factor REST Is Lost in Aggressive Breast Cancer. **6**, (2010).
 28. Lee, A. R., Che, N., Lovnicki, J. M., Dong, X. & Lee, A. R. Development of Neuroendocrine Prostate Cancers by the Ser/Arg Repetitive Matrix 4-Mediated RNA Splicing Network. **8**, (2018).
 29. Kreisler, A. *et al.* Regulation of the NRSF/REST gene by methylation and CREB affects the cellular phenotype of small-cell lung cancer. *Oncogene* **29**, 5828–5838 (2010).
 30. Ravache, M., Weber, C., Mérienne, K. & Trottier, Y. Transcriptional activation of REST by Sp1 in huntington’s disease models. *PLoS One* **5**, (2010).
 31. Canzonetta, C. *et al.* DYRK1A-Dosage Imbalance Perturbs NRSF/REST Levels, Deregulating Pluripotency and Embryonic Stem Cell Fate in Down Syndrome. *Am. J. Hum. Genet.* **83**, 388–400 (2008).
 32. Datta, M. & Bhattacharyya, N. P. Regulation of RE1 protein silencing transcription factor (REST) expression by HIP1 protein interactor (HIPPI). *J. Biol. Chem.* **286**, 33759–33769 (2011).
 33. Nishihara, S., Tsuda, L. & Ogura, T. The canonical Wnt pathway directly regulates NRSF/REST expression in chick spinal cord. *Biochem. Biophys. Res. Commun.* **311**, 55–63 (2003).
 34. Packer, A. N., Xing, Y., Harper, S. Q., Jones, L. & Davidson, B. L. The bifunctional microRNA miR-9/miR-9* regulates REST and CoREST and is downregulated in Huntington’s disease. *J. Neurosci.* **28**, 14341–14346 (2008).

35. Liu, J. J. *et al.* miR-218 involvement in cardiomyocyte hypertrophy is likely through targeting REST. *Int. J. Mol. Sci.* **17**, (2016).
36. Westbrook, T. F. *et al.* Westbrook et al., 2008 SCF β TRCP Controls Oncogenic Transformation and Neural Differentiation Through REST Degradation.pdf. *Nature* **452**, 370–374 (2008).
37. Guardavaccaro, D., Frescas, D., Dorrello, N. V., Peschiaroli, A., Multani, A. S., Cardozo, T., Lasorella, A., Iavarone, A., Chang, S., Hernando, E., & Pagano, M. Control of chromosome stability by the beta-TrCP-REST-Mad2 axis. *Nature*, **452**, 365–369 (2008).
38. Nesti, E. Harnessing the master transcriptional repressor rest to reciprocally regulate neurogenesis. *Neurogenesis* **2**, (2015).
39. Kaneko, N., Hwang, J. Y., Gertner, M., Pontarelli, F. & Suzanne Zukin, R. Casein Kinase 1 suppresses activation of REST in insulted hippocampal neurons and halts ischemia-induced neuronal death. *J. Neurosci.* **34**, 6030–6039 (2014).
40. Karlin, K. L., Mondal, G., Hartman, J. K., Tyagi, S., Kurley, S. J., Bland, C. S., Hsu, T. Y., Renwick, A., Fang, J. E., Migliaccio, I., Callaway, C., Nair, A., Dominguez-Vidana, R., Nguyen, D. X., Osborne, C. K., Schiff, R., Yu-Lee, L. Y., Jung, S. Y., Edwards, D. P., Hilsenbeck, S. G., ... Westbrook, T. F. The oncogenic STP axis promotes triple-negative breast cancer via degradation of the REST tumor suppressor. *Cell reports.* **9**, 1318–1332. (2014).
41. Nesti, E., Corson, G. M., McCleskey, M., Oyer, J. A. & Mandel, G. C-terminal domain small phosphatase 1 and MAP kinase reciprocally control REST stability and neuronal differentiation. *Proc. Natl. Acad. Sci. U. S. A.* **111**, E3929–E3936 (2014).
42. Burkholder, N. T. *et al.* Phosphatase activity of small C-terminal domain phosphatase 1 (SCP1) controls the stability of the key neuronal regulator RE1-silencing transcription factor (REST). *J. Biol. Chem.* **293**, 16851–16861 (2019).
43. Huang, Z. *et al.* Deubiquitylase HAUSP stabilizes REST and promotes maintenance of neural progenitor cells. *Nat. Cell Biol.* **13**, 142–152 (2011).
44. Chen, R., Li, Y., Buttyan, R. & Dong, X. Implications of PI3K/AKT inhibition on REST

- protein stability and neuroendocrine phenotype acquisition in prostate cancer cells. *Oncotarget* **8**, 84863–84876 (2017).
45. Conaco, C., Otto, S., Han, J. J. & Mandel, G. Reciprocal actions of REST and a microRNA promote neuronal identity. *Proc. Natl. Acad. Sci. U. S. A.* **103**, 2422–2427 (2006).
 46. Zuo, Z. *et al.* Why Do Long Zinc Finger Proteins have Short Motifs? *bioRxiv* **30**, (2019).
 47. Miller, J., McLachlan, A. D. & Klug, A. Repetitive zinc-binding domains in the protein transcription factor IIIA from *Xenopus* oocytes. *EMBO J.* **4**, 1609–1614 (1985).
 48. Najafabadi, H. S. *et al.* C2H2 zinc finger proteins greatly expand the human regulatory lexicon. *Nat. Biotechnol.* **33**, 555–562 (2015).
 49. Andres, M. E. *et al.* CoREST: A functional corepressor required for regulation of neural- specific gene expression. *Proc. Natl. Acad. Sci. U. S. A.* **96**, 9873–9878 (1999).
 50. Ballas, N. *et al.* Regulation of neuronal traits by a novel transcriptional complex. *Neuron* **31**, 353–365 (2001).
 51. Wu, Q. *et al.* The BRG1 ATPase of human SWI/SNF chromatin remodeling enzymes as a driver of cancer. *Epigenomics* **9**, 919–931 (2017).
 52. Ooi, L., Belyaev, N. D., Miyake, K., Wood, I. C. & Buckley, N. J. BRG1 chromatin remodeling activity is required for efficient chromatin binding by repressor element 1-silencing transcription factor (REST) and facilitates REST-mediated repression. *J. Biol. Chem.* **281**, 38974–38980 (2006).
 53. Roopra, A. *et al.* Transcriptional Repression by the Neuron-Restrictive Silencer Factor (REST/NRSF) is Mediated via the Sin3/Histone Deacetylase complex. *Biochem. Soc. Trans.* **28**, A88–A88 (2000).
 54. Roopra, A., Qazi, R., Schoenike, B., Daley, T. J. & Morrison, J. F. Localized domains of G9a-mediated histone methylation are required for silencing of neuronal genes. *Mol. Cell* **14**, 727–738 (2004).
 55. Murai, K., Naruse, Y., Shaul, Y., Agata, Y. & Mori, N. Direct interaction of NRSF with

- TBP: Chromatin reorganization and core promoter repression for neuron-specific gene transcription. *Nucleic Acids Res.* **32**, 3180–3189 (2004).
56. Yeo, M. *et al.* Small CTD phosphatases function in silencing neuronal gene expression. *Science (80-.)*. **307**, 596–600 (2005).
 57. Ballas, N. & Mandel, G. The many faces of REST oversee epigenetic programming of neuronal genes. *Curr. Opin. Neurobiol.* **15**, 500–506 (2005).
 58. Lunyak, V. V., Prefontaine, G. G. & Rosenfeld, M. G. REST and peace for the neuronal-specific transcriptional program. *Ann. N. Y. Acad. Sci.* **1014**, 110–120 (2004).
 59. Sugitani, Y., Ogawa, M. & Noda, T. Neocortical development. *Tanpakushitsu Kakusan Koso.* **49**, 247–254 (2004).
 60. Miller, F. D. & Gauthier, A. S. Timing Is Everything: Making Neurons versus Glia in the Developing Cortex. *Neuron* **54**, 357–369 (2007).
 61. Noctor, S. C., Martinez-Cerdeño, V., Ivic, L. & Kriegstein, A. R. Cortical neurons arise in symmetric and asymmetric division zones and migrate through specific phases. *Nat. Neurosci.* **7**, 136–144 (2004).
 62. Rash, B. G. & Grove, E. A. Area and layer patterning in the developing cerebral cortex. *Curr. Opin. Neurobiol.* **16**, 25–34 (2006).
 63. Kwan, K. Y., Šestan, N. & Anton, E. S. Transcriptional co-regulation of neuronal migration and laminar identity in the neocortex. *Development* **139**, 1535–1546 (2012).
 64. O'Leary, D. D., & Sahara, S. Genetic regulation of arealization of the neocortex. *Current opinion in neurobiology*, **18**, 90–100 (2008)
 65. Kang, P. *et al.* Sox9 and NFIA Coordinate a Transcriptional Regulatory Cascade during the Initiation of Gliogenesis. *Neuron* **74**, 79–94 (2012).
 66. Deneen, B. *et al.* The Transcription Factor NFIA Controls the Onset of Gliogenesis in the Developing Spinal Cord. *Neuron* **52**, 953–968 (2006).
 67. Stolt, C. C. *et al.* The Sox9 transcription factor determines glial fate choice in the developing spinal cord. *Genes Dev.* **17**, 1677–1689 (2003).
 68. Molofsky, A. V. & Deneen, B. Astrocyte development: A Guide for the Perplexed.

- Glia* **63**, 1320–1329 (2015).
69. Ullian, E. M., Christopherson, K. S. & Barres, B. A. Role for glia in synaptogenesis. *GLIA* vol. 47 209–216 (2004).
 70. Kanski, R., Van Strien, M. E., Van Tijn, P. & Hol, E. M. A star is born: New insights into the mechanism of astrogenesis. *Cell. Mol. Life Sci.* **71**, 433–447 (2014).
 71. Nechiporuk, T. *et al.* The REST remodeling complex protects genomic integrity during embryonic neurogenesis. *Elife* **5**, 1–28 (2016).
 72. Chen, Z. F., Paquette, A. J. & Anderson, D. J. NRSF/REST is required in vivo for repression of multiple neuronal target genes during embryogenesis. *Nat. Genet.* **20**, 136–142 (1998).
 73. Singh, S. K., Kagalwala, M. N., Parker-Thornburg, J., Adams, H. & Majumder, S. REST maintains self-renewal and pluripotency of embryonic stem cells. *Nature* **453**, 223–227 (2008).
 74. Hwang, J. Y., & Zukin, R. S. REST, a master transcriptional regulator in neurodegenerative disease. *Current opinion in neurobiology*, **48**, 193–200 (2018).
 75. Abrajano, J. J. *et al.* REST and CoREST modulate neuronal subtype specification, maturation and maintenance. *PLoS One* **4**, (2009).
 76. Negrini, S., Prada, I., D’Alessandro, R. & Meldolesi, J. REST: An oncogene or a tumor suppressor? *Trends Cell Biol.* **23**, 289–295 (2013).
 77. Mukherjee, S., Brulet, R., Zhang, L. & Hsieh, J. REST regulation of gene networks in adult neural stem cells. *Nat. Commun.* **7**, 1–14 (2016).
 78. Bergsland, M., Covacu, R., Perez Estrada, C., Svensson, M. & Brundin, L. Nitric oxide-induced neuronal to glial lineage fate-change depends on NRSF/REST function in neural progenitor cells. *Stem Cells* **32**, 2539–2549 (2014).
 79. Guillemot, F. Cell fate specification in the mammalian telencephalon. *Prog. Neurobiol.* **83**, 37–52 (2007).
 80. Kohyama, J. *et al.* BMP-induced REST regulates the establishment and maintenance of astrocytic identity. *J. Cell Biol.* **189**, 159–170 (2010).
 81. Imayoshi, I. & Kageyama, R. Review bHLH Factors in Self-Renewal , Multipotency , and Fate Choice of Neural Progenitor Cells. *Neuron* **82**, 9–23 (2014).

82. Lee, H., Tan, K., Cheah, P. & Ling, K. Potential Role of JAK-STAT Signaling Pathway in the Neurogenic-to-Gliogenic Shift in Down Syndrome Brain. **2016**, (2016).
83. Tanigaki, K. *et al.* Notch1 and Notch3 instructively restrict bFGF-responsive multipotent neural progenitor cells to an astroglial fate. *Neuron* **29**, 45–55 (2001).
84. Namihira, M. *et al.* Committed Neuronal Precursors Confer Astrocytic Potential on Residual Neural Precursor Cells. *Dev. Cell* **16**, 245–255 (2009).
85. Nakashima, K. *et al.* BMP2-mediated alteration in the developmental pathway of fetal mouse brain cells from neurogenesis to astrocytogenesis. *Proc. Natl. Acad. Sci. U. S. A.* **98**, 5868–5873 (2001).
86. He, F. *et al.* A positive autoregulatory loop of Jak-STAT signaling controls the onset of astroglialogenesis. *Nat. Neurosci.* **8**, 616–625 (2005).
87. Covey, M. V., Streb, J. W., Spektor, R. & Ballas, N. REST regulates the pool size of the different neural lineages by restricting the generation of neurons and oligodendrocytes from neural stem/progenitor cells. *Dev.* **139**, 2878–2890 (2012).
88. Covacu, R., Estrada, C. P., Arvidsson, L., Svensson, M. & Brundin, L. Change of Fate Commitment in Adult Neural Progenitor Cells Subjected to Chronic Inflammation. (2014) doi:10.1523/JNEUROSCI.0231-14.2014.
89. Covacu, R., Danilov, A. I., Rasmussen, B. S., Hallén, K., Moe, M. C., Lobell, A., Johansson, C. B., Svensson, M. A., Olsson, T., & Brundin, L. Nitric oxide exposure diverts neural stem cell fate from neurogenesis towards astroglialogenesis. *Stem cells (Dayton, Ohio)*, **24**, 2792–2800 (2006).
90. Oberheim, N. A., Wang, X., Goldman, S. & Nedergaard, M. Astrocytic complexity distinguishes the human brain. *Trends Neurosci.* **29**, 547–553 (2006).
91. Volterra, A. & Meldolesi, J. Astrocytes, from brain glue to communication elements: The revolution continues. *Nature Reviews Neuroscience* vol. 6 626–640 (2005).
92. Garcia-Manteiga, J. M., D'alessandro, R. & Meldolesi, J. News about the role of the transcription factor REST in neurons: From physiology to pathology. *Int. J. Mol. Sci.* **21**, (2020).
93. Rodenas-Ruano, A., Chávez, A. E., Cossio, M. J., Castillo, P. E., & Zukin, R. S. REST-

- dependent epigenetic remodeling promotes the developmental switch in synaptic NMDA receptors. *Nature neuroscience*, **15**, 1382–1390 (2012).
94. Loe-Mie, Y. *et al.* SMARCA2 and other genome-wide supported schizophrenia-associated genes: Regulation by REST/NRSF, network organization and primate-specific evolution. *Hum. Mol. Genet.* **19**, 2841–2857 (2010).
 95. Zuccato, C. *et al.* Huntingtin interacts with REST/NRSF to modulate the transcription of NRSE-controlled neuronal genes. *Nat. Genet.* **35**, 76–83 (2003).
 96. Shimojo, M. Huntingtin regulates RE1-silencing transcription factor/neuron-restrictive silencer factor (REST/NRSF) nuclear trafficking indirectly through a complex with REST/NRSF-interacting LIM domain protein (RILP) and dynactin p150 Glued. *J. Biol. Chem.* **283**, 34880–34886 (2008).
 97. Suo, H., Wang, P., Tong, J., Cai, L., Liu, J., Huang, D., Huang, L., Wang, Z., Huang, Y., Xu, J., Ma, Y., Yu, M., Fei, J., & Huang, F. NRSF is an essential mediator for the neuroprotection of trichostatin A in the MPTP mouse model of Parkinson's disease. *Neuropharmacology*, **99**, 67–78. (2015).
 98. Yu, M. *et al.* NRSF/REST neuronal deficient mice are more vulnerable to the neurotoxin MPTP. *Neurobiol. Aging* **34**, 916–927 (2013).
 99. Baldelli, P. & Meldolesi, J. The transcription repressor REST in adult neurons: Physiology, pathology, and diseases. *eNeuro* **2**, (2015).
 100. Noh, K. M. *et al.* Repressor element-1 silencing transcription factor (REST)-dependent epigenetic remodeling is critical to ischemia-induced neuronal death. *Proc. Natl. Acad. Sci. U. S. A.* **109**, (2012).
 101. Calderone, A. *et al.* Ischemic insults derepress the gene silencer REST in neurons destined to die. *J. Neurosci.* **23**, 2112–2121 (2003).
 102. Liang, H., Geng, L., Shi, X., Zhang, C. & Wang, S. silencer factor knockdown promotes neurological recovery after ischemia. **8**, 101012–101025 (2017).
 103. Costigan, M., Scholz, J., & Woolf, C. J. Neuropathic pain: a maladaptive response of the nervous system to damage. *Annual review of neuroscience*, **32**, 1–32 (2009).
 104. Uchida, H., Sasaki, K., Ma, L. & Ueda, H. Neuron-restrictive silencer factor causes

- epigenetic silencing of Kv4.3 gene after peripheral nerve injury. *Neuroscience* **166**, 1–4 (2010).
105. Thompson, R. & Chan, C. NRSF and its epigenetic effectors: New treatments for neurological disease. *Brain Sci.* **8**, (2018).
 106. Blom, T. *et al.* Molecular genetic analysis of the REST/NRSF gene in nervous system tumors. *Acta Neuropathol.* **112**, 483–490 (2006).
 107. Lepagnol-Bestel, A. M. *et al.* Nrsf silencing induces molecular and subcellular changes linked to neuronal plasticity. *Neuroreport* **18**, 441–446 (2007).
 108. Su, X. *et al.* Abnormal Expression of REST/NRSF and Myc in Neural Stem/Progenitor Cells Causes Cerebellar Tumors by Blocking Neuronal Differentiation. *Mol. Cell. Biol.* **26**, 1666–1678 (2006).
 109. Conti, L. *et al.* REST Controls Self-Renewal and Tumorigenic Competence of Human Glioblastoma Cells. **7**, (2012).
 110. McClelland, S., Flynn, C., Dubé, C., Richichi, C., Zha, Q., Ghestem, A., Esclapez, M., Bernard, C., & Baram, T. Z. Neuron-restrictive silencer factor-mediated hyperpolarization-activated cyclic nucleotide gated channelopathy in experimental temporal lobe epilepsy. *Annals of neurology*, **70**, 454–464 (2011).
 111. McClelland, S. *et al.* The transcription factor NRSF contributes to epileptogenesis by selective repression of a subset of target genes. *Elife* **3**, e01267 (2014).
 112. Carminati, E. *et al.* Mild Inactivation of RE-1 Silencing Transcription Factor (REST) Reduces Susceptibility to Kainic Acid-Induced Seizures. **13**, 1–10 (2020).
 113. Pozzi, D. *et al.* REST / NRSF-mediated intrinsic homeostasis protects neuronal networks from hyperexcitability. **32**, 2994–3007 (2013).
 114. Bender, R. A. *et al.* Localization of HCN1 Channels to Presynaptic Compartments : Novel Plasticity That May Contribute to Hippocampal Maturation. **27**, 4697–4706 (2007).
 115. Shimojo, M. & Hersh, L. B. Characterization of the REST / NRSF-interacting LIM domain protein (RILP): localization and interaction with REST / NRSF. 1130–1138 (2006) doi:10.1111/j.1471-4159.2005.03608.x.
 116. Bassuk, A. G. *et al.* ARTICLE A Homozygous Mutation in Human PRICKLE1 Causes

- an Autosomal-Recessive Progressive Myoclonus Epilepsy-Ataxia Syndrome. *Am. J. Hum. Genet.* **83**, 572–581 (2008).
117. Charbord, J., Poydenot, P., Bonnefond, C., Feyeux, M., Casagrande, F., Brinon, B., Francelle, L., Aurégan, G., Guillermier, M., Cailleret, M., Viegas, P., Nicoleau, C., Martinat, C., Brouillet, E., Cattaneo, E., Peschanski, M., Lechuga, M., & Perrier, A. L. High throughput screening for inhibitors of REST in neural derivatives of human embryonic stem cells reveals a chemical compound that promotes expression of neuronal genes. *Stem cells (Dayton, Ohio)*, **31**, 1816–1828 (2013).
 118. Ueda, H., Kurita, J. I., Neyama, H., Hirao, Y., Kouji, H., Mishina, T., Kasai, M., Nakano, H., Yoshimori, A., & Nishimura, Y. A mimetic of the mSin3-binding helix of NRSF/REST ameliorates abnormal pain behavior in chronic pain models. *Bioorganic & medicinal chemistry letters*, **27**, 4705–4709 (2017).
 119. Hai-ying, C., Nagano, K., Ezzikouri, S. & Yamaguchi, C. Establishment of an intermittent cold stress model using *Tupaia belangeri* and evaluation of compound C737 targeting neuron-restrictive silencer factor. **65**, 285–292 (2016).
 120. Dobson, T., Hatcher, R. J., Swaminathan, J., Das, C. M., Shaik, S., Tao, R. H., Milite, C., Castellano, S., Taylor, P. H., Sbardella, G., & Gopalakrishnan, V. Regulation of *USP37* Expression by REST-Associated G9a-Dependent Histone Methylation. *Molecular cancer research : MCR*, **15**, 1073–1084 (2017).
 121. Kurita, J. I., Hirao, Y., Nakano, H., Fukunishi, Y., & Nishimura, Y. Sertraline, chlorprothixene, and chlorpromazine characteristically interact with the REST-binding site of the corepressor mSin3, showing medulloblastoma cell growth inhibitory activities. *Scientific reports*, **8**, 13763. (2018).
 122. Callegari, K., Maegawa, S., Bravo-alegria, J. & Gopalakrishnan, V. Pharmacological inhibition of LSD1 activity blocks REST-dependent medulloblastoma cell migration. 1–13 (2018).
 123. Dobson, T., Hatcher, R. J., Swaminathan, J., Das, C. M., Shaik, S., Tao, R. H., Milite, C., Castellano, S., Taylor, P. H., Sbardella, G., & Gopalakrishnan, V. Regulation of *USP37* Expression by REST-Associated G9a-Dependent Histone Methylation. *Molecular cancer research : MCR*, **15**, 1073–1084 (2017).

124. Liu, Y. *et al.* Demethylation of Repressor Element-1 Silencing Transcription (REST) Suppresses the Malignant Phenotype of Breast Cancer via MMP9. **25**, 445–454 (2017).
125. Minucci, S. *et al.* Valproic acid defines a novel class of HDAC inhibitors inducing differentiation of transformed cells. **20**, 6969–6978 (2001).
126. Didonna, A., & Opal, P. The promise and perils of HDAC inhibitors in neurodegeneration. *Annals of clinical and translational neurology*, **2**, 79–101. (2015).
127. Barres, B. A. The Mystery and Magic of Glia: A Perspective on Their Roles in Health and Disease. *Neuron* **60**, 430–440 (2008).
128. Pfrieger, F. W. & Barres, B. A. Synaptic efficacy enhanced by glial cells in vitro. *Science (80-.)*. **277**, 1684–1687 (1997).
129. Jensen, C. J., Massie, A. & De Keyser, J. Immune players in the CNS: The astrocyte. *J. Neuroimmune Pharmacol.* **8**, 824–839 (2013).
130. Allen, N. J. & Barres, B. A. Signaling between glia and neurons: Focus on synaptic plasticity. *Curr. Opin. Neurobiol.* **15**, 542–548 (2005).
131. Peters, A. A fourth type of neuroglial cell in the adult central nervous system. *J. Neurocytol.* **33**, 345–357 (2004).
132. Aloisi, F. Immune function of microglia. *Glia* **36**, 165–179 (2001).
133. Bradl, M. & Lassmann, H. Oligodendrocytes: Biology and pathology. *Acta Neuropathol.* **119**, 37–53 (2010).
134. Vasile, F., Dossi, E. & Rouach, N. Human astrocytes: structure and functions in the healthy brain. *Brain Struct. Funct.* **222**, 2017–2029 (2017).
135. Sofroniew, M. V. & Vinters, H. V. Astrocytes: Biology and pathology. *Acta Neuropathol.* **119**, 7–35 (2010).
136. Chung, W., Allen, N. J. & Eroglu, C. Astrocyte & synapse. *Cold Spring Harb. Lab. Press* **7**, 1–19 (2015).
137. Theodosis, D. T., Poulain, D. A. & Oliet, S. H. R. Activity-dependent structural and functional plasticity of astrocyte-neuron interactions. *Physiol. Rev.* **88**, 983–1008 (2008).

138. Haydon, P. G. Glia: Listening and talking to the synapse. *Nat. Rev. Neurosci.* **2**, 185–193 (2001).
139. Nedergaard, M., Ransom, B. & Goldman, S. A. New roles for astrocytes: Redefining the functional architecture of the brain. *Trends Neurosci.* **26**, 523–530 (2003).
140. Rossi, D. *et al.* Defective tumor necrosis factor- α -dependent control of astrocyte glutamate release in a transgenic mouse model of Alzheimer disease. *J. Biol. Chem.* **280**, 42088–42096 (2005).
141. Perea, G. & Araque, A. Astrocytes potentiate transmitter release at single hippocampal synapses. *Science (80-.)*. **317**, 1083–1086 (2007).
142. Pyka, M. *et al.* Chondroitin sulfate proteoglycans regulate astrocyte-dependent synaptogenesis and modulate synaptic activity in primary embryonic hippocampal neurons. *Eur. J. Neurosci.* **33**, 2187–2202 (2011).
143. Kucukdereli, H. *et al.* Control of excitatory CNS synaptogenesis by astrocyte-secreted proteins hevin and SPARC. *Proc. Natl. Acad. Sci. U. S. A.* **108**, (2011).
144. Ullian, E. M., Ullian, E. M., Sapperstein, S. K., Christopherson, K. S. & Barres, B. A. Control of Synapse Number by Glia. **657**, (2012).
145. Allen, N. J. *et al.* Astrocyte glypicans 4 and 6 promote formation of excitatory synapses via GluA1 AMPA receptors. *Nature* **486**, 410–414 (2012).
146. Albrecht, D. *et al.* SPARC prevents maturation of cholinergic presynaptic terminals. *Mol. Cell. Neurosci.* **49**, 364–374 (2012).
147. Simard, M. & Nedergaard, M. The neurobiology of glia in the context of water and ion homeostasis. *Neuroscience* **129**, 877–896 (2004).
148. Benfenati, V. & Ferroni, S. Water transport between CNS compartments: Functional and molecular interactions between aquaporins and ion channels. *Neuroscience* **168**, 926–940 (2010).
149. Agre, P., King, L. S., Yasui, M., Guggino, W. B., Ottersen, O. P., Fujiyoshi, Y., Engel, A., & Nielsen, S. Aquaporin water channels--from atomic structure to clinical medicine. *The Journal of physiology*, **542**, 3–16 (2002).
150. Nagelhus, E. A., Mathiisen, T. M., & Ottersen, O. P. Aquaporin-4 in the central

- nervous system: cellular and subcellular distribution and coexpression with KIR4.1. *Neuroscience*, **129**(4), 905–913 (2004).
151. Verkman A. S. More than just water channels: unexpected cellular roles of aquaporins. *Journal of cell science*, **118**, 3225–3232 (2005).
 152. Nielsen, S. *et al.* Specialized Membrane Domains for Water Transport in Glial Cells : High-Resolution Immunogold Cytochemistry of Aquaporin-4 in Rat Brain. **17**, 171–180 (1997).
 153. Ma, T., Epstein, C. J. & Verkman, A. S. Generation and phenotype of a transgenic knockout mouse lacking the mercurial-insensitive water channel aquaporin-4 . Generation and Phenotype of a Transgenic Knockout Mouse Lacking the. **100**, 957–962 (1997).
 154. Binder, D. K., Papadopoulos, M. C., Haggie, P. M. & Verkman, A. S. In Vivo Measurement of Brain Extracellular Space Diffusion by Cortical Surface Photobleaching. **24**, 8049–8056 (2004).
 155. Szu, J. I. & Binder, D. K. The Role of Astrocytic Aquaporin-4 in Synaptic Plasticity and Learning and Memory. **10**, 1–16 (2016).
 156. Binder, D. K., Yao, X., Zador, Z., Sick, T. J. & Verkman, A. S. Increased Seizure Duration and Slowed Potassium Kinetics in Mice Lacking Aquaporin-4 Water Channels. **636**, 631–636 (2006).
 157. Hayashi, Y. *et al.* Induction of various blood-brain barrier properties in non-neural endothelial cells by close apposition to co-cultured astrocytes. *Glia* **19**, 13–26 (1997).
 158. Greene, C., Hanley, N. & Campbell, M. Claudin - 5 : gatekeeper of neurological function. *Fluids Barriers CNS*, **16**, 3 (2019).
 159. Macvicar, B. A. & Newman, E. A. Astrocyte regulation of blood flow in the brain. *Cold Spring Harb. Perspect. Biol.* **7**, 1–15 (2015).
 160. Gordon, G. R. J., Howarth, C. & Macvicar, B. A. Bidirectional control of arteriole diameter by astrocytes. *Exp. Physiol.* **96**, 393–399 (2011).
 161. Golovina, V. A. & Blaustein, M. P. Unloading and refilling of two classes of spatially resolved endoplasmic reticulum Ca²⁺ stores in astrocytes. *Glia* **31**, 15–28 (2000).

162. Cornell-Bell, A. H., Finkbeiner, S. M., Cooper, M. S., & Smith, S. J. Glutamate induces calcium waves in cultured astrocytes: long-range glial signaling. *Science (New York, N.Y.)*, **247**(4941), 470–473 (1990).
163. Meier, S. D., Kafitz, K. W. & Rose, C. R. Developmental profile and mechanisms of GABA-induced calcium signaling in hippocampal astrocytes. *Glia* **56**, 1127–1137 (2008).
164. Salter, M. W. & Hicks, J. L. ATP causes release of intracellular Ca²⁺ via the phospholipase C β /IP3 pathway in astrocytes from the dorsal spinal cord. *J. Neurosci.* **15**, 2961–2971 (1995).
165. James, G. & Butt, A. M. P2Y and P2X purinoceptor mediated Ca²⁺ signalling in glial cell pathology in the central nervous system. *Eur. J. Pharmacol.* **447**, 247–260 (2002).
166. Vardjan, N., Parpura, V., & Zorec, R. Loose excitation-secretion coupling in astrocytes. *Glia*, **64**, 655–667 (2016).
167. Bazargani, N. & Attwell, D. Astrocyte calcium signaling: The third wave. *Nat. Neurosci.* **19**, 182–189 (2016).
168. Carmignoto, G. & Haydon, P. G. Astrocyte calcium signaling and epilepsy. *Glia* **60**, 1227–1233 (2012).
169. Bezzi, P. *et al.* CXCR4-activated astrocyte glutamate release via TNF α : Amplification by microglia triggers neurotoxicity. *Nat. Neurosci.* **4**, 702–710 (2001).
170. Ventura, R. & Harris, K. M. Three-dimensional relationships between hippocampal synapses and astrocytes. *J. Neurosci.* **19**, 6897–6906 (1999).
171. Olsen, M. L. & Sontheimer, H. Functional implications for Kir4.1 channels in glial biology: From K⁺ buffering to cell differentiation. *J. Neurochem.* **107**, 589–601 (2008).
172. Schousboe, A. & Waagepetersen, H. S. Role of astrocytes in glutamate homeostasis: Implications for excitotoxicity. *Neurotox. Res.* **8**, 221–225 (2005).
173. Schröder, W., Seifert, G., Hüttmann, K., Hinterkeuser, S. & Steinhäuser, C. AMPA receptor-mediated modulation of inward rectifier K⁺ channels in astrocytes of

- mouse hippocampus. *Mol. Cell. Neurosci.* **19**, 447–458 (2002).
174. Fakler, B. & Ruppersberg, J. P. Functional and molecular diversity classifies the family of inward-rectifier K^{+} channels. *Cell. Physiol. Biochem.* **6**, 195–209 (1996).
 175. Butt, A. M. & Kalsi, A. Inwardly rectifying potassium channels (Kir) in central nervous system glia: A special role for Kir4.1 in glial functions. *J. Cell. Mol. Med.* **10**, 33–44 (2006).
 176. Takumi, T. *et al.* A novel ATP-dependent inward rectifier potassium channel expressed predominantly in glial cells. *Journal of Biological Chemistry* vol. 270 16339–16346 (1995).
 177. Kofuji, P. *et al.* Genetic inactivation of an inwardly rectifying potassium channel (kir4.1 Subunit) in mice: Phenotypic impact in retina. *J. Neurosci.* **20**, 5733–5740 (2000).
 178. Hibino, H., Fujita, A., Iwai, K., Yamada, M. & Kurachi, Y. Differential assembly of inwardly rectifying K^{+} channel subunits, Kir4.1 and Kir5.1, in brain astrocytes. *J. Biol. Chem.* **279**, 44065–44073 (2004).
 179. Bordey, A. & Sontheimer, H. Postnatal development of ionic currents in rat hippocampal astrocytes in situ. *J. Neurophysiol.* **78**, 461–477 (1997).
 180. Olsen, M. L., Higashimori, H., Campbell, S. L., Hablitz, J. J. & Sontheimer, H. Functional expression of Kir4.1 channels in spinal cord astrocytes. *Glia* **53**, 516–528 (2006).
 181. Kofuji, P. & Newman, E. A. Potassium buffering in the central nervous system. *Neuroscience* **129**, 1043–1054 (2004).
 182. Djukic, B., Casper, K. B., Philpot, B. D., Chin, L. S. & McCarthy, K. D. Conditional knock-out of Kir4.1 leads to glial membrane depolarization, inhibition of potassium and glutamate uptake, and enhanced short-term synaptic potentiation. *J. Neurosci.* **27**, 11354–11365 (2007).
 183. Walz, W. Role of astrocytes in the clearance of excess extracellular potassium. *Neurochem. Int.* **36**, 291–300 (2000).
 184. Buono, R. J. *et al.* Association between variation in the human KCNJ10 potassium

- ion channel gene and seizure susceptibility. *Epilepsy Res.* **58**, 175–183 (2004).
185. Kaiser, M. *et al.* Progressive loss of a glial potassium channel (KCNJ10) in the spinal cord of the SOD1 (G93A) transgenic mouse model of amyotrophic lateral sclerosis. *J. Neurochem.* **99**, 900–912 (2006).
 186. Pivonkova, H., Benesova, J., Butenko, O., Chvatal, A. & Anderova, M. Impact of global cerebral ischemia on K⁺ channel expression and membrane properties of glial cells in the rat hippocampus. *Neurochem. Int.* **57**, 783–794 (2010).
 187. Bataveljić, D., Nikolić, L., Milosević, M., Todorović, N. & Andjus, P. R. Changes in the astrocytic aquaporin-4 and inwardly rectifying potassium channel expression in the brain of the amyotrophic lateral sclerosis SOD1G93A rat model. *Glia* **60**, 1991–2003 (2012).
 188. Tong, X. *et al.* Astrocyte Kir4.1 ion channel deficits contribute to neuronal dysfunction in Huntington's disease model mice. *Nat. Neurosci.* **17**, 694–703 (2014).
 189. Ferraro, T. N. *et al.* Fine mapping of a seizure susceptibility locus on mouse Chromosome 1: Nomination of Kcnj10 as a causative gene. *Mamm. Genome* **15**, 239–251 (2004).
 190. Barbeito, L. H. *et al.* A role for astrocytes in motor neuron loss in amyotrophic lateral sclerosis. *Brain Res. Rev.* **47**, 263–274 (2004).
 191. Scholl, U. I. *et al.* Seizures, sensorineural deafness, ataxia, mental retardation, and electrolyte imbalance (SeSAME syndrome) caused by mutations in KCNJ10. *Proc. Natl. Acad. Sci. U. S. A.* **106**, 5842–5847 (2009).
 192. Tobin, J. *et al.* Epilepsy, Ataxia, Sensorineural Deafness, Tubulopathy, and. (2009).
 193. Chever, O., Djukic, B., McCarthy, K. D. & Amzica, F. Implication of Kir4.1 channel in excess potassium clearance: An in vivo study on anesthetized glial-conditional Kir4.1 knock-out mice. *J. Neurosci.* **30**, 15769–15777 (2010).
 194. Rosenberg, P. A. & Aizenman, E. Hundred-fold increase in neuronal vulnerability to glutamate toxicity in astrocyte-poor cultures of rat cerebral cortex. *Neurosci. Lett.* **103**, 162–168 (1989).
 195. Rosenberg, P. A., Amin, S. & Leitner, M. Glutamate uptake disguises neurotoxic

- potency of glutamate agonists in cerebral cortex in dissociated cell culture. *J. Neurosci.* **12**, 56–61 (1992).
196. Trophic Interactions between Astroglial Cells and Hippocampal Neurons in Culture Author (s): Gary A . Banker Reviewed work (s): Source : Science , New Series , Vol . 209 , No . 4458 (Aug . 15 , 1980), pp . 809-810 Published by : American Association. **209**, 809–810 (2012).
 197. Gegelashvili, G. & Schousboe, A. Cellular distribution and kinetic properties of high-affinity glutamate transporters. *Brain Res. Bull.* **45**, 233–238 (1998).
 198. Danbolt, N. C. Glutamate uptake. *Prog. Neurobiol.* **65**, 1–105 (2001).
 199. Hertz, L. & Rodrigues, T. B. Astrocytic-neuronal-astrocytic pathway selection for formation and degradation of glutamate/GABA. *Front. Endocrinol. (Lausanne)*. **5**, 10–13 (2014).
 200. Tani, H. *et al.* A local glutamate-glutamine cycle sustains synaptic excitatory transmitter release. *Neuron* **81**, 888–900 (2014).
 201. Todd, A. C., Marx, M. C., Hulme, S. R., Bröer, S. & Billups, B. SNAT3-mediated glutamine transport in perisynaptic astrocytes in situ is regulated by intracellular sodium. *Glia* **65**, 900–916 (2017).
 202. Billups, D., Marx, M. C., Mela, I. & Billups, B. Inducible presynaptic glutamine transport supports glutamatergic transmission at the calyx of Held synapse. *J. Neurosci.* **33**, 17429–17434 (2013).
 203. Todd, A. C. & Hardingham, G. E. The regulation of astrocytic glutamate transporters in health and neurodegenerative diseases. *Int. J. Mol. Sci.* **21**, 1–32 (2020).
 204. Zerangue, N., Arriza, J. L., Amara, S. G. & Kavanaugh, M. P. Differential modulation of human glutamate transporter subtypes by arachidonic acid. *J. Biol. Chem.* **270**, 6433–6435 (1995).
 205. Owe, S. G., Marcaggi, P. & Attwell, D. The ionic stoichiometry of the GLAST glutamate transporter in salamander retinal glia. *J. Physiol.* **577**, 591–599 (2006).
 206. Perego, C. *et al.* The GLT-1 and GLAST glutamate transporters are expressed on morphologically distinct astrocytes and regulated by neuronal activity in primary

- hippocampal cocultures. *J. Neurochem.* **75**, 1076–1084 (2000).
207. Stanimirovic, D. B., Ball, R., Small, D. L. & Muruganandam, A. Developmental regulation of glutamate transporters and glutamine synthetase activity in astrocyte cultures differentiated in vitro. *Int. J. Dev. Neurosci.* **17**, 173–184 (1999).
208. Rothstein, J. D. *et al.* Localization of neuronal and glial glutamate transporters. *Neuron* **13**, 713–725 (1994).
209. Takayasu, Y., Iino, M., Takatsuru, Y., Tanaka, K. & Ozawa, S. Functions of glutamate transporters in cerebellar Purkinje cell synapses. *Acta Physiol.* **197**, 1–12 (2009).
210. Lehre, K. P., Davanger, S. & Danbolt, N. C. Localization of the glutamate transporter protein GLAST in rat retina. *Brain Res.* **744**, 129–137 (1997).
211. Berger, U. V. & Hediger, M. A. Distribution of the glutamate transporters GLAST and GLT-1 in rat circumventricular organs, meninges, and dorsal root ganglia. *J. Comp. Neurol.* **421**, 385–399 (2000).
212. Schreiner, A. E. *et al.* Laminar and subcellular heterogeneity of GLAST and GLT-1 immunoreactivity in the developing postnatal mouse hippocampus. *J. Comp. Neurol.* **522**, 204–224 (2014).
213. Benveniste, H., Drejer, J., Schousboe, A. & Diemer, N. H. Elevation of the Extracellular Concentrations of Glutamate and Aspartate in Rat Hippocampus During Transient Cerebral Ischemia Monitored by Intracerebral Microdialysis. *J. Neurochem.* **43**, 1369–1374 (1984).
214. Erecińska, M., & Silver, I. A. Metabolism and role of glutamate in mammalian brain. *Progress in neurobiology*, **35**, 245–296. (1990).
215. Swanson, R. A. *et al.* Neuronal regulation of glutamate transporter subtype expression in astrocytes. *J. Neurosci.* **17**, 932–940 (1997).
216. Tanaka, K. *et al.* Epilepsy and exacerbation of brain injury in mice lacking the glutamate transporter GLT-1. *Science (80-.)*. **276**, 1699–1702 (1997).
217. Bruijn, L. I. *et al.* ALS-linked SOD1 mutant G85R mediates damage to astrocytes and promotes rapidly progressive disease with SOD1-containing inclusions. *Neuron* **18**, 327–338 (1997).

218. Lin, C. L. G. *et al.* Aberrant RNA processing in a neurodegenerative disease: The cause for absent EAAT2, a glutamate transporter, in amyotrophic lateral sclerosis. *Neuron* **20**, 589–602 (1998).
219. Tessler, S., Danbolt, N. C., Faull, R. L. M., Storm-Mathisen, J. & Emson, P. C. Expression of the glutamate transporters in human temporal lobe epilepsy. *Neuroscience* **88**, 1083–1091 (1999).
220. Chotibut, T. *et al.* Ceftriaxone reduces L-dopa-induced dyskinesia severity in 6-hydroxydopamine parkinson's disease model. *Mov. Disord.* **32**, 1547–1556 (2017).
221. Jacob, C. P. *et al.* Alterations in expression of glutamatergic transporters and receptors in sporadic Alzheimer's disease. *J. Alzheimer's Dis.* **11**, 97–116 (2007).
222. Liévens, J. C. *et al.* Impaired glutamate uptake in the R6 Huntington's disease transgenic mice. *Neurobiol. Dis.* **8**, 807–821 (2001).
223. Estrada-Sánchez, A. M., Montiel, T., Segovia, J. & Massieu, L. Glutamate toxicity in the striatum of the R6/2 Huntington's disease transgenic mice is age-dependent and correlates with decreased levels of glutamate transporters. *Neurobiol. Dis.* **34**, 78–86 (2009).
224. Right, N. of this is. The Emerging Role of Glutamate in the Pathophysiology and Treatment of Schizophrenia Donald. *Agron. J.* **75**, 1005 (1983).
225. Karlsson, R. M., Tanaka, K., Heilig, M. & Holmes, A. Loss of Glial Glutamate and Aspartate Transporter (Excitatory Amino Acid Transporter 1) Causes Locomotor Hyperactivity and Exaggerated Responses to Psychotomimetics: Rescue by Haloperidol and Metabotropic Glutamate 2/3 Agonist. *Biol. Psychiatry* **64**, 810–814 (2008).
226. Kiryk, A. *et al.* Behavioral characterization of GLT1 (+/-) mice as a model of mild glutamatergic hyperfunction. *Neurotox. Res.* **13**, 19–30 (2008).
227. Hoshi, A. *et al.* Altered expression of glutamate transporter-1 and water channel protein aquaporin-4 in human temporal cortex with Alzheimer's disease. *Neuropathol. Appl. Neurobiol.* **44**, 628–638 (2018).
228. Kobayashi, E. *et al.* Activated forms of astrocytes with higher GLT-1 expression

- are associated with cognitive normal subjects with Alzheimer pathology in human brain. *Sci. Rep.* **8**, 2–13 (2018).
229. Mookherjee, P. *et al.* GLT-1 loss accelerates cognitive deficit onset in an Alzheimer's disease animal model. *J. Alzheimer's Dis.* **26**, 447–455 (2011).
 230. Zumkehr, J. *et al.* Ceftriaxone ameliorates tau pathology and cognitive decline via restoration of glial glutamate transporter in a mouse model of Alzheimer's disease. *Neurobiol. Aging* **36**, 2260–2271 (2015).
 231. Scimemi, A. *et al.* Amyloid- β 1-42 slows clearance of synaptically released glutamate by mislocalizing astrocytic GLT-1. *Ann. Intern. Med.* **158**, 5312–5318 (2013).
 232. Malik, A. R. & Willnow, T. E. Excitatory amino acid transporters in physiology and disorders of the central nervous system. *Int. J. Mol. Sci.* **20**, 1–37 (2019).
 233. Bradford, J. *et al.* Expression of mutant huntingtin in mouse brain astrocytes causes age-dependent neurological symptoms. *Proc. Natl. Acad. Sci. U. S. A.* **106**, 22480–22485 (2009).
 234. Plaitakis, A. & Caroscio, J. T. Abnormal glutamate metabolism in amyotrophic lateral sclerosis. *Ann. Neurol.* **22**, 575–579 (1987).
 235. Rothstein, J. D. *et al.* Abnormal excitatory amino acid metabolism in amyotrophic lateral sclerosis. *Ann. Neurol.* **28**, 18–25 (1990).
 236. Sasaki, S., Komori, T. & Iwata, M. Excitatory amino acid transporter 1 and 2 immunoreactivity in the spinal cord in amyotrophic lateral sclerosis. *Acta Neuropathol.* **100**, 138–144 (2000).
 237. Trotti, D. *et al.* Amyotrophic lateral sclerosis-linked glutamate transporter mutant has impaired glutamate clearance capacity. *J. Biol. Chem.* **276**, 576–582 (2001).
 238. Doi, T., Ueda, Y., Nagatomo, K. & Willmore, L. J. Role of glutamate and GABA transporters in development of pentylenetetrazol-kindling. *Neurochem. Res.* **34**, 1324–1331 (2009).
 239. Petr, G. T. *et al.* Conditional deletion of the glutamate transporter GLT-1 reveals that astrocytic GLT-1 protects against fatal epilepsy while neuronal GLT-1 contributes significantly to glutamate uptake into synaptosomes. *J. Neurosci.* **35**,

- 5187–5201 (2015).
240. Hubbard, J. A., Szu, J. I., Yonan, J. M. & Binder, D. K. Regulation of astrocyte glutamate transporter-1 (GLT1) and aquaporin-4 (AQP4) expression in a model of epilepsy. *Exp. Neurol.* **283**, 85–96 (2016).
 241. Kong, Q. *et al.* Increased glial glutamate transporter EAAT2 expression reduces epileptogenic processes following pilocarpine-induced status epilepticus. *Neurobiol. Dis.* **47**, 145–154 (2012).
 242. Billups, B. *et al.* Physiological and pathological operation of glutamate transporters. *Prog. Brain Res.* **116**, 45–57 (1998).
 243. Robinson, M. B. The family of sodium-dependent glutamate transporters: A focus on the GLT-1/EAAT2 subtype. *Neurochem. Int.* **33**, 479–491 (1998).
 244. Inyushin, M. *et al.* NIH Public Access. **51**, 1707–1713 (2011).
 245. Dallérac, G., Chever, O. & Rouach, N. How do astrocytes shape synaptic transmission? Insights from electrophysiology. *Front. Cell. Neurosci.* **7**, 1–19 (2013).
 246. De-zolt, S. *et al.* Genomewide production of multipurpose alleles for the functional analysis of the mouse genome. **102**, 7221–7226 (2005).
 247. High-efficiency deleter mice show that FLPe is an alternative to Cre-loxP. **25**, 139–140 (2000).
 248. Kaeser, P. S. *et al.* RIM proteins tether Ca²⁺ channels to presynaptic active zones via a direct PDZ-domain interaction. *Cell* **144**, 282–295 (2011).
 249. Jaudon, F. *et al.* Kidins220/ARMS controls astrocyte calcium signaling and neuron–astrocyte communication. *Cell Death Differ.* **27**, 1505–1519 (2020).
 250. De Palma, M. & Naldini, L. Transduction of a gene expression cassette using advanced generation lentiviral vectors. *Methods Enzymol.* **346**, 514–529 (2002).
 251. Ferroni, S. *et al.* <Ferroni-2003-Arachidonic acid activates an ope.pdf>. **372**, 363–372 (2003).
 252. Chiacchiarretta, M. *et al.* Graphene Oxide Upregulates the Homeostatic Functions of Primary Astrocytes and Modulates Astrocyte-to-Neuron Communication. *Nano Lett.* **18**, 5827–5838 (2018).

253. Codeluppi, S. *et al.* Influence of rat substrain and growth conditions on the characteristics of primary cultures of adult rat spinal cord astrocytes. *J. Neurosci. Methods* **197**, 118–127 (2011).
254. Magoun, H. W. Growth of purified astrocytes in a chemically defined medium. **78**, 7205–7209 (1981).
255. Ferroni, S., Marchinip, C., Schubert, P. & Rapisarda, C. Two distinct inwardly rectifying conductances are expressed in long term dibutyl-AMP treated rat cultured cortical astrocytes. **367**, 319–325 (1995).
256. Valente, P. *et al.* Cell adhesion molecule L1 contributes to neuronal excitability regulating the function of voltage-gated Na⁺ channels. *J. Cell Sci.* **129**, 1878–1891 (2016).
257. Prestigio, C. *et al.* Spike-Related Electrophysiological Identification of Cultured Hippocampal Excitatory and Inhibitory Neurons. *Mol. Neurobiol.* **56**, 6276–6292 (2019).
258. Watt, A. J., Rossum, M. C. W. Van, Macleod, K. M., Nelson, S. B. & Turrigiano, G. G. Activity Coregulates Quantal AMPA and NMDA Currents at Neocortical Synapses. **26**, 659–670 (2000).
259. Poskanzer, K. E., & Molofsky, A. V. Dynamism of an Astrocyte In Vivo: Perspectives on Identity and Function. *Annual review of physiology*, **80**, 143–157 (2018).
260. Olsen, M. L. *et al.* New Insights on Astrocyte Ion Channels: Critical for Homeostasis and Neuron-Glia Signaling. **35**, 13827–13835 (2015).
261. Seifert, G. *et al.* Analysis of Astroglial K⁺ Channel Expression in the Developing Hippocampus Reveals a Predominant Role of the Kir4.1 Subunit. **29**, 7474–7488 (2009).
262. Benfenati, V., Caprini, M., Nobile, M., Rapisarda, C. & Ferroni, S. Guanosine promotes the up-regulation of inward rectifier potassium current mediated by Kir4.1 in cultured rat cortical astrocytes. *J. Neurochem.* **98**, 430–445 (2006).
263. Zurolo, E. *et al.* Regulation of Kir4.1 expression in astrocytes and astrocytic tumors: A role for interleukin-1 β . *J. Neuroinflammation* **9**, 1–17 (2012).
264. Olsen, M. L., Higashimori, H., Campbell, S. L., Hablitz, J. J., & Sontheimer, H.

- Functional expression of Kir4.1 channels in spinal cord astrocytes. *Glia*, **53**, 516–528 (2006).
265. Abrahamsen, B. *et al.* Allosteric Modulation of an Excitatory Amino Acid Transporter : The Subtype-Selective Inhibitor UCPH-101 Exerts Sustained Inhibition of EAAT1 through an Intramonomeric Site in the Trimerization Domain. **33**, 1068–1087 (2013).
266. Shimamoto, K., Brun, B. L. E., Yasuda-kamatani, Y., Sakaitani, M. & Shigeri, Y. A Potent Blocker of Excitatory Amino Acid Transporters. **201**, 195–201 (1998).
267. Bergles, D. E. & Jahr, C. E. Synaptic Activation of Glutamate Transporters in Hippocampal Astrocytes. **19**, 1297–1308 (1997).
268. Pajarillo, E. *et al.* Astrocytic transcription factor REST upregulates glutamate transporter EAAT2, protecting dopaminergic neurons from manganese-induced excitotoxicity. *J. Biol. Chem.* **297**, 101372 (2021).
269. Stevens, C. F. Quantal release of neurotransmitter and long-term potentiation. *Neuron* **10**, 55–63 (1993).
270. Seth, K. A. & Majzoub, J. A. Repressor Element Silencing Transcription Factor/Neuron-restrictive Silencing Factor (REST/NRSF) Can Act as an Enhancer as Well as a Repressor of Corticotropin-releasing Hormone Gene Transcription. *J. Biol. Chem.* **276**, 13917–13923 (2001).
271. Bessis, A., Champtiaux, N., Chatelin, L. & Changeux, J. P. The neuron-restrictive silencer element: A dual enhancer/silencer crucial for patterned expression of a nicotinic receptor gene in the brain. *Proc. Natl. Acad. Sci. U. S. A.* **94**, 5906–5911 (1997).
272. Kallunki, P., Edelman, G. M. & Jones, F. S. The neural restrictive silencer element can act as both a repressor and enhancer of L1 cell adhesion molecule gene expression during postnatal development. *Proc. Natl. Acad. Sci. U. S. A.* **95**, 3233–3238 (1998).
273. Neusch, C., Rozengurt, N., Jacobs, R. E., Lester, H. A. & Kofuji, P. Kir4.1 potassium channel subunit is crucial for oligodendrocyte development and in vivo myelination. *J. Neurosci.* **21**, 5429–5438 (2001).

274. Neusch, C. *et al.* Lack of the Kir4.1 channel subunit abolishes K⁺ buffering properties of astrocytes in the ventral respiratory group: Impact on extracellular K⁺ regulation. *J. Neurophysiol.* **95**, 1843–1852 (2006).
275. Ransom, B. R. & Goldring, S. Slow hyperpolarization in cells presumed to be glia in cerebral cortex of cat. *J. Neurophysiol.* **36**, 879–892 (1973).
276. Hagiwara, S. & Takahashi, K. The anomalous rectification and cation selectivity of the membrane of a starfish egg cell. *J. Membr. Biol.* **18**, 61–80 (1974).
277. Sakmann, B. & Trube, G. Conductance properties of single inwardly rectifying potassium channels in ventricular cells from guinea-pig heart. *J. Physiol.* **347**, 641–657 (1984).
278. Ransom, C. B. & Sontheimer, H. Biophysical and pharmacological characterization of inwardly rectifying K⁺ currents in rat spinal cord astrocytes. *J. Neurophysiol.* **73**, 333–346 (1995).
279. Verkhratsky, A. & Steinhäuser, C. Ion channels in glial cells. *Brain Res. Rev.* **32**, 380–412 (2000).
280. Vezzani, A., Maroso, M., Balosso, S., Sanchez, M. A. & Bartfai, T. IL-1 receptor/Toll-like receptor signaling in infection, inflammation, stress and neurodegeneration couples hyperexcitability and seizures. *Brain. Behav. Immun.* **25**, 1281–1289 (2011).
281. Aronica, E., Ravizza, T., Zurolo, E. & Vezzani, A. Astrocyte immune responses in epilepsy. *Glia* **60**, 1258–1268 (2012).
282. D’Ambrosio, R., Maris, D. O., Grady, M. S., Winn, H. R. & Janigro, D. Impaired K⁺ homeostasis and altered electrophysiological properties of post-traumatic hippocampal glia. *J. Neurosci.* **19**, 8152–8162 (1999).
283. Leis, J. A., Bekar, L. K. & Walz, W. Potassium homeostasis in the ischemic brain. *Glia* **50**, 407–416 (2005).
284. Bordey, A. & Sontheimer, H. Modulation of glutamatergic transmission by Bergmann glial cells in rat cerebellum in situ. *J. Neurophysiol.* **89**, 979–988 (2003).
285. D’Ambrosio, R. The role of glial membrane ion channels in seizures and epileptogenesis. *Pharmacol. Ther.* **103**, 95–108 (2004).

286. Perera, A. *et al.* TET3 is recruited by REST for context-specific hydroxymethylation and induction of gene expression. *Cell Rep.* **11**, 283–294 (2015).
287. Bersten, D. C., Wright, J. A., McCarthy, P. J. & Whitelaw, M. L. Regulation of the neuronal transcription factor NPAS4 by REST and microRNAs. *Biochim. Biophys. Acta - Gene Regul. Mech.* **1839**, 13–24 (2014).
288. Chamberlin, N. L., Traub, R. D. & Dingledine, R. Role of EPSPs in initiation of spontaneous synchronized burst firing in rat hippocampal neurons bathed in high potassium. *J. Neurophysiol.* **64**, 1000–1008 (1990).
289. Tureček, R. & Trussell, L. O. Control of synaptic depression by glutamate transporters. *J. Neurosci.* **20**, 2054–2063 (2000).
290. Dvorzhak, A., Vagner, T., Kirmse, K. & Grantyn, R. Functional indicators of glutamate transport in single striatal astrocytes and the influence of Kir4.1 in normal and huntington mice. *J. Neurosci.* **36**, 4959–4975 (2016).
291. Tzingounis, A. V. & Wadiche, J. I. Glutamate transporters: Confining runaway excitation by shaping synaptic transmission. *Nat. Rev. Neurosci.* **8**, 935–947 (2007).
292. Hibino, H. *et al.* Inwardly rectifying potassium channels: Their structure, function, and physiological roles. *Physiol. Rev.* **90**, 291–366 (2010).
293. Olsen, M. L., Campbell, S. L. & Sontheimer, H. Differential distribution of Kir4.1 in spinal cord astrocytes suggests regional differences in K⁺ homeostasis. *J. Neurophysiol.* **98**, 786–793 (2007).
294. Higashi, K. *et al.* An inwardly rectifying K⁺ channel, Kir4.1, expressed in astrocytes surrounds synapses and blood vessels in brain. *Am. J. Physiol. - Cell Physiol.* **281**, 922–931 (2001).
295. Murphy-Royal, C. *et al.* Surface diffusion of astrocytic glutamate transporters shapes synaptic transmission. *Nat. Neurosci.* **18**, 219–226 (2015).
296. Pecoraro-Bisogni, F. *et al.* REST-Dependent Presynaptic Homeostasis Induced by Chronic Neuronal Hyperactivity. *Mol. Neurobiol.* **55**, 4959–4972 (2018).
297. Prestigio, C. *et al.* Rest/nrsf drives homeostatic plasticity of inhibitory synapses in a target-dependent fashion. *Elife* **10**, 1–34 (2021).

10. Acknowledgements

I thank Professor Fabio Benfenati for his mentoring, supervision, and for giving me the opportunity to be part of the inspiring environment of the NSYN.

I thank Professor Pierluigi Valente for scientific discussions, for his help in developing this project and for contributing to the production of this thesis.

I would like to thank Professor Fabrizia Cesca for useful scientific suggestions and for contributing to the production of this manuscript.

I want to acknowledge Professor Stefano Ferroni for his valuable experimental advices.

I thank Dr. Martina Albini for imaging and molecular assays and Dr. Antonella Marte for the help with biochemical assays.

Lastly, I would like to thank all my colleagues at NSYN for being precious support to me both in and out of the lab and for sharing with me unforgettable moments.